Institute for Space Nuclear Power Studies
Department of Chemical and Nuclear Engineering
The University of New Mexico
Albuquerque, New Mexico 87131

CONCEPTUAL STUDIES ON THE INTEGRATION OF A NUCLEAR REACTOR SYSTEM TO A MANNED ROVER FOR MARS MISSIONS

MOHAMED S. EL-GENK AND NICHOLAS J. MORLEY

FINAL REPORT NO. UNM-ISNPS-NAG3-992

NASA Grant No. NAG 3-992
Performance Period Feb. 1989 - Nov. 1990

July 1991

CONCEPTUAL STUDIES ON THE INTEGRATION OF A NUCLEAR REACTOR POWER SYSTEM TO A MANNED ROVER FOR MARS MISSIONS

ABSTRACT

Multiyear civilian manned missions to explore the surface of Mars are thought by NASA to be possible early in the next century. Expeditions to Mars, as well as permanent bases, are envisioned to require enhanced piloted vehicles to conduct science and exploration activities. Piloted rovers, with 30 kWe user net power (for drilling, sampling and sample analysis, onboard computer and computer instrumentation, vehicle thermal management, and astronaut life support systems) in addition to mobility, are being considered.

The rover design, for this study, included a four car train type vehicle complete with a hybrid solar photovoltaic/regenerative fuel cell auxiliary power system (APS). This system was designed to power the primary control vehicle. The APS supplies life support power for four astronauts and a limited degree of mobility allowing the Primary Control Vehicle to limp back to either a permanent base or an accent vehicle. The results showed that the APS described above, with a mass of 667 kg, was sufficient to provide life support power and a top speed of five km/h for 6 hours per day. It was also seen that the factors that had the largest effect on the APS mass were the life support power, the number of astronauts, and the PV cell efficiency. From the results of the auxiliary PV mass study several points can be made:

(1) The life support power requirements significantly affect the mass and size of the PV panels. For this reason, every effort should be made to design an energy efficient life support system and attempt to reduce astronaut requirements if possible,

(2) In addition to the life support power, the PV panel efficiency and the number of astronauts on board the rover also play a major role in determining the size and mass of the PV panels for the auxiliary power system.

(3) Parameters that affect the mass of the auxiliary PV power system to a lesser extent, but are still important to the overall mass and size determination are the cruising speed of the PCV, and the surface density of the PV cells.

(4) The parameter that has an insignificant effect on the auxiliary power system mass, but strongly impacts the volume of the fuel cells, is the reserve capacity of the RFC's.

(5) In order to minimize the size and mass of the auxiliary power system, traversing should be done at night.

The primary power requirement of 100 kWe was met using an SP-100 type nuclear reactor coupled to a dynamic conversion system and a man-rated radiation shield. The masses of the shield, reactor,and the radiator were directly dependent on the reactor power, while this power was dictated by the electrical output and the conversion system parameters. The following four conversion systems were investigated for use in the PPS: Free Piston Stirling Engine (FPSE), He/Xe Closed Brayton Cycle (CBC), CO_2 Open Brayton Cycle (OBC), and Thermoelectric conversion. Of the systems studied, the FPSE and CBC systems yield the lowest overall PPS mass, with the Stirling system (15-16 tonnes) giving slightly lower system mass than the Brayton system (18-19.5 tonnes). Because the shield was such a large portion of the overall system mass, its size must be kept as low as possible. Therefore the system with the highest conversion efficiency has the lowest overall mass.

Since the efficiencies calculated for both the Stirling and Brayton cycles were projected upper limits a parametric analysis was completed to see what

effect lower efficiencies would have on the total rover mass. The analysis show that while the masses of each system increased by reducing the efficiencies to 29% for the Stirling and 25% for the Brayton, both systems still had a total mass that is significantly lower than the thermoelectric and the open Brayton systems.

It was seen that major mass component for the PPS was the radiation shield. While it was possible to design an effective man-rated radiation shield (satisfying the dose rate limit of 0.3 Sv/y to the rover crew) for a manned Mars rover using a single layer each of tungsten and lithium hydride, the shield would not be mass efficient. A double layered W and LiH shield was more effective and significantly lighter. The thickness and positions of the tungsten layers, within the shield, were varied to determine the impact of secondary gammas produced in the W on the dose rate and total shield mass.

The combined shield of LiH and W/depleted U was slightly heavier than a double layered W-LiH shield. The mass of the optimized man-rated W-LiH shield for the Mars rover vehicle powered by a nuclear reactor system increases with the thermal power of the reactor raised to the 0.3797 power, and varies from 8600 to 20580 kg over the power range of 100 to 1000 kW_{th}, respectively. These shield masses were based on a conservative design correlation developed based on the results of 1-D neutronics analysis. Results show that shield mass estimates could be as much as 15 percent higher than those based on 2-D neutronics calculations.

TABLE OF CONTENTS

TABLE OF CONTENTS

TABLE OF CONTENTS

TABLE OF CONTENTS

LIST OF FIGURES

LIST OF FIGURES

LIST OF FIGURES

LIST OF TABLES

NOMENCLATURE

A	:Area (m^2)
β	:$\ln(E_n)$
$\dot{D}$	:Dose rate (mrem/h)
E	:Energy (MeV)
F	:View factor
k	:Ratio of specific heat at constant volume to constant pressure
G	:Solar radiation (W/m^2)
M	:Mass (kg)
n	:number
P	:Power (kW)
P	:Pressure
p	:Power/astronaut (kW/astro.)
PA	:Net user power (kW_e)
Q	:Quality factor (rem/rad)
R	:Radius (cm)
SM	:Specific mass (kg/kW_e)
SMA	:Mass per unit area (kg/m^3)
T	:Temperature (K)
t	:Time (h)
V	:Velocity (km/h)
x	:Separation distance of the tungsten shields (cm)
α	:Absorptivity
ε	:Surface emissivity
η	:Efficiency
ϕ	:Flux (part/cm^2 sec)
ϕ'	:Flux required for 1 mrem/hr dose rate (part/cm^2 sec/mrem/h)
σ	:Stefan-Boltzmann constant (5.67×10^{-8} W/m^2K)
χ	:Traction parameter

NOMENCLATURE

μ_a/ρ : Mass absorption coefficient (cm^2/g)

ξ : Thickness of the tungsten shield (cm)

Subscripts

a : astronaut

ae : auxiliary reserve in EU

ap : auxiliary reserve in PCV

as : auxiliary reserve in SC

am : ambient

c : collection

d : daylight

e : electrical

EU : experimental unit

fc : fuel cell

g : gamma

ls : life support

m : mobility

n : neutron

PCV : primary control vehicle

r : reactor

rad : radiator

rej : rejection

SC : supply car

shield : shield

th : thermal

tis : in tissue

1 : first layer of tungsten

2 : second layer of tungsten

1. INTRODUCTION

1.1 Background

For centuries the red planet has intrigued man. The nearest outward neighbor to the earth, Mars, has been the focus of much speculation as the home for alien life, although today it is known that the planet houses no intelligent life forms. The first successful probe to Mars was Mariner 4, which on July 14, 1965 flew to within 10,000 kilometers of Mars. In 1969 two more Mariner missions were sent to fly by Mars to photograph the surface. Mariner 9, the final Mariner mission, was sent in 1971 to photograph the two Martian moons, Phobos and Deimos, and perform a photographic survey of the Martian surface. This survey set the stage for the first two successful landing missions on Mars. On July 20, 1976 the Viking I lander touched down on the Chryse Plain on the surface of Mars. A month and a half later the Viking II lander also came to rest on the surface of our sister planet [Ezell and Ezell, 1984]. Although both the Viking missions were highly successful, NASA has not revisited Mars.

The first step in the return to Mars may be an unmanned Mars rover Sample Return (MRSR) mission. A possible MRSR mission scenario would place two spacecraft in orbit about Mars and land a small (<1000 kg) robotic rover on the surface of the planet. The rover's power would be supplied by one or two radioisotope thermoelectric generators [Shock, 1989]. This rover would collect up to 100 kg of soil, rocks, and atmospheric samples over a period of 11 to 18 months. These samples would in turn be transferred to an ascent vehicle for return to Earth. In addition to collecting samples for return to earth, the rover would be capable of performing additional experiments over the lifetime of its extended mission. The Solar System Exploration Committee (SSEC) of the NASA advisory Council is strongly recommending that a Mars Sample Return

mission be undertaken before the end of the century [Bents, 1989]. This unmanned MRSR mission would then pave the way for manned exploration of our neighbor planet by plotting the terrain and studying, in depth, the environment which will be encountered.

An evolutionary strategy is currently planned for manned missions to Mars. This strategy begins with an initial exploration of Mars and builds towards the establishment of an *in situ* propellant facility and ultimately a permanent manned base. Some of the mission design guidelines include an initial crew size of four growing to eight, reusability of selected vehicle elements, and aerobraking at both Mars and Earth. The program is to be carried out through a series of unmanned cargo flights and manned exploration missions [Andrews, 1989].

1.2 **Power System Options**

Multiyear civilian manned missions to explore the surface of Mars are thought by NASA to be possible early in the next century. Expeditions to Mars, as well as permanent bases, are envisioned to require enhanced piloted vehicles to conduct science and exploration. Piloted rovers, with extended range, have been identified as a viable means of achieving global access of Mars. For these missions, a rover vehicle with 30 kW_e user net power is being considered. The operations covered by this power include: drilling, sampling and sample analysis, onboard computer and computer instrumentation, vehicle thermal management, and astronaut life support systems. In addition to the 30 kW_e user power, electric power will be needed to drive the rover across the Martian terrain. The only power system option that can provide this level of power at a reasonable mass penalty is a nuclear reactor heat source with a static or dynamic conversion system. Fore the auxiliary power system, which

will by used in the event of a primary power system failure there are several possible system options.

1.2.1 Auxiliary Power System Options

These options include photovoltaic (PV) collection systems, radioisotope thermoelectric generators (RTG's), dynamic isotope power systems (DIPS), and high performance fuel cells. The following is a brief discussion of each of these systems.

1.2.1.1 Photovoltaic Power Systems

Photovoltaic (PV) power systems have been flown by NASA since the late 1950's with the launch of the Vanguard satellite in 1958. Those first cells, while only delivering milliwatts of power (used to operate a tracking oscillator), operated for over six years demonstrating the reliability the PV systems [Ralph, 1989]. The cells used for this mission were p on n silicon cells, which exhibited ~5% efficiency at air mass zero (AM0). After 1962, NASA switched to n on p type silicon cells in order to improve the radiation resistance of the PV's. During the 60's the efficiency of PV cells was increased to 12% by the introduction of gridded front contacts. This substantial increase in efficiency was further improved during the 1970's and 80's which saw cells improved to their current level of 15% AM0 [Ralph, 1989]. Although efficiencies of 18.1% have been measured in the laboratory with simulated AM0 conditions, it is predicted that an efficiency of 22% can be obtained with the use of techniques such as light trapping and surface passivation [Ralph, 1989]. The efficiency has increased over the years as has the resistance of the cells to radiation damage.

Although Silicon has been the primary material used for the construction of photovoltaic cells in America's space program (due to the experience with the material, ease of manufacturing, and low cost of materials), several other

materials are now under consideration. The use of GaAs as Photovoltaic cell material also has certain inherent advantages. By using GaAs typical efficiencies for single junction cells of ~19% are currently being seen. The maximum calculated efficiency for GaAs cells is 27.5%. By going to dual junction cells of GaAs on Ge substrate, efficiencies of up to 22% have been obtained in the laboratory [Ralph, 1989]. For these cascade cells a maximum calculated efficiency of 35.7% is predicted [Landis et al., 1989]. While Gallium Arsinide cells have been used for many years in terrestrial applications, production for the space program has only recently begun. The primary disadvantage of these cells is their high cost.

Another emerging technology in the area of space photovoltaics is the use of ultrathin films. Although there are several materials being researched, the primary candidates are amorphous silicon (α-Si) and copper indium diselenide ($CuInSe_2$). Thin film cells have several inherent advantages in that they have a high radiation tolerance, high specific power, can be formed into flexible blankets, and have a large manufacturing experience. However, thin films are handicapped by lower efficiencies, lack of spacecraft experience, and the fact that they are not currently produced on lightweight substrates [Landis et al., 1989]. Although the spacecraft experience and light weight substraits are easily overcome by the increase in experience with the cells, the maximum efficiency is limited by the physical properties of the materials. Laboratory efficiencies of 10% are now being produced for α-Si cells; however, by using multiple junction designs this could increase to greater than 15% in the future. Projected power-to-weight ratios for 10% cells should reach 350 W_e/kg AM0 in earth orbit [Ralph, 1989].

The experience and information relating to silicon PV solar cells is quite extensive. However, while photovoltaic solar cells have been shown to be

extremely useful on orbital spacecraft, their effectiveness is directly dependent on the availability and intensity of the solar insolation. The solar insolation in turn is a function of the inverse squared distance the cell is from the sun. As one travels further from the sun the available insolation decreases. Since the orbit of Mars places it ~1.5 times further from the sun than the earth is, the average solar insolation is only 590 W/m^2 compared to the 1371 W/m^2 for an earth orbit [Appelbaum and Flood, 1989]. If this value is used with a projected efficiency of 30 %, the rover's 30 kW_e user power alone would require ~340 m^2 of panels. Although this area is already prohibitive it does not take into consideration the decrease in insolation due to atmospheric effects, nor include the energy losses due to storage for night consumption, and the power required by the rover for mobility.

1.2.1.2 Radioisotope Thermoelectric Generators (RTG's)

Radioisotope thermoelectric generators (RTG's) are another possibility for an auxiliary power system for the manned rover. RTG's are extremely reliable long term static power supplies which operate on the thermoelectric energy (TE) conversion principle. Thermal energy is produced internally by the natural decay of Plutonium-238 ($t_{1/2}$=87.7 yr) and is carried across an array of TE couples and rejected by radiative heat transfer through external fins [Kelly, 1987]. The temperature difference between the heat source and the fins is the driving force for the TE conversion [Angrist, 1976]. RTG's have been demonstrated to be safe and reliable with millions of hours of flight experience. The first RTG (SNAP 3B) launched in 1961 was used to power the Navy's Transit 4a and 4b navigation satellites. Although this small unit only produced 4W_e beginning of mission (BOM) power, it successfully operated for over six years.

The next generation RTG's were developed under the SNAP program and showed a substantial increase in power and specific power. The SNAP 19 and 27 RTG's were flown on the Viking and Apollo missions and produced a specific power of $\leq$2.2 W_e/kg. The SNAP RTG's employed lead-telluride (Pb-Te) thermoelectric couples for energy conversion [Hartman, 1988]. Pioneer 10 and 11 missions are also each powered by four SNAP 19 RTG's. Pioneer 10 has passed the mean orbit of Pluto and should have sufficient power to transmit data through 1990 (18 years after being launched) [Skrabeck, 1987]. Again, these units operated in excess of the predicted performance. The Multi-Hundred Watt (MHW) RTG was the next step in RTG design. These systems, which were used to supply power to DOD's LES 8 and 9 spacecraft and NASA's Voyager 1 and 2, yielded a specific power of ~4.0 W_e/kg (BOM). The MHW RTG used silicon germanium thermocouples (unicouples) for energy conversion and modular Pu-238 fuel sphere packs for the heat source [Hartman, 1988].

The current generation of RTG uses the modular General Purpose Heat Source (GPHS) and unicouple thermoelectrics. The GPHS-RTG developed under sponsorship of the Department of Energy, has a specific power of 5.3 W_e/kg in ground tests for both NASA's 4.2 year Galileo mission to Jupiter and the joint NASA/ESA 4.7 year Ulysses solar polar mission. The GPHS-RTG has a mass of 55.9 kg [Bennett et al., 1986].

Under current design is the Modular-RTG (MOD-RTG). This next generation RTG has the distinguishing feature of true modularity. By varying the number of modules assembled, power levels ranging from 20-342 W_e can be obtained. The heat source for the MOD-RTG is again the Pu-238 GPHS; however, the TE converters are improved SiGe/GaP multicouples (each multicouple contains 40 thermoelectric legs). MOD-RTG's are predicted to have specific power up to 7.7 W_e/kg [Hartman, 1988].

Although RTG's are extremely reliable, they have some inherent drawbacks. First, the net conversion efficiency of a static thermoelectric converter system is in the range of 4-8%. This implies that for the 30 kW_e specified user net power of the rover, a total of 500 kW_t would be needed (assuming an optimistic 6% efficiency), requiring ~882 kg Pu-238. In addition to being in short supply at present, the use of Pu-238 in a rover RTG power supply is highly unlikely due to economical and safety considerations.

Another RTG drawback is that heat must be rejected during the journey to Mars, because the energy produced by the radioactive decay of the Pu-238 is continuous. Also, the power level is always decreasing (~1.3% per year electrical power loss due to fuel decay) [Kelly, 1987]. For these reasons and the low specific power, RTGs are not a viable alternative for the rover's auxiliary power source.

1.2.1.3 Dynamic Radioisotope Power System

Another system that utilizes the GPHS isotope heat sources is the Dynamic Radioisotope Power System (DIPS). This type of system can be designed to produce power in the 1 to 15 kW_e range with potential growth up to 20 kW_e. Currently the DIPS program is being conducted under joint DOE/DOD sponsorship [Bennett, 1988]. In DIPS the radioisotope heat source is coupled to a dynamic energy conversion system which provides a higher conversion efficiency than TE's. Three thermodynamic cycles have been studied for use with DIPS; Closed Brayton Cycle, Organic Rankine Cycle (ORC), and stirling cycle. Schematic diagrams for the CBC and ORC are shown in Figures 1 and 2 [Bennett, 1988], respectively. Although system efficiencies up to 5 times that obtained using RTGs are possible, currently projected specific mass, ~150

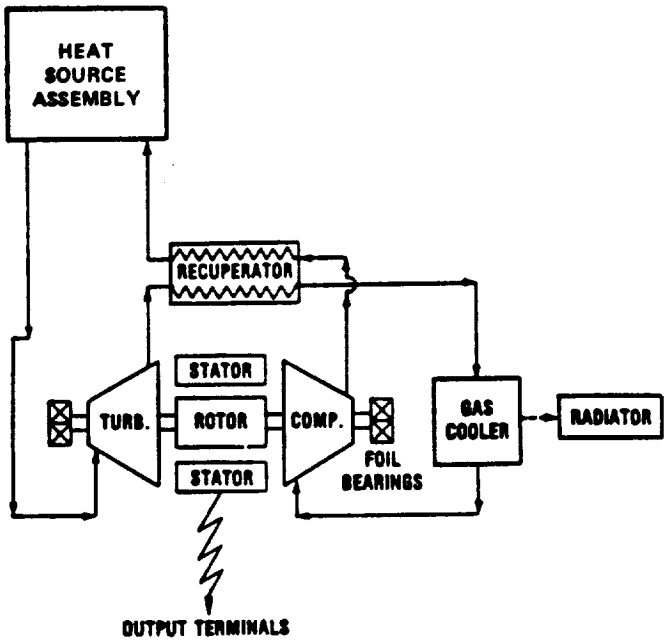

Figure 1. Schematic of Closed Brayton Cycle for DIPS [Bennett, 1988].

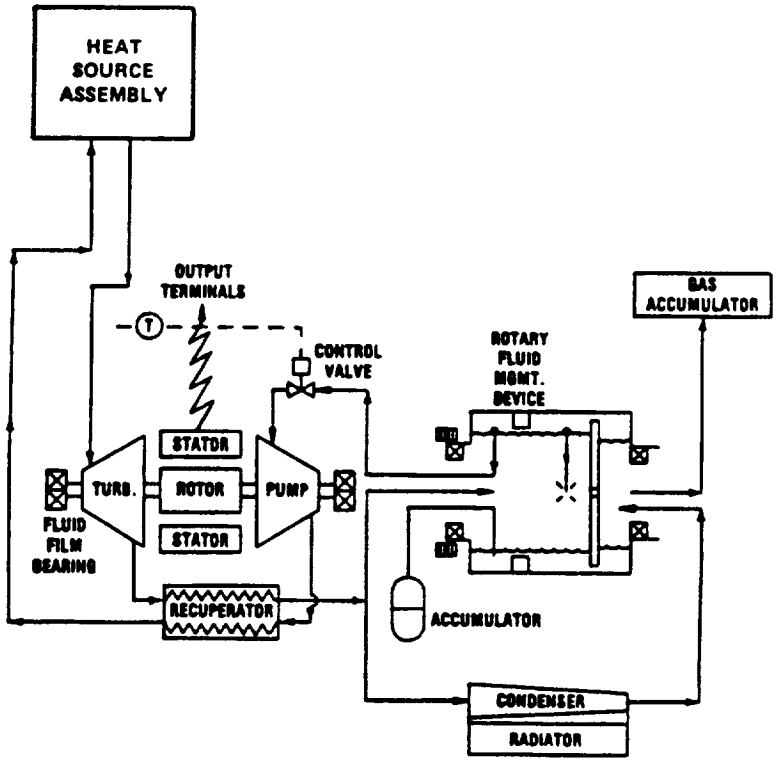

Figure 2. Schematic of Organic Rankine Cycle for DIPS [Bennett, 1988].

kg/kW_e (6.6 W_e/kg), [Angelo and Buden, 1985; Pearson, 1988] of DIPS may limit their usefulness in a large, high power Mars rover. Also, DIPS must still contend with the same power degradation and heat rejection during transit issues as RTGs.

1.2.1.4 High Performance Fuel Cells

High performance fuel cells such as Hydrogen-Oxygen primary fuel cells are a very efficient way to store energy. The major drawback with these systems is that they are an energy storage device rather than a production system. Thus, as the mission length and the total energy storage increases, the mass of the reactant storage becomes prohibitively large. Although Hydrogen/Oxygen fuel cells are not an acceptable primary energy source for the rover, they will be considered as a part of an auxiliary backup system in case of primary power system failure.

1.2.2 Nuclear Reactor Power Systems for Primary Power

Nuclear reactor power systems exhibit many highly desirable characteristics as a primary power source for a manned Mars rover. First, the reactor core will produce virtually no heat until it has been brought up to power after safely landing on the surface of Mars. Second, the power output of the system can be controlled and adjusted to the level needed. Unlike PV systems, the power and size is not dependent on the distance from the sun and the rotation of the planet. Current efforts in the area of space reactors are focused on the NASA/DOD/DOE SP-100 Program. This program is currently following a development plan that will provide the technical data base and the verified analytical design codes needed to design, fabricate and qualify space reactor power systems to meet future mission requirements.

The SP-100 nominal reactor is a fast spectrum lithium cooled reactor power system being developed under a joint DOE/DOD/NASA agreement. The goal of the SP-100 program is to develop a space nuclear reactor power system in the 100 - 1000 kWe range (GE 1988). The reactor core is coupled to 12 primary coolant loops, referred to as the primary heat transfer system (PHTS), each equipped with a thermoelectric-electromagnetic (TEM) pump for circulating the Lithium coolant. The heat is transported from the reactor core by liquid lithium to the thermoelectric (TE) power conversion assemblies (PCA) where it is partially converted to electricity. The residual the heat is then transported by circulating lithium in the secondary loops to the heat pipe radiator where it is rejected into space. Each integrated power module (IPM) consists of a primary coolant loop and a secondary coolant loop having its own radiator panel, TEM pump, and PCA. Both loops are thermally coupled in the TEM pump and the PCA. To accommodate the change in lithium volume during operation and initial thaw upon deployment in orbit, each primary and secondary loop is equipped with a void accumulator/gas separator and a bellows type accumulator, respectively. The separator function of the accumulator in the primary loop is to remove helium gas produced in the reactor core by neutron-lithium reaction.

The nominal thermal power of the reactor is approximately 2.4 MW_t and the system electric output is 110 kWe resulting in an overall conversion efficiency of ~4.5%. The SP-100 system is equipped with a W-LiH shadow shield that provides for a neutron fluence of 1013 and a gamma dose of 0.5 Mrad for a 7-year operation time. The SP-100 fuel elements are highly enriched uranium/nitride with a Nb-.99%Zr-.01%C (PWC-11) cladding. The coolant is liquid lithium, while the structure of the reactor is composed primarily of PWC-11. The core has an active height of 34-cm with a radius of 17-cm.

The control system for the SP-100 consists of BeO reflector shutter panels. When the shutters are opened more neutrons escape reducing k_{eff} of the core. In this work the beryllium reflector shutter panels are replaced by rotating BeO/B4C control drums (see Figure 3). This is done because, unlike the SP-100 reference mission, which employs a shadow shield that is not man-rated, the reactor for the vehicle will require (as a minimum) an oriented 4-π shield to insure adequate protection for the crew. Such a shield configuration limits the usefulness of a shutter control system. The current design of the SP-100 yields a specific mass of approximately 40 kg/kW_e ($25W_e/kg$). This design includes a shadow shield with a cone half angle of 17°. This will significantly increase the specific mass of the system. Even with the shield requirements the reactor system is felt to be the best alternative to give the rover sufficient power for global access.

However, application of the SP-100 reactor power system to a manned Mars rover will require the resolution of a variety of technical issues in order to efficiently and effectively integrate the system into the rover vehicle. These issues include minimization of shield mass and optimization of shield configuration, optimal integration of the heat rejection system with the rover configuration, thermal management, protection from the harsh Martian environment, and contingency systems. The objective of thesis is to answer the questions that arise from these issues. While Chapters 2 and 3 focuses on the rover design and assessment of power requirements for traversing, Chapters 4, 5, and 6 will report the results of parametric analysis to: (a) identify the suitable conversion system/heat rejection combination, (b) the radiation shielding design and integration of nuclear reactor with the rover, and (c) mass optimization of the rover.

1.2.3 Objectives

This research investigates the utilization of an SP-100 reactor power system to fulfil the primary power requirements for a manned Mars rover. The integration of a nuclear reactor power system into a manned Mars rover (see Figure 1) will require the resolution of a variety of technical issues. These issues include minimization of the man-rated shield mass and optimization of shield configuration, integration of the heat rejection radiator with the rover configuration, protection of the crew from nuclear radiation while having the flexibility to sample the Martian surface, and selection of an auxiliary power system for an emergency return scenario. In an attempt to address some of these issues the research focuses on assessing the auxiliary and traversing power requirements for the rover vehicle. A parametric analysis is performed to: (a) determine the sensitivity of the total mass of the rover vehicle to the number of astronauts on board, the desired cruising speed and the scenario for an emergency return in case the primary power system fails; (b) identify the type of energy conversion system for minimizing the mass of the nuclear power system, including the man rated shield; and (c) optimize the configuration and composition of the man-rated radiation shield to reduce the radiation dose to the crew.

2. ROVER LAYOUT AND DESIGN

2.1 Design Considerations for a Manned Rover

The integration of a nuclear reactor power system with a manned Mars rover requires a detailed description of the design and functional requirements of the rover. These requirements included:

1) a 7-year lifetime with intermittent operations,
2) unlimited range,
3) life support for 4 astronauts,
4) an SP-100 type reactor coupled to a static or dynamic conversion systems,
5) a net user power of 30 kW_e, and
6) materials consistent with 7 year life in Martian environment.

It should be noted that the SP-100 reactor containment and piping are fabricated from Nb-1Zr, such material is not compatible with the CO_2 Martian environment. Therefore, this issue will have to be addressed through the use of a special protective coating or other suitable means to protect the structure from being attacked by CO_2. The material compatibility however is outside the scope of this study, hence it will not be addressed further.These requirements form the starting point for a more detailed description of the rover in order to determine the mobility power requirements, and hence, determine the electric power output of the nuclear reactor system.

Currently, there is little information on the design of a multi-purpose global access rover for Mars; however, extensive investigations on moon based rovers

have been completed [16,17]. Since many of the design parameters for a lunar rover are similar to those of a Martian vehicle many parallels may be drawn.

The first step in understanding the characteristics of the rover vehicle is to define the design capabilities and requirements of the rover. However, the Martian scenario exhibits several unique qualities. Three major considerations for the Martian rover are: (1) The extreme distance from the Earth demands the lowest specific mass in order to minimize the launch and transportation cost; (2) The rover power system should contain the highest degree of reliability and redundancy with capabilities for an adequate auxiliary power system in case of a complete malfunction of the primary power system, (3) The rover must be compatible with a Martian atmosphere composed primarily of CO_2.

2.2 **Rover Configuration**

There is a wide variety of possible configurations for a planetary surface rover, and many parameters which can affect their mobility power requirements. The soil/vehicle interaction is the most critical power variable and is a function of traction type. Different traction types including wheels, tracks, and walkers have been studied. In the area of wheels alone there are several options available including rigid, pneumatic tires, wire mesh tires, elliptical wheels, hemispherical (and cone) wheels, and hub-less wheels [Bekker, 1969].

Typical rover configurations could vary from a large single vehicle to an articulated crank mounted wheeled vehicle, to a multi-car overland train [Cataldo, 1989]. In order to minimize radiation shield mass radiation sensitive equipment and the crew must be located a sufficient distance from the reactor. This important requirement is most easily met with the multi-car overland train rover option, which allows the crew and radiation sensitive equipment to be

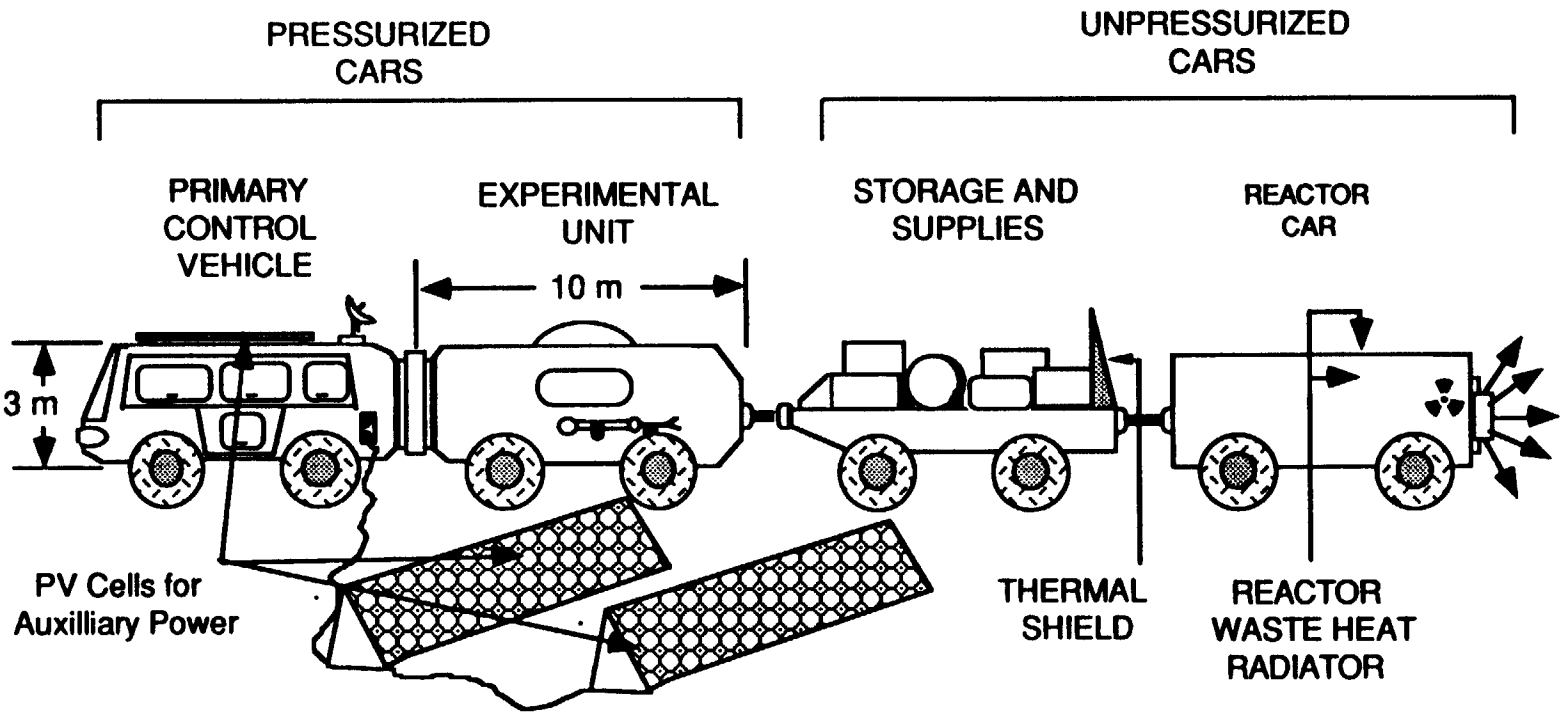

FIGURE 3: Layout for Train-Type Manned Mars Rover

located in the forward cars, while the reactor and radiation insensitive equipment and supplies are located at the rear of the train. The proposed configuration for the manned Mars rover is shown in Figure 3. It consists of four units: the Primary Control Vehicle (PCV), the Experimental Unit (EU), the Supply Car (SC), and the Reactor Car (RC). The function and the component mass breakdown for each of the units are discussed separately in the following sections.

2.3 **Primary Control Vehicle and Auxiliary Power System**

The Primary Control Vehicle (PCV) is a double wall, pressurized, climate controlled car. The PCV houses the driving, navigation, and general control systems for the rover vehicle. The basic car design accommodates four astronauts. The PCV also includes the sleeping quarters, galley, a work station, life support systems and an auxiliary power system. The basic exterior dimensions of the vehicle are 3x3x10 meters, which provides an interior volume of approximately 80 m^3. A generalized configuration for the PCV is shown in Figure 4.

2.3.1 Auxiliary System Layout

In the case of primary power system (PPS) failure the immediate concern is the survival of the rover crew. Due to the extreme distance from the earth it is essential that the rover be equipped with an emergency power system to maintain life support systems and a degree of rover mobility for several days, in the event of a PPS failure . For this purpose a PV/regenerative fuel cell power system is employed, see Figure 5 (a and b). Figure 5a illustrates the system configuration during solar energy collection. Here the PV's not only supply energy for the PCV, but also to electrolyze H_2O into H_2 and O_2 for the

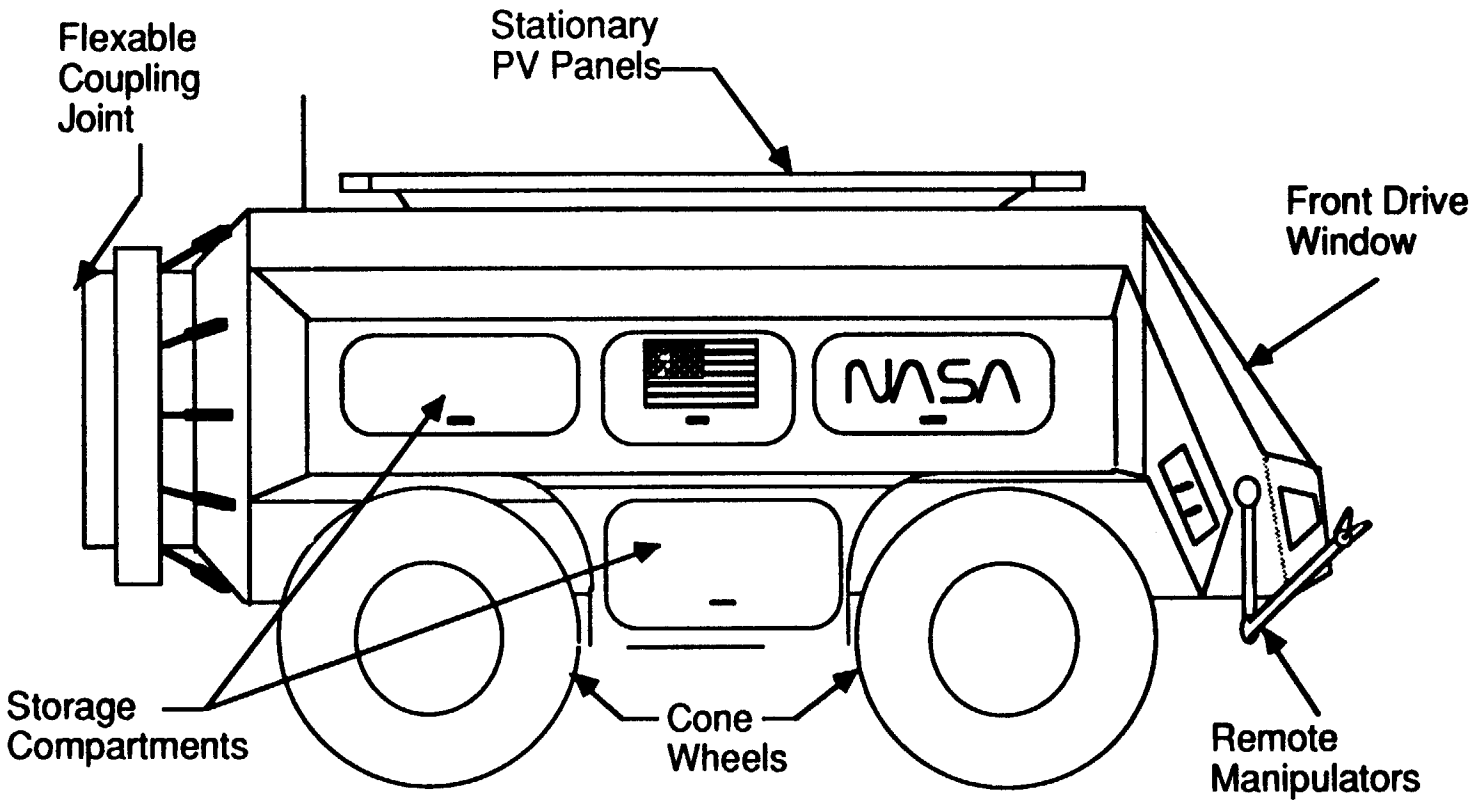

FIGURE 4 : Layout for Primary Control Vehicle

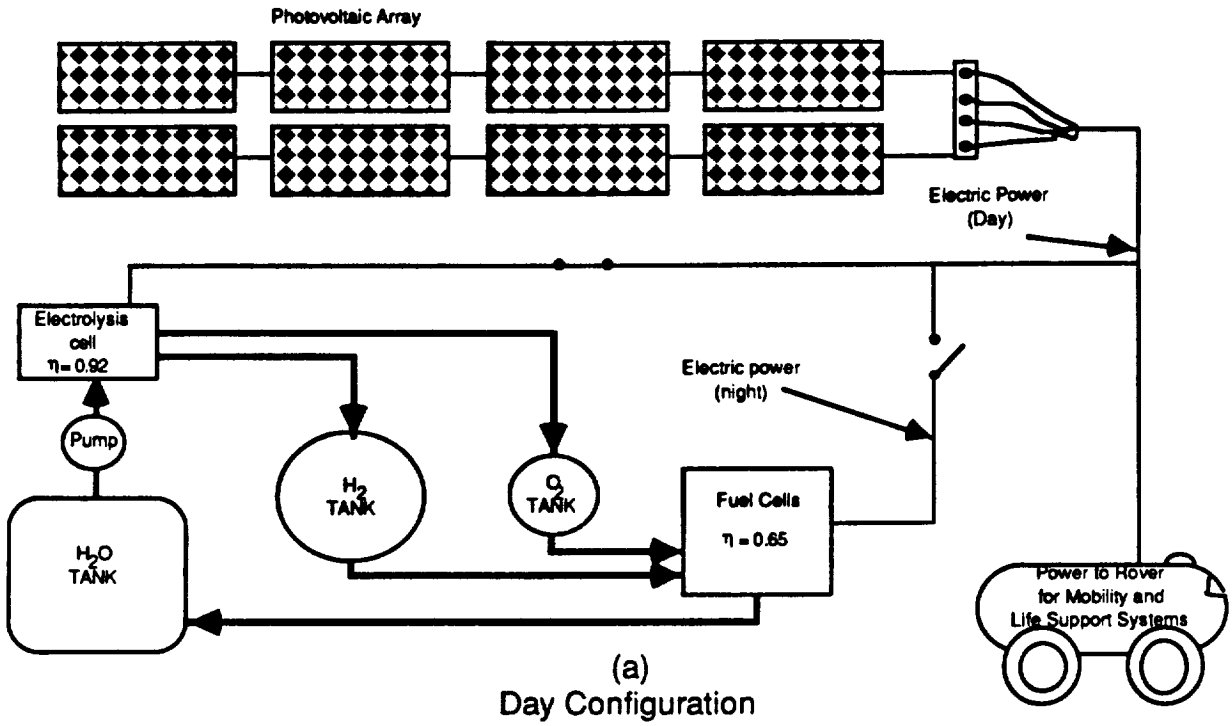

(a)
Day Configuration

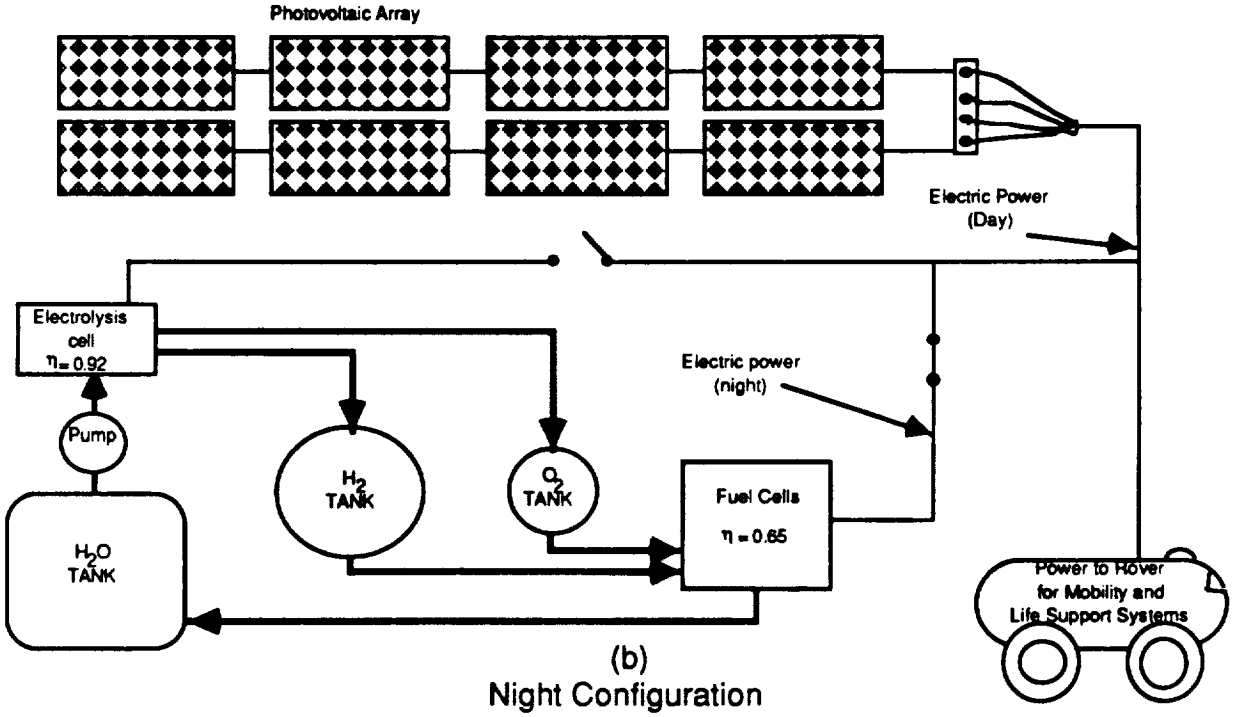

(b)
Night Configuration

Figure 5: Auxiliary Power System Configuration

regenerative fuel cells (RFC's). In Figure 5b the night configuration is shown. Here, no energy is being collected by the PV's and total rover power is supplied by the RFC's.

Since the primary mission concern in the event of a PPS failure is shifted from the experimental objectives to the survival of the crew, all nonessential equipment and supplies are to be jettisoned. The scenario calls for disconnecting the PCV from the rest of the train. The PCV then travels at a reduced speed back to a preestablished base or the mission assent vehicle. The PCV is equipped with up to three days worth of life support power stored in the Hydrogen/Oxygen RFC; the total mass of the fuel cell system including reactant is 720 kg. This Figure is based on a crew of 4 astronauts, a life support power of 1 kW_e/astronaut, and a system specific energy of 400 $W_e \cdot h/kg$ [Eagle Engineering, 1988]. For this storage a total reactant mass of 107 kg is required (12 kg H_2 and 95 kg O_2). For reactant storage tanks pressurized to ~2MPa [Angrist, 1976] a total storage volume of 9.5 m^3 is necessary.

2.3.2 Mass Estimates of Auxiliary PV Panels

In addition to the fuel cells, the auxiliary power system will include a set of Photovoltaic (PV) arrays in order to recharge the fuel cells on a daily basis and provide for both life support and mobility power. The mass of the PV array is a function of the total mass of the PCV (this includes the PV array itself), the driving scenario (daily range and cruising speed), and the efficiency of the RFC cycle.

The PV panels mass can be given in a general form by:

$$M_{pv} = P_{aux} SM_{pv}, \qquad (1)$$

where P_{aux} is the auxiliary power and SM_{pv} is the specific mass (kg/kWe) of the

PV array. The auxiliary power required from the PV's can be divided into power required for life support, P_{ls}, and power required for mobility, P_m. While the life support power is constant for a given number of astronauts, the power requirements for mobility will be dependent on the terrain, emergency cruising speed, daily range, and the total mass of the PCV according to the following equation:

$$P_m = \chi(8.0\text{x}10^{-5}\ \text{kW}\cdot\text{h/km}\cdot\text{kg})M_{tpcv}\cdot V. \qquad (2)$$

The value of $8.0\text{x}10^{-5}$ kW·h/km·kg for the soil traction coefficients is based on the average energy consumption of the Apollo Lunar rovers [Cataldo, 1989]. The traction factor modifier χ is a correction factor to account for the difference in soil conditions and the difference in gravitational acceleration between the Moon and Mars and V is the PCV return velocity in km/h. Although the calculation seems straight forward at first, it is important to note that the PCV mass also includes not only the values shown in Table 1, but also the mass of the PV array.

The mass for the the PV panels, which is a function of several parameter, can be expressed as:

$$M_{pv} = \frac{SM_{pv}}{t_c}\left[n_a\, p_{ls}\left[t_c+(t_d-t_c)/\eta_{fc}\right] + \chi\left(8.0\text{x}10^{-5}\text{kW}\cdot\text{hr/km}\cdot\text{kg}\right)\left(M_{PCV}+M_{pv}\right)V(t_m/\eta_{fc})\right] \qquad (3a)$$

and by rearranging:

$$M_{pv} = \frac{n_a\, p_{ls}\left[t_c+(t_d-t_c)/\eta_{fc}\right] + \chi\left(8.0\text{x}10^{-5}\text{kW}\cdot\text{hr/km}\cdot\text{kg}\right)M_{PCV}\,V(t_m/\eta_{fc})}{\left[t_c/SM_{pv} - \chi\left(8.0\text{x}10^{-5}\text{kW}\cdot\text{hr/km}\cdot\text{kg}\right)V\,(t_m/\eta_{fc})\right]}. \qquad (3b)$$

Table 1. Primary Control Vehicle Mass Breakdown
Based on Four Astronauts
(From EEI Report 88-188)

	Mass (kg)
Structure and Pressure Vessel	
Inner Shell	490
Outer Shell	500
Other Structures	200
Insulation	130
Galley	70[a]
Personal Hygiene	90[a]
Emergency Equipment	30
Man-Locks	230
EMUs	680[a]
Avionics	90
Environment Control and Life Support	200[a]
Workstation	40
Drive Stations	80
Sleep Quarters	500[a]
Experiments and Payload	500
Crew	360[a]
Active Thermal System	
Radiator	160
Pump	20
Heat Exchanger	50
Piping	100
Refrigerant	300
Wheels and Locomotion	300
Fuel Cells	740
Total	5860

[a]Values will vary depending on the number of astronaut

Equation (3b) gives the mass of the PV panels in terms of the collection time, t_c, the mobility time during both the day and night (t_m), the number of astronauts (n_a), the cruising speed (V), the traction factor modifier (χ), and the specific mass of the PV's (SM_{pv}). The total mass of the PCV then becomes the sum of the tabulated masses in Table 1 plus that calculated for the PVs by equation (3b).

Determining the total PCV mass then becomes an issue of accurately estimating the PV parameters and identifying the sensitivity with which each of these parameters affect the PV mass. For the base case scenario the mass of the PCV and the number of astronauts have already been set at 5860 kg (Table 1) and four, respectively. Since the gravitational acceleration on Mars is approximately twice that of the Moon a value of 2.0 is used for χ. This value is comparable to the estimated values for the rolling resistance of the Martian soil of 0.35 and a rover drive efficiency of 50% [AeroVironment, 1989]. Although the value of 2.0 for χ is 15% lower than that suggested by AeroVironment, it is still considered a reasonable value.

The time parameters including PV collection (t_c) and rover mobility (t_m) are dependent on the driving scenario assumed; however, for the base case a collection time of 12.3 h (12.3 h is the number sun light hours at 0 degrees latitude during both the Martian Aphelion and Perihelion) and a mobility time of 6 hours were used. A discussion on the selection of these base case values will be presented later in this report. Although the cruising speed for the emergency return, like the mobility and collection times, will be determined by the specific return scenario, a maximum speed of 5 km/h was assumed. An efficiency of 60% was used for the RFC system [Eagle Engineering, 1988]. The final parameter, the Specific Mass of the PVs, was calculated using an average surface solar insolation, G, on the planet's surface of 250 W/m^2, a PV efficiency,

η_{pv}, of 20%, and a panel surface density, SMA, of 2.3 kg/m^2 as:

$$SM_{pv} = SMA/(G \cdot \eta_{pv}/1000\ W/kW). \quad (4)$$

The base case values for the variable in equations 3b and 4 are listed in Table 2.

Table 2. Base Case Auxiliary Power System Variables

Photovoltaic panel efficiency	η_{pv}	= 20%
Average solar insolation	G	= 250 W/m^2
Specific mass area of PV panels	SMA	= 2.3 kg/m^2
Fuel cell reserve life support energy storage (PCV)	t_{ap}	= 72 h
Fuel cell reserve life support energy storage (EU)	t_{ae}	= 72 h
Fuel cell reserve life support energy storage (SC)	t_{as}	= 24 h
Emergency return speed	auxspd	= 5 km/h
Power required for life support	P_{ls}	= 1kW/astro.
PV collection time	t_c	= 12.3h
Day Mobility	t_{md}	= 0 h
Night Mobility	t_{mn}	= 6 h
Efficiency of the fuel cell cycle	η_{fc}	= 0.6
Specific mass of the fuel cells	SM_{fc}	= 2.5 kg/kw·h

From the Base case parameters, PV panels having a mass of 667 kg are required to power the PCV during the emergency return. This corresponds to a PV panel area of 290 m^2. If the panels were dimensioned such that they were 10 m wide (the same as the length of the PCV), a 29 m length of PV panels would be needed. While this is not felt to be impossible to accomplish, a substantial increase in panel size would limit the auxiliary power system's usefulness to supply power for an emergency return trip, due to the large

storage volume and difficulty in deployment which would be associated with large panels. It is, therefore, important to evaluate the effects of reasonable variation in the base case parameters on the mass and area of the PV array.

In order to minimize the PV mass it is important that the collection time be maximized and the mobility scenario be optimized for minimum power requirement. Therefore, it is assumed that energy collection takes place for 12.3 h, representing all daylight hours, during which the PV panels are deployed and the PCV is not moving. Table 3 list the dark periods (in hours) at several Northern latitudes for both the Aphelion and Perihelion planetary positions [Kaplan, 1988]. Given 24.62 h as the length of a Mars Sidereal day and an equatorial location, the collection time can be determined by:

$$t_c = 12.3 \text{ hr} - t_{md} \qquad (5)$$

When determining the total mass of the PV panels it is important to consider the advantages and disadvantages of choosing a particular emergency return mobility scenario. The operating region for equatorial deployment is shown in Figure 6. The four curves presented in this Figure represent PV mass values for the base case parameters given in Table 2. The effect, upon the PV mass, of varying the collection time (or mobility during the day) and the mobility during the night, t_{mn}, is presented. Starting from the base case of 6 hours of night mobility (@5 km/h this represents a daily travel of 30 km/day) and a 12.3 h collection time (0 h day mobility) a Photovoltaic mass of 667 kg is required. It is recognized that driving during the night can place additional constraints on the rover crew, but it reduces the mass of the PV panels, therefore, the merits of nighttime travel are discussed.

Keeping the travel time constant at 6 h, a PV mass of 1500 kg is needed if traveling is limited to daylight hours. This increase from 667 kg to 1500 kg (more than twice the base case mass) is due to the shortened collection time for the PV panels, compounded by the increased storage and consequent energy

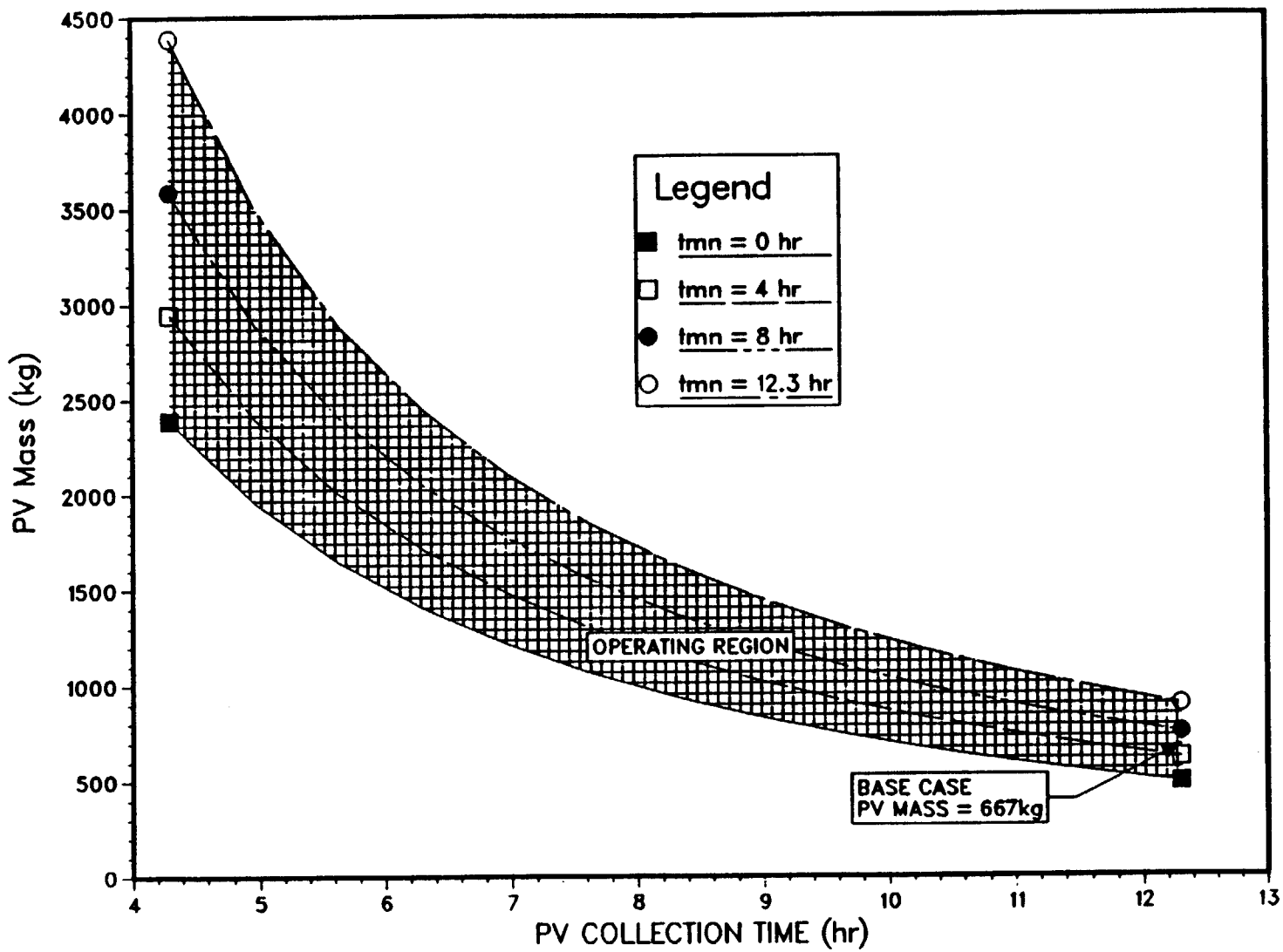

FIGURE 6: Operating Regime for Auxiliary Power System

loss during energy storage and recovery from the fuel cells. In addition to the mass increase, the size of the array becomes prohibitively large. For example, by traveling during the day instead of night, the 290 m^2 surface area is more than doubled to 652 m^2. Therefore, in order to effectively reduce the size and mass of the PV, night travel during an emergency return is required.

Table 3. Martian Seasonal Information

Northern Hemisphere Summer (Aphelion)

Latitude (degrees)	Mean Radius (km)	Ratio (night/day)	Dark Period (hours)
0	3393.0	1.00	12.31
9	3351.2	0.910	11.73
21	3167.6	0.793	10.89
33	2845.6	0.670	9.88
44	2440.7	0.538	8.61
55	1946.1	0.361	6.54
65	1433.9	0.000	0.00

Northern Hemisphere Winter (Perihelion)

Latitude (degrees)	Mean Radius (km)	Ratio (night/day)	Dark Period (hours)
0	3393.0	1.00	12.31
9	3351.2	1.10	12.90
21	3167.6	1.262	13.74
33	2845.6	1.493	14.75
44	2440.7	1.858	16.01
55	1946.1	2.768	18.09
65	1433.9	undefined	24.62

When the collection time is held constant as in the base case, and the night mobility time is increased to 12.3 h (this assumes instantaneous

deployment of the PV's), the PV mass increases to 900 kg. This value is still considerably less than the 1500 kg for only 6 hours of day travel. Had the additional 6.3 h been driven during the day instead, a PV mass of ~2000 kg would be needed, requiring a total PV area of 870 m^2, or 3 times that needed for the base case.

The PV mass optimization surface, in terms of nighttime travel and daytime collection at 0 latitude (or daytime travel = 12.3h-t_c), is shown in Figure 7. It is apparent that the lowest PV mass requirement is that corresponding to 0 hrs of night travel and 12.3 hrs collection time (0 hrs day mobility). This scenario could be used in the case where a rescue mission is launched from a Martian base or orbiting space craft. This PV mass of 490 kg corresponds to the PV panels needed only to maintain life support. By traveling along the night mobility axis to 6 h, the base case in Table 2 is again reached. It is important to note that by increasing the night travel from 0 to 12.3 h, the PV mass is effectively doubled, while increasing the day travel from 0 to 8 h, increases the mass of the PV panels by a factor of 5. For this reason the night driving scenario is preferred.

To illustrate the typical duty cycle that can be used, a log of daily activities is presented in Figure 8 for the base case scenario (see Table 2). This diagram shows the activities performed for a full Martian day, during an emergency return. It is assumed that the RFC's are fully charged (three days life support power) at sunset. One full hour each is devoted to folding and deploying of the PV panels. Although the actual time needed for these activities will depend on the amount of automation, an hour was determined to be more than sufficient for each activity, should the automatic deployment mechanisms fail. The schedule also allows for three meals and eight hours sleep each day. The 6 h driving

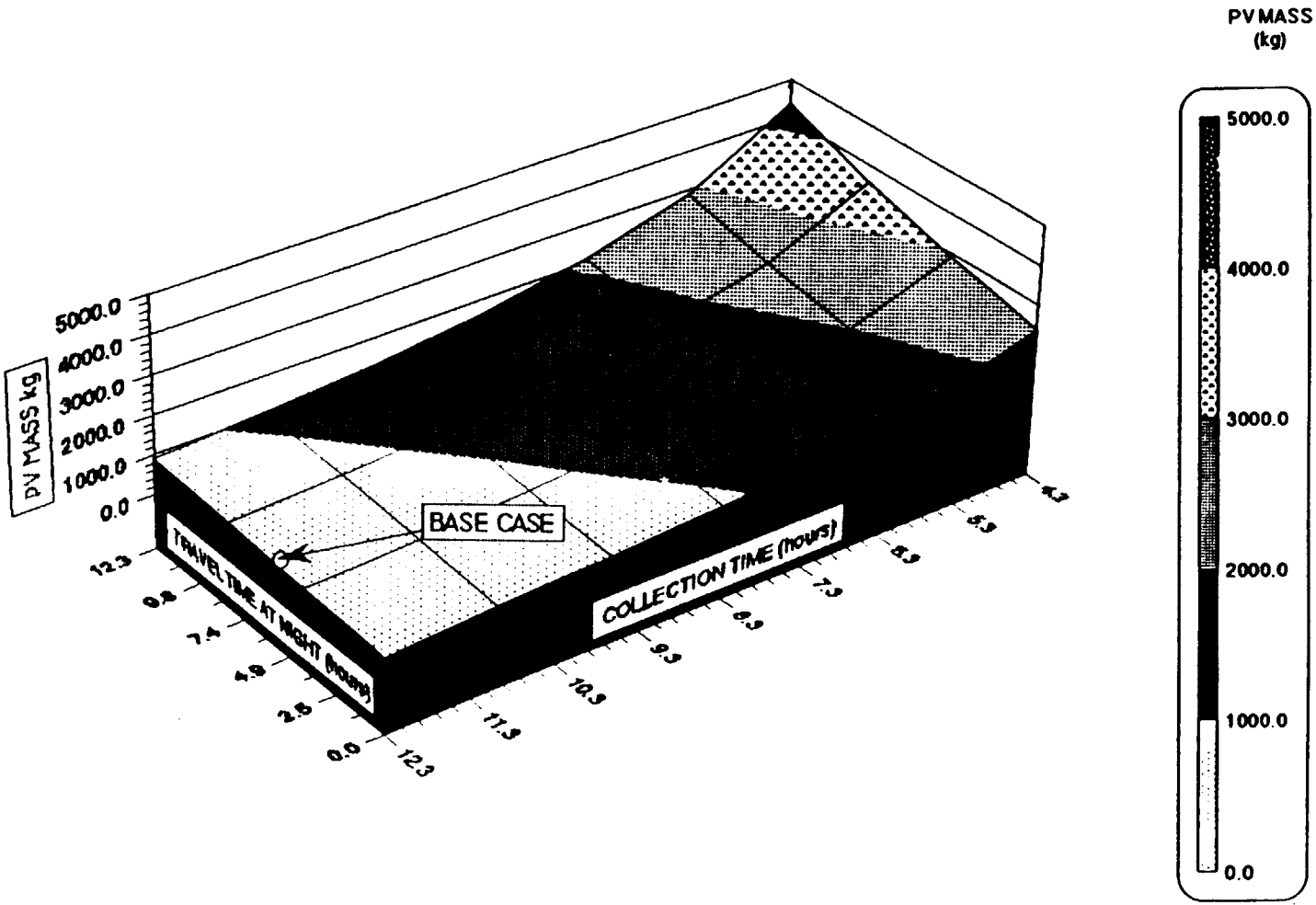

FIGURE 7: Auxiliary Power Systems Operating Surface

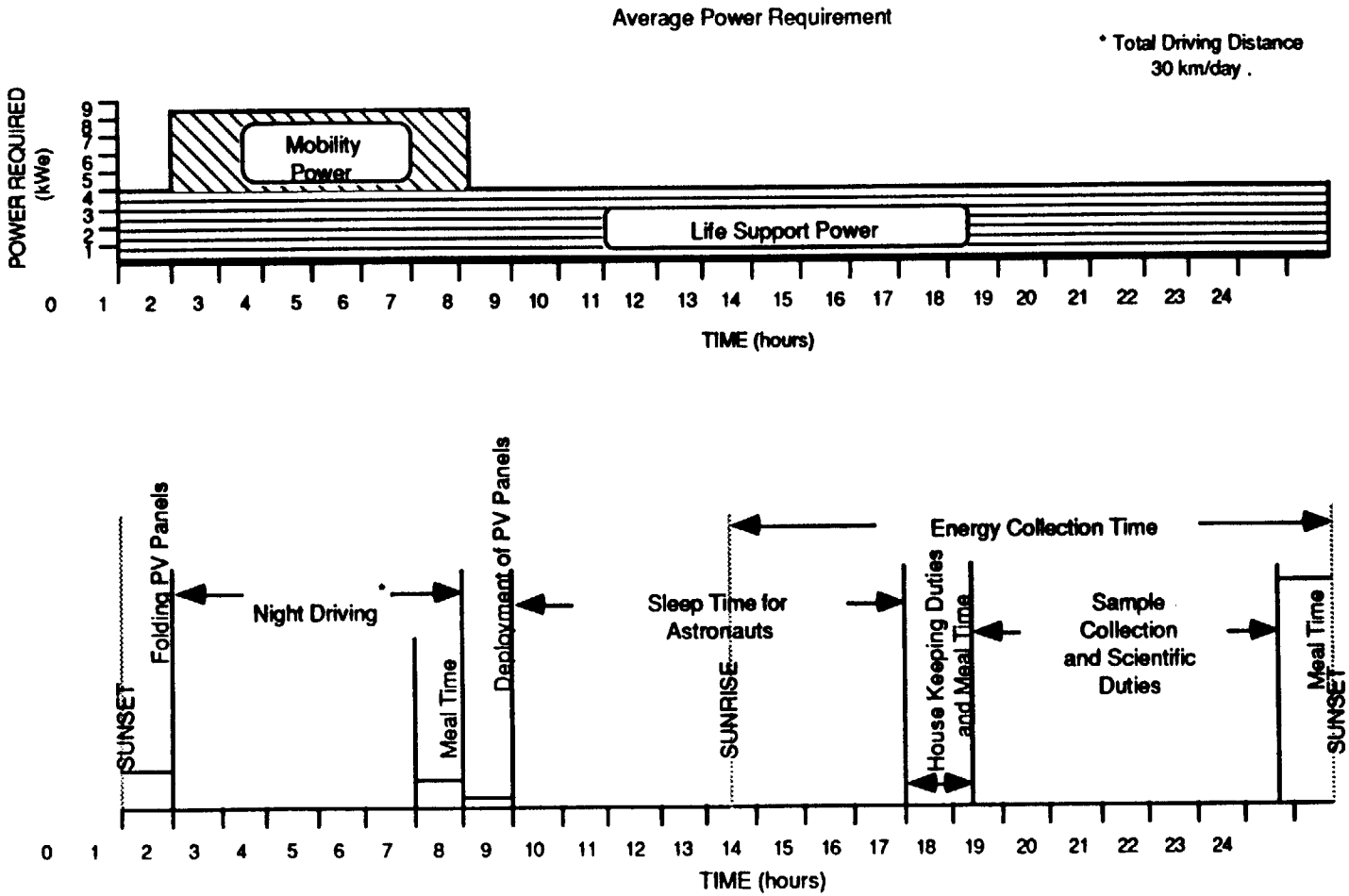

FIGURE 8: Base Case Mission Scenario for Emergency Return @ 5km/hr

scenario allows for a total traveling distance of 30 km/day. It is important to reemphasize that in the scenario delineated in Figure 6, the entire 12.3 h of daylight is used for solar energy collection. The daylight hours during which the crew is awake, are designated for sample collection and scientific duties. The power utilization curve shown above the duty cycle represents the average power requirements based on life support power of 1 kW_e/astro and a maximum cruising speed of 5 km/h. In the case where daily range must be increased, the night driving time can be increased from 6 to 10.3 h. For this scenario the total PV required mass is 820 kg. This 20% increase in mass and area of the PV panels over the base case mass can increase the daily travel distance by 70% (from 30 km/h to 51 km/day). For a 1000 km return trip only 25 days will be required as compared with the 33 days for the base case. A possible duty cycle for the 10.3 h daily driving time is shown in Figure 9. Here the time allocated to scientific duties is decreased from 6 hrs to 2.7 hrs in order to free up time for travel. In Figure 7, the average power utilization of the longer driving time scenario is shown above the duty cycle.

Figure 10 is a plot of PV mass contours as a function of both the collection time and the nighttime travel time. Similar to the surface in Figure 7, this plot allows for all the night/day driving combinations to be examined for given a mass requirement for the PV panels. In Figure 10, the minimum night driving scenario, maximum night driving scenario, and the base case scenario masses are all labeled with their respective locations on the contour. The lowest PVmass of 490 kg, represents the mass of PV panels needed to only supply sufficient energy to run the life support systems.

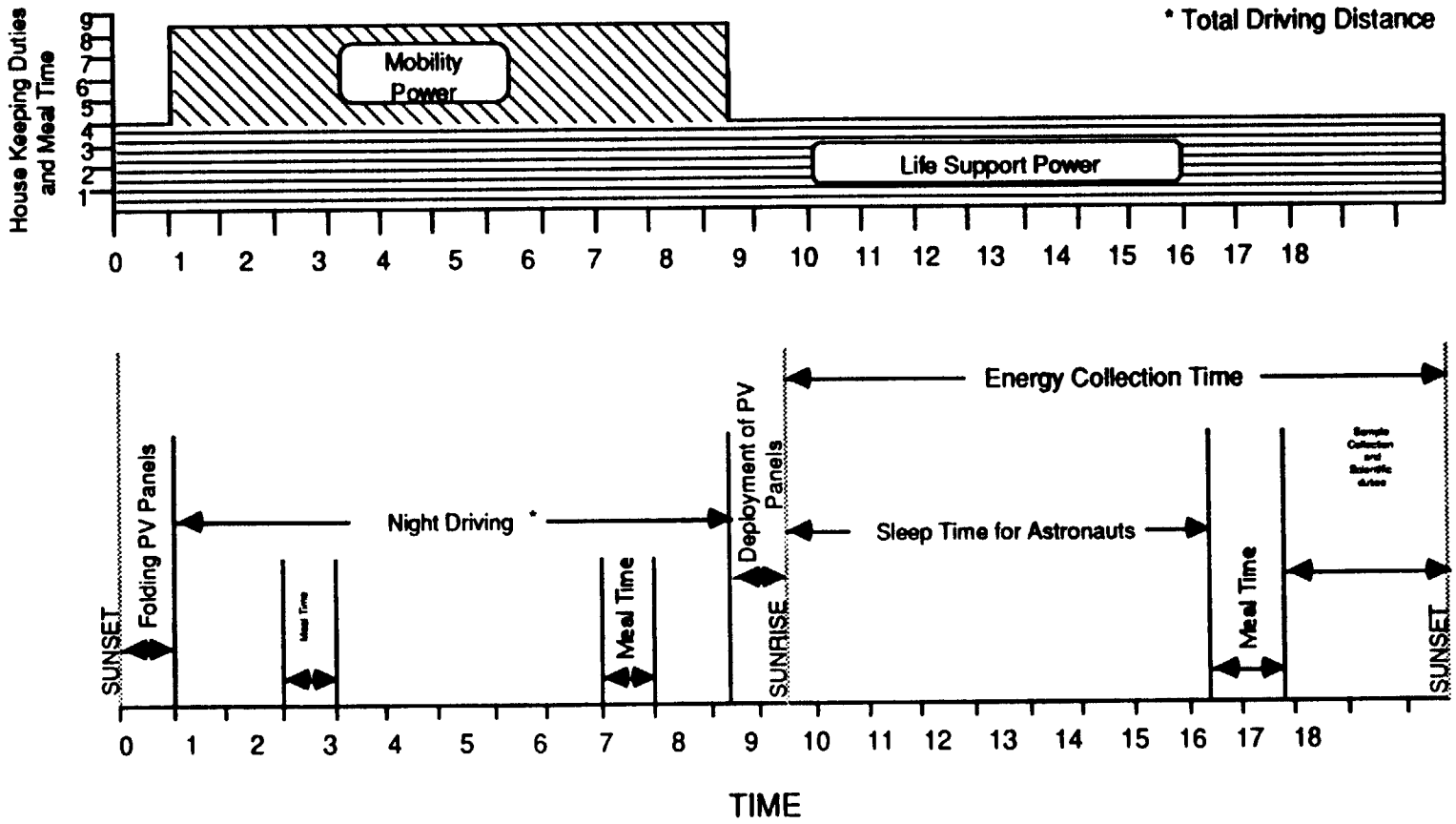

FIGURE 9: Maximum Night Travel Mission Scenario for Emergency Return @ 5km/hr

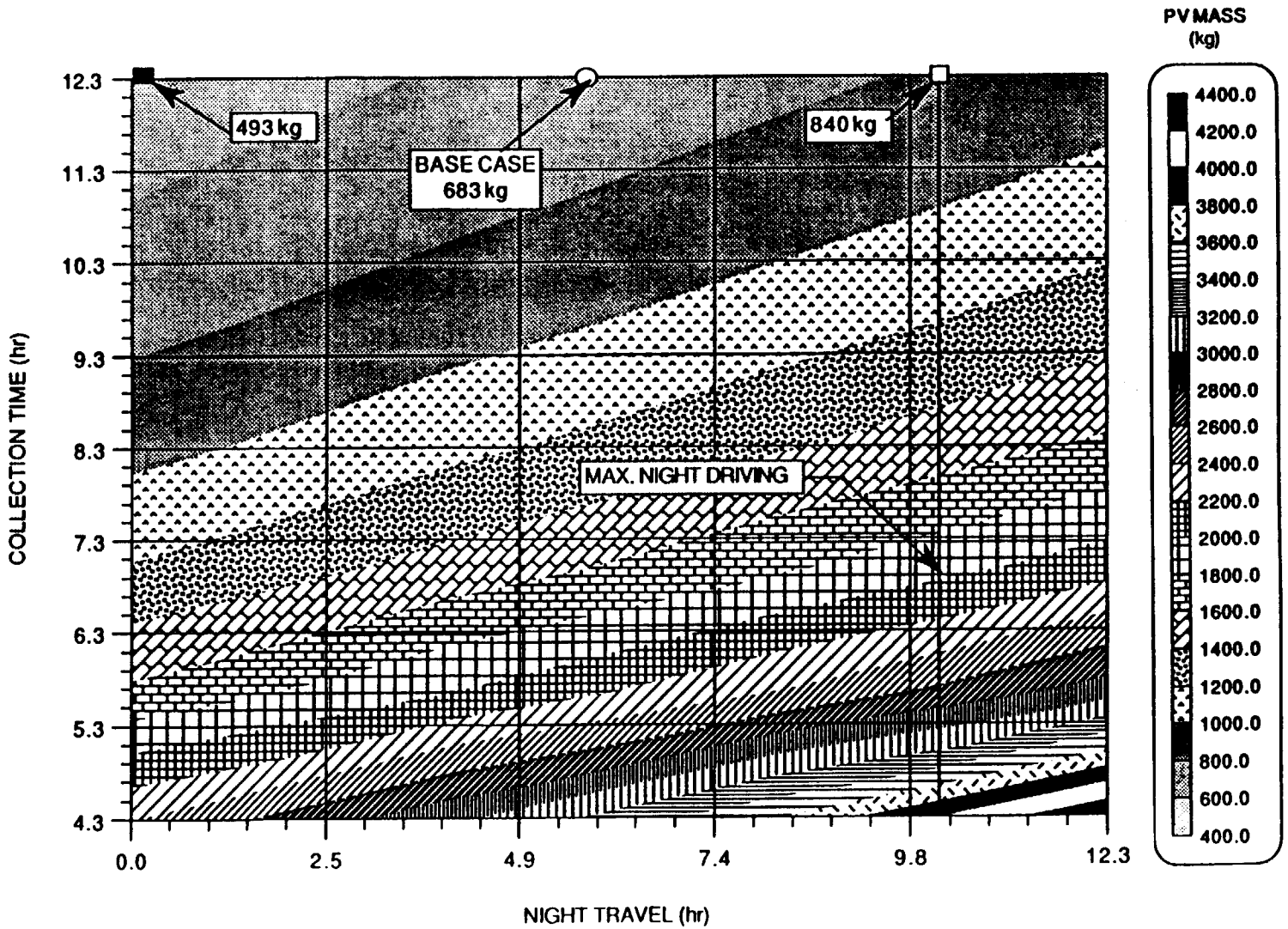

FIGURE 10: PV Mass Contours

2.4 **Parametric Analysis of Design Parameters on PV Mass**

Because of the conceptual nature of the rover design the exact values for the parameters to determine the auxiliary power system mass are unknown. Even though care has been taken to use values judged to be reasonable, given current technology and expected advances, a degree of uncertainty in the results is still introduced. For this reason a parametric analysis was performed to examine the sensitivity of the mass of the auxiliary power system to various operation and design parameters in equation 3b. These parameters include cruising speed, number of astronauts, life support power per astronaut, average PV specific power, efficiency and specific mass of the PV panels, and the amount of fuel cell reactants stored. The results of the parametric analysis are presented and discussed in the following subsections.

2.4.1 Effect of Cruising Speed

The easiest variable to control in equation 3b is the Primary Control Vehicle's cruising speed. While decreasing the cruising speed reduces the mobility power requirements for a given traveling distance, it increases the duration of the return trip. Therefore, the appropriate cruising speed should be selected based on considerations of power requirements and traveling range. In Figure 11, the required mass of the PV panels is plotted against the the PCV cruising speed with life support (kW_e/astro) as a parameter. The points corresponding to 0 km/h cruising speed show the PV mass required to only maintain life support. The effect of cruising speed on PV mass is seen to be a relatively weak function.

2.4.2 Effect of Life Support Power Requirements

As Figure 11 shows, maintaining a constant cruising speed of 5 km/h, and doubling the life support power to 2 kW_e, increases the PV mass from 667 kg to just under 1200 kg. The strong dependence of the PV mass on the life support power is due to two considerations. First, unlike the cruising speed the life support power is continuous throughout the day. Second, for a crew of four astronauts doubling the life support power per astronaut increases the total life support power requirement by a factor of 4. Further increase of the life support power to 3 kW_e/astro will bring the PV mass requirement to nearly 1700 kg for the base case. As demonstrated in Figure 11, an auxiliary power system that is designed for 1 kW_e/astro at a cruising speed of 10 km/h would not be able to deliver sufficient power to maintain the life support at 2 kW_e/astro, even without mobility. These results suggest that great care should be taken to minimize the life support power requirements.

2.4.3 Effect of PV Specific Power

In Figure 12 the PV mass is plotted against the PCV cruising speed for different values of the PV specific power . The specific power values in Figure 12 are simply the average solar insolation (G = 250 W/m^2) multiplied by the efficiency of the array (from 8 to 40%). As Figure 12 shows, lowering the specific power of the PV panels increases the rate at which the PV mass increases with cruising speed. This rate increase is caused by the fact that PV panels with lower specific power require a larger collection area of the PV panels, resulting in a larger mass. In turn, this increased mass requires more power to move. In Figure 12, beginning at the base case, increasing the

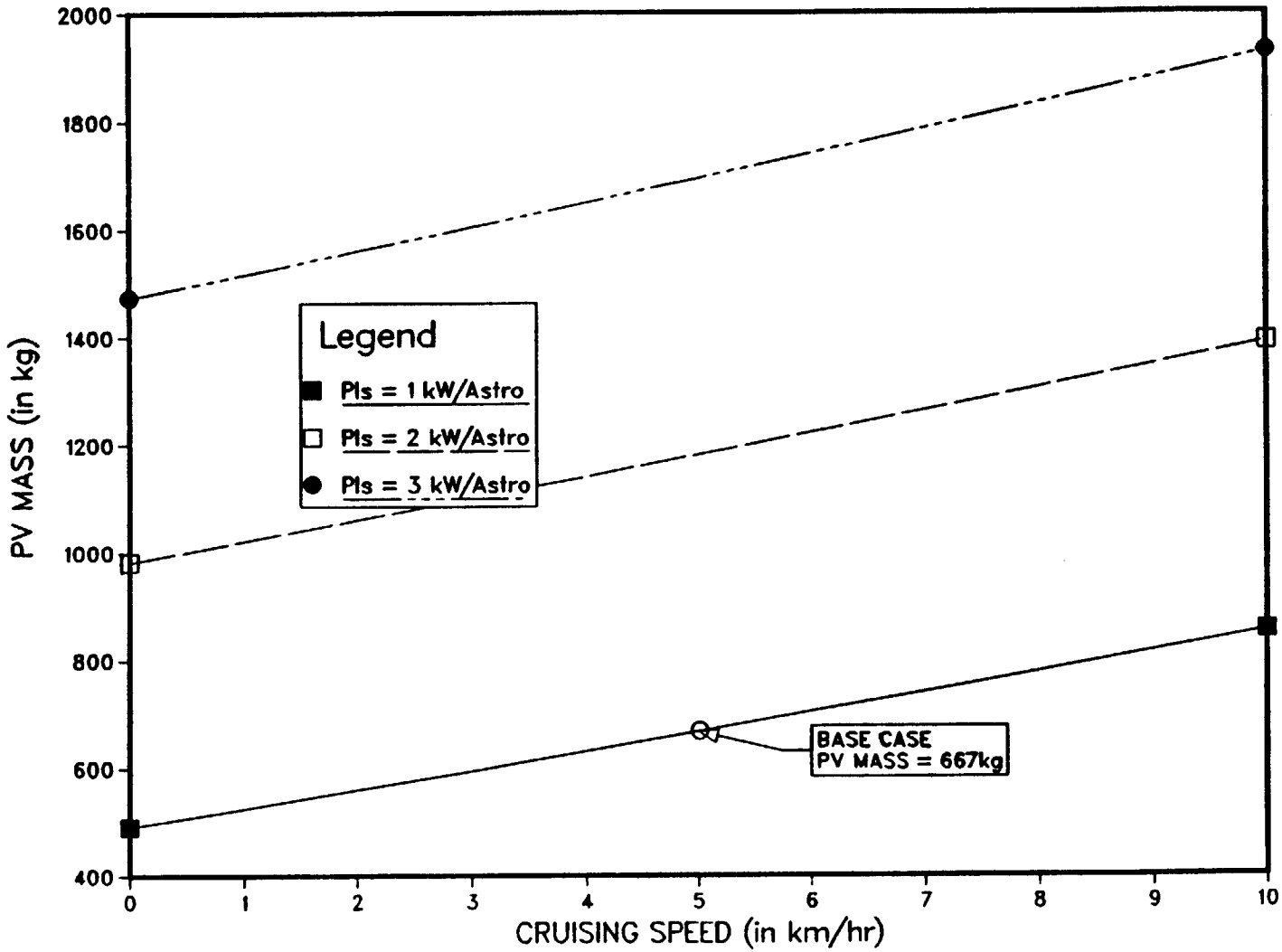

FIGURE 11: Effect of Life Support Power on PV Mass

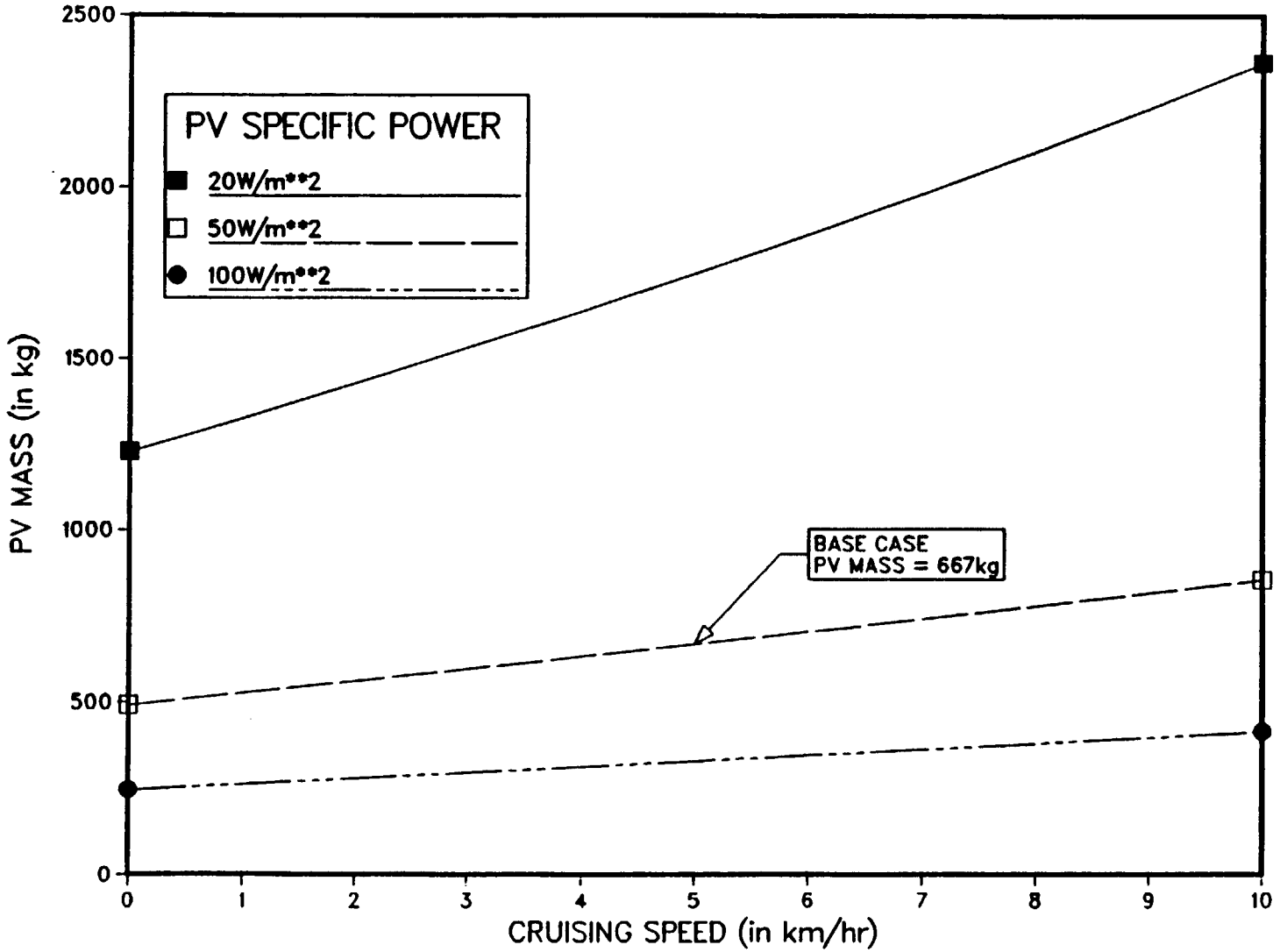

FIGURE 12: Effect of PV Specific Power on PV Mass

specific power to 100 W/m^2 brings the PV mass down to 300 kg. Conversely, decreasing the PV specific power to 20 W/m^2 raises the PV mass to as much as 1750 kg. The sensitivity of the PV mass to its specific power is much greater than that of the cruising speed at high specific power values (>50 W/m^2); however, as the specific power decreases the sensitivity of the PV mass to the cruising speed increases drastically. These results suggest that the savings in the PV mass by lowering the cruising speed becomes less significant as the PV panel becomes more efficient. Therefore, future advances in PV technology should serve to shorten the travel time on Mars for the same PV panel mass. Another factor that could effect the specific power of the PV panels are the frequent dust storms that occur on Mars. These storms can significantly reduce the amount of sunlight received by the PV array (thus effectively reducing G). This reduction in received light can easily reduce the specific power by a factor of 2 for several days. The loss of power from the PV arrays could, however, be compensated for by using the reserve in the fuel cell storage system.

2.4.4 Effect of PV Panel Efficiency

The Specific Power of the PV panel, SP_{pv}, is related to the PV cell efficiency, η_{pv}, as:

$$SP_{pv} = G \cdot \eta_{pv}, \tag{6}$$

where G is the average solar insolation available at the surface of the planet. An expected range of 20 to 30% for cell efficiency is shown in Figure 13. It should be noted that the base case value of 20% was chosen because it represents the projected efficiency for amorphous silicon (a-Si) cells which are light, flexible, and easily stored. If the PV efficiency increases to 25%, the same PV panel mass needed for the base case cruising speed of 5 km/h could power the PCV at a cruising speed over 10 km/h. Moreover, increasing the efficiency

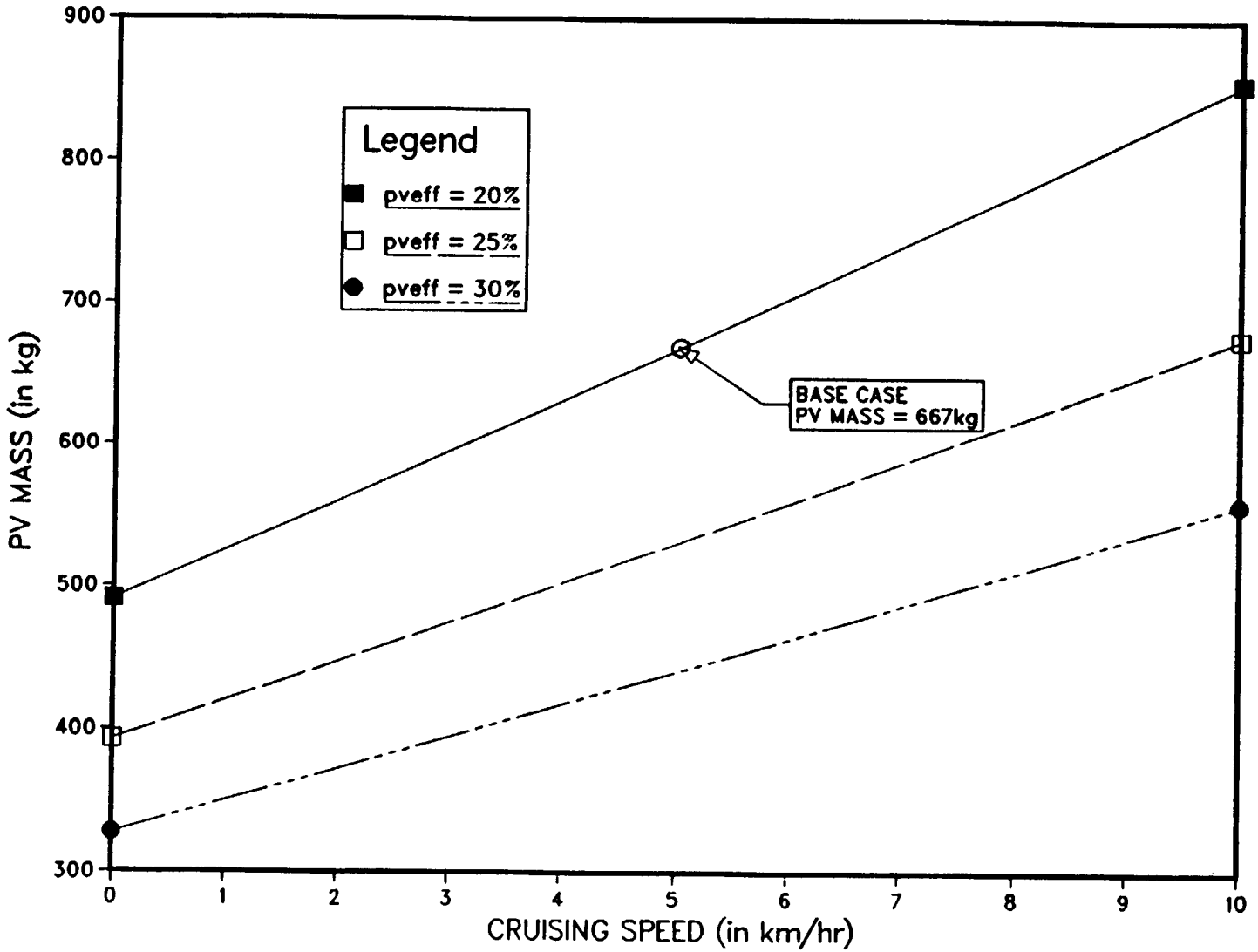

FIGURE 13: Effect of PV Panel Efficiency on PV Mass

to 30% would increase the PV effectiveness to the point where a 10 km/h speed for 6 hours of mobility would require less PV mass than that required for life support alone at 20% efficiency. Therefore, future advances in PV technology are expected to have significant impact on reducing the PV mass.

2.4.5 Effect of PV Surface Density

Another parameter that is completely independent of the efficiency is the PV surface density, or the amount of mass per square meter of PV panels. The value used for this parameter in the base case is 2.3 kg/m^2. This value is based on current silicon cell technology for a sun tracking system, with projected cell efficiency of 20%. With the α-Si cells the specific mass is expected to decline to as low as 1.0 kg/m^2, resulting in a 200% reduction in the mass of the PV panels for the base case. While the mass of the PV cells decreases as the surface density goes down, the total PV area required does not decrease significantly. The PV panel area, however, decreases as the PV cell efficiency increases. Therefore, the trade off is whether to use a larger, less efficient, yet lighter α-Si panels, or smaller, more efficient, but heavier tracking GeAs panels. In either case, the values presented for the base case should be conservative.

Figure 14 demonstrates the effect of a surface density for 1.0, 1.65, and 2.3 kg/m^2. Note that by using a surface density 1.0 kg/m^2, the total PV mass decreases from the base case (SD = 2.3 kg/m^2) 667kg down to as low as 280kg, but the array area only decreases from 290 m^2 to 280 m^2. This is because the mass of the PV panels represents a small fraction of the total PCV mass.

2.4.6 Effects of the Number of Astronauts and Reserve Energy Storage

The final two parameters that affect the mass of the PV system are the number of astronauts on board and the amount of reserve energy storage of the

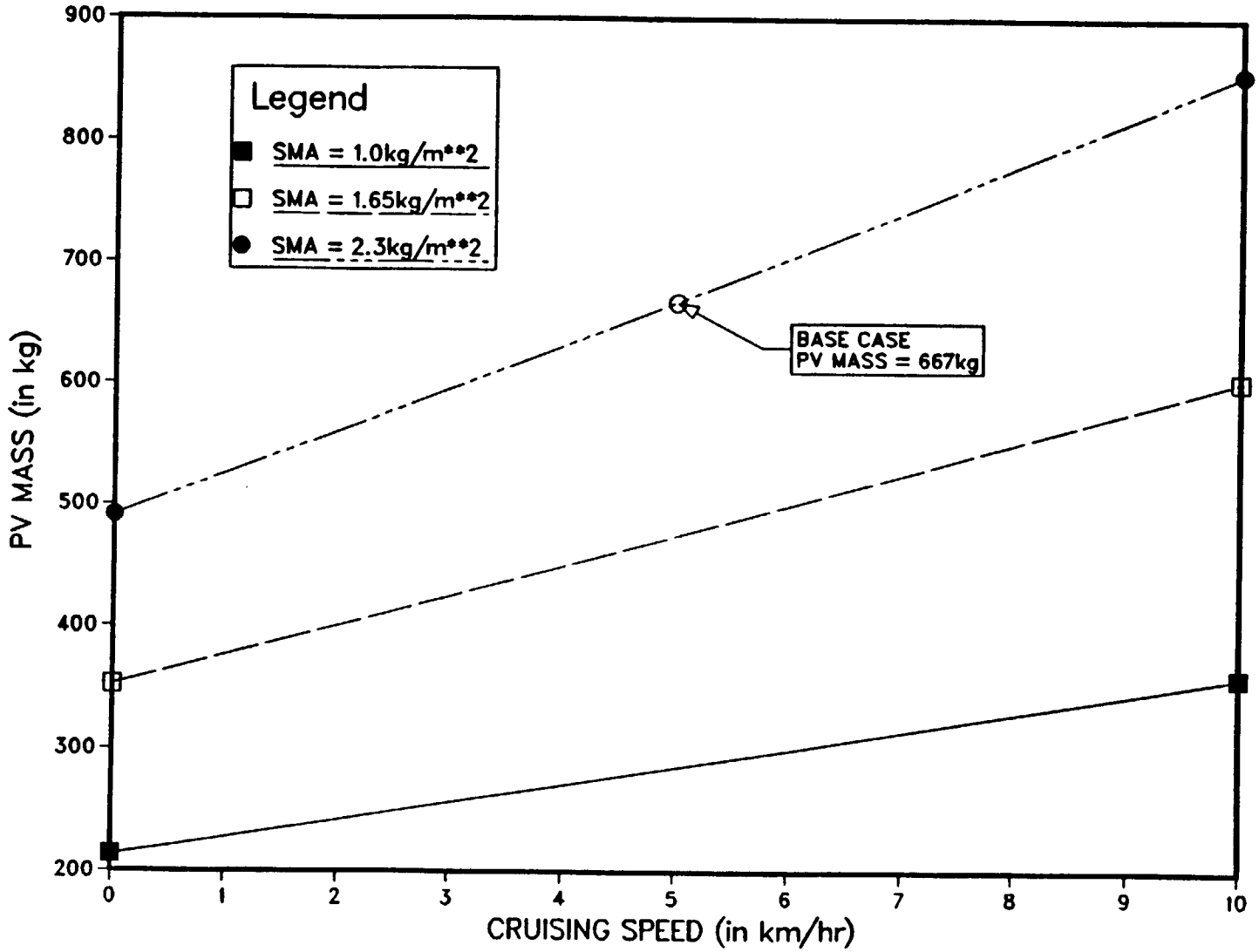

FIGURE 14: Effect of PV Panel Surface Density on PV Mass

regenerative fuel cells. While both affect the PV mass by increasing the PCV mass and mobility power requirements, the number of astronauts has a profound effect on the life support power requirements, which is such a significant portion of the total auxiliary power needs. In Figure 15 the mass of the auxiliary PV panels is plotted versus the PCV cruising speed for 2, 4, and 6 astronauts with the base case life support power of $1kW_e$/astronaut. As Figure 15 shows, the change in slope with the number of astronauts is hardly noticeable, yet the offset between the three curves due to the difference in life support power requirements is significant. These results again emphasize the importance of employing an efficient life support system. As demonstrated in Figure 15, a PV system that provides for four astronauts at a cruising speed of 10 km/h, is sufficient to sustain six astronauts at a reduced speed of ~3 km/h.

Increasing the amount of reactants for the reserve fuel cells does not significantly change the mass of the PV panels, since the increase in the reactant mass only affects the mobility power requirement. Also, because the reactant mass is a small fraction of the total PCV mass, increasing the fuel cell capacity from 24 to 168 h (1 day to 1 week) has only a small affect on the PV panel mass (see Figure 16). Since the fuel cells on board the PCV are regenerative types and the reactants are not stored as cryogenic liquids, but as compressed gases, it is not their weight, but their storage volume that becomes prohibitive. For example, a one day supply of reactants requires a total storage volume of 3.1 m^3 (1.05 m^3 for O_2 and 2.05 m^3 for H_2), while for 72 h, the storage volume will be 9.5 m^3 (3.2 m^3 for O_2 and 6.3 m^3 for H_2). For one week storage, a reactant volume of 22.1 m^3 will be needed (7.4 m^3 for O_2 and 14.7 m^3 for H_2).

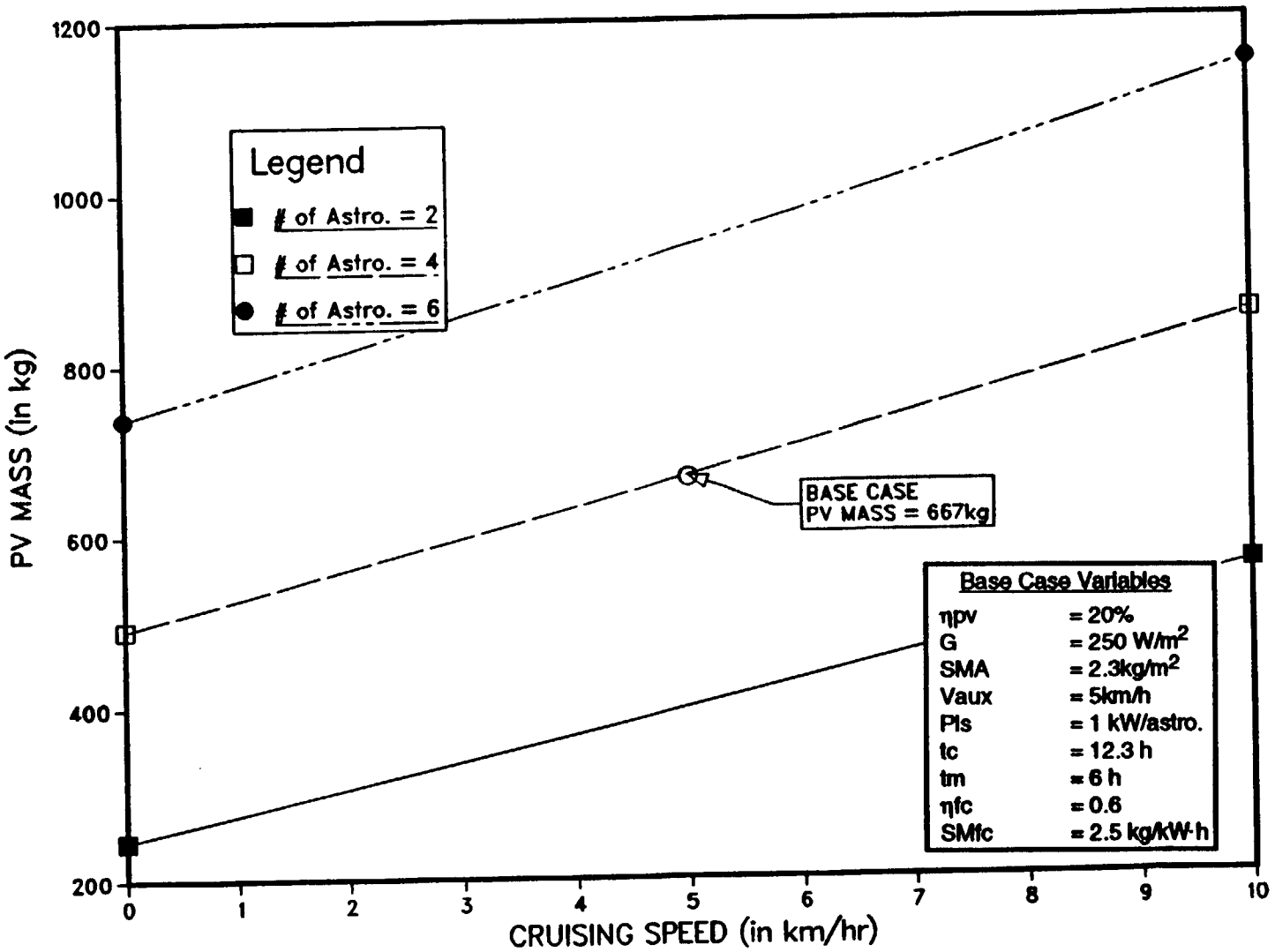

FIGURE 15: Effect of the Number of Astronauts on PV Mass

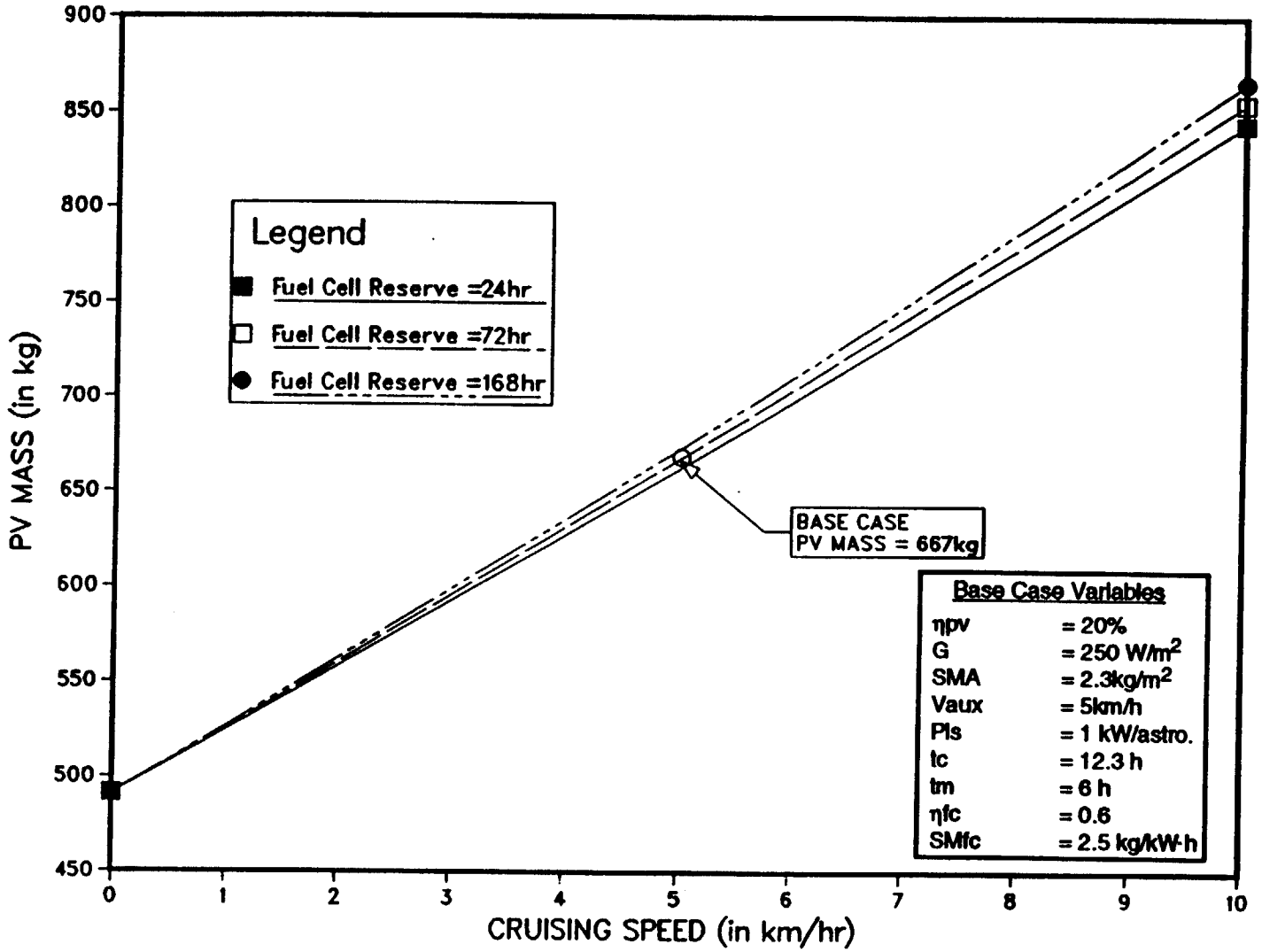

FIGURE 16: Effect of Fuel Cell Reactant Storage Capacity on PV Mass

To summarize the results of the auxiliary PV mass study several points can be made:

(1) The life support power requirements significantly affect the mass and size of the PV panels. For this reason, every effort should be made to design an energy efficient life support system and attempt to reduce astronaut requirements if possible.

(2) In addition to the life support power, the PV panel efficiency and the number of astronauts on board the rover also play a major role in determining the size and mass of the PV panels for the auxiliary power system.

(3) Parameters that affect the mass of the auxiliary PV power system to a lesser extent, but are still important to the overall mass and size determination are the cruising speed of the PCV, and the surface density of the PV cells.

(4) The parameter that has an insignificant effect on the auxiliary power system mass, but strongly impacts the volume of the fuel cells, is the reserve capacity of the RFC's.

(5) In order to minimize the size and mass of the auxiliary power system, traversing should be done at night; the daytime travel should be limited to as short a time as possible.

(6) The PV mass calculated for the base case scenario appears to be reasonable. Therefore, the mass of 667 kg was added to the PCV mass of 5860 kg from Table 1, giving a total PCV mass of 6527 kg.

2.5 **Experimental Unit**

The Experimental Unit (EU) is similar to the Primary Control Vehicle in that it is a double walled pressurized car capable of maintaining a crew of four astronauts in a climate controlled environment (see Figure 3). This car provides

facilities for sample collection and laboratory analysis as well as additional living space for extended missions. The EU also houses the control systems for the primary power system (PPS). The components and equipment pertaining to the EU are listed along with their respective mass estimates in Table 4. Again, these masses are based on the Eagle Engineering Inc. Report on Lunar Surface Transportation Systems, but have been modified to suit the manned Mars rover mission.

Since the EU is not equipped with a PV/RFC auxiliary power system. In the event of a PPS failure, the EU would be detached from the PCV and abandoned. In the event of a minor, short term, potentially repairable malfunction in the PPS, the EU is equipped with three days worth of life support power in the form of primary fuel cell (PFC). The reactants for these cells are stored in liquid form in order to decrease the required volume. These reactants are included to give the rover crew additional time during which they could initiate repairs, before they would be forced to begin an emergency return.

2.6 **Supply and Storage Car**

The Supply and Storage Car (SC) is much simpler than either the PCV or the EU. The SC is an open trailer which carries all the radiation hardened equipment and tools (see Figure 3). At the rear of the car, a thermal shield is installed to protect the contents of the car from the thermal radiation rejected by the waste heat radiator surface mounted on the reactor car. The SC also contains an additional 24 h worth of reactants for the PFC in order to supplement that in the EU. This yields a total of one weeks worth of reserve energy between the PCV, EU, and SC. The mass breakdown for the SC is given in Table 5.

Table 4. Experimental Unit Mass Breakdown
(EEI Report 88-188)

	Mass (kg)
Structure and Pressure Vessel	
Inner Shell	490
Outer Shell	500
Other Structures	200
Insulation	130
Galley	70
Personal Hygiene	90
Emergency Equipment	30
Man-Locks	230
Work Station	40
EMU's	340
Reactor Control Systems	100
Avionics	90
Environment Control and Life Support	200
Showers	80
Experiments and Payload	900
Active Thermal System	
Radiator	160
Pump	20
Heat Exchanger	50
Piping	100
Refrigerant	300
Wheels and Locomotion	300
Fuel Cells (Reactants)	720
Total	5500

Table 5. Storage Car Mass Breakdown (EEI Report 88-188)

	MASS kg
Thermal Shield	200
Wheels and Locomotion	300
Other Structure	500
Experimental Equipment	887
Fuel Cells (Reactants)	240
Additional Supplies and Equip.	1000
Total	3127

2.7 **Reactor Car**

The reactor car houses the reactor systems, energy conversion systems, waste heat rejection equipment, and shielding for the protection of the crew. The mass of the Reactor Car (RC) cannot be determined by simply tabulating the components and summing their masses because mobility power depends upon the mass of the rover (including the RC), and the mass of the reactor system is a function of the total power needed. Therefore, an iterative approach similar to that taken for the PV auxiliary system, is needed to determine the total power required.

A model was developed to determine the total electric power requirements of the PPS as a function of: mass of rover Utility Cars (RUC, including the PCV, EU, SC), cruising speed, number of astronauts, user net power, mobility traction parameter, and the specific mass of the PPS. The total electric power delivered by the reactor system is given by the general form:

$$P_t = PA + \chi(8.0\times10^{-5}\ \text{kW·h/km·kg})M_t \cdot V. \qquad (7)$$

The mass of the reactor power system, which is proportional to its power output, can be given as:

$$M_r = SM_r \cdot P_t. \tag{8a}$$

The reactor power system mass includes the mass of the following subsystems: reactor, primary heat transport, shield, energy conversion, secondary heat transport and power management. In addition, the frame and drive system mass of the Reactor Car were also estimated at 10% of the total load mass. Hence equation (8a) becomes:

$$M_r = 1.1(SM_r \cdot P_t). \tag{8b}$$

The total rover mass (M_t) is the sum of the masses of the individual rover cars:

$$M_t = M_{pcv}+M_{eu}+M_{sc}+1.1(SM_r \cdot P_t). \tag{9}$$

Substituting equation (9) into equation (7) and rearranging results in the following general form for the total power requirement as:

$$P_t = P_a + \frac{\chi(8.0\times10^{-5}\text{kW}\cdot\text{h/km}\cdot\text{kg})[M_{PCV}+M_{EU}+M_{SC}]\cdot V}{1 - \chi(8.8\times10^{-5}\text{kW}\cdot\text{h/km}\cdot\text{kg})\ SM_r \cdot V}. \tag{10}$$

It can be seen from equation (10) that the total power requirement for the manned Mars rover depends on five primary variables: P_a, χ, SM_r, V, and the masses of the Utility Vehicles (M_{pcv}, M_{eu}, M_{sc}). The next chapter presents the results of parametric analysis investigating the effects of each of these variables on the total rover power requirements .

3. PARAMETRIC ANALYSIS OF TOTAL MASS AND POWER REQUIREMENTS FOR MANNED MARS ROVER

In this analysis, the values for the number of astronauts, the cruising speed, the surface traction parameter, power system specific mass, and the utility car mass were varied so that their effects on the total rover mass and the net electric power needed could be evaluated. The parameters for the base case are listed in Table 6.

Table 6. Base Case Rover Variables

Additional Power above mobility requirements	P_a	= 30 kW_e
Mobility traction parameter	χ	= 0.16W·h/km·kg
Drive Efficiency	η_{dr}	= 50%
Specific mass of the Power system	SM_r	= 100 kg/KW_e
Mass of the Primary Control Vehicle (w/o PV's)	M_{pcv}	= 5860 kg
Mass of the Experimental Unit	M_{eu}	= 5400 kg
Mass of the Supply Car	M_{sc}	= 3100 kg
Minimum rover speed	minspd	= 0 km/h
Maximum rover speed	maxspd	= 30 km/h
Number of astronauts	N_a	= 4

3.1 **Effect of Number of Astronauts**

Variation of the number of astronauts has a minimal effect on the total rover mass. Increasing the number of astronauts raises the mass of the PCV in Table 1, and also increases the auxiliary power system mass and mobility power requirements. This mass increase, however, is a small fraction of the total rover mass and does not significantly affect the mobility power. This means the power system mass is relatively insensitive to the number of astronauts. Figure 17 shows that for a cruising speed of 20 km/h, increasing the number of

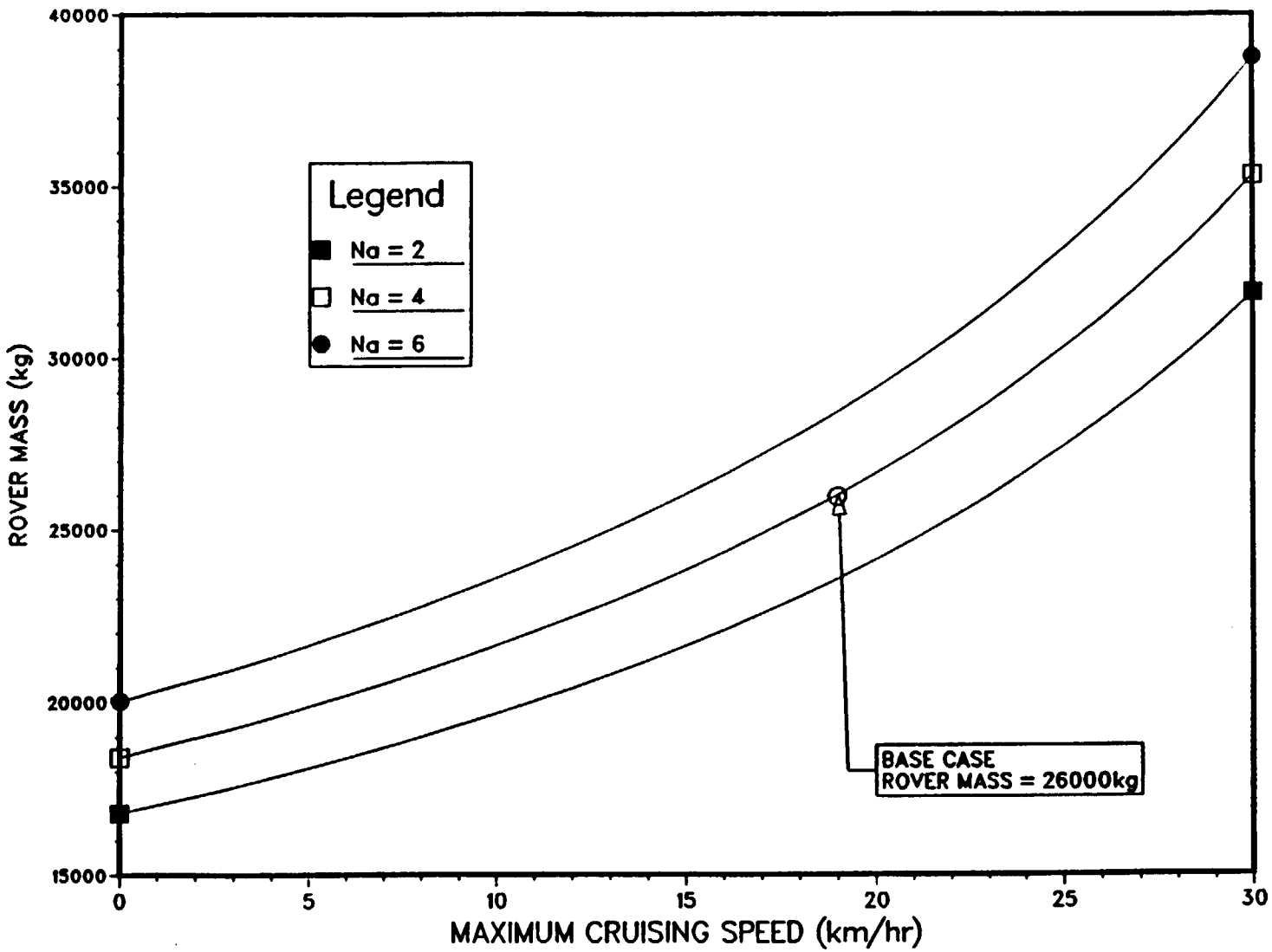

FIGURE 17: Effect of the Number of Astronauts on Total Rover Mass

astronauts from 4 to 6, increases the total rover mass by only 8% (from 25,000 kg to 27,000 kg). Most of this mass increase (~1600 kg) reflects the weight of the additional two astronauts, their gear, and the increase in the auxiliary power system mass to provide for the additional astronauts. The remaining mass (less than 400 kg) represents the incremental increase in the mass of the primary power system for meeting the increased mobility and life support power needs.

3.2 Effect of the Cruising Speed and Soil Traction Parameter

The maximum cruising speed of the rover could vary significantly with the terrain encountered; however, 30 km/h was selected as an upper limit. Since the gravitational acceleration on Mars is almost twice that on the moon, the weight of the rover vehicle force will increase proportionally and the vehicle will exhibit a higher rolling resistance. The wheel design and soil consistency may also vary, which will affect the mobility power requirement. It is, therefore, also necessary to study the effects of varying the soil traction parameter.

The results delineated in Figure 17 show the strong dependence of the total rover mass on the cruising speed. The mass corresponding to a zero speed represents the mass of the rover vehicles, including that of the PPS, needed to meet the User power requirement (excluding mobility). As this figure shows, increasing the cruising speed increases the mobility power requirements, resulting in higher masses for the PPS and the rover vehicle. As Figure 17 shows, for the base case, the total mass of the rover is 26 metric tons at a cruising speed is 19 km/h. As the cruising speed increases to 30 km/h, the total rover mass for the base case of four astronauts increases to 32 metric tons (~12% increase), and the power requirements for the PPS increase to 160 kW_e (a 60% increase)

The effects on mobility power of varying the maximum cruising speed and soil traction parameter are illustrated in Figure 18. Here the mobility power

requirement is plotted against the maximum cruising speed, from 0 to 30 km/h, for three different surface traction values (8.0×10^{-5}, 1.6×10^{-4}, and 2.4×10^{-4} kW·h/kg·km). Starting with the base case of 1.6×10^{-4} kW·h/kg·km ($\chi = 2.0$), and a cruising speed of 19 km/h, the required power level is 70 kW_e for mobility (P_t = 100kW_e). Increasing the cruising speed to 30 km/h will require increasing mobility power 120% to 153 kW_e. The effect of variation in the surface traction parameter becomes highly significant at higher values of the cruising speed. For example, at a cruising speed of 19 km/h, increasing the traction value from 1.6×10^{-4} to 2.4×10^{-4} kW·h/kg·km doubles the mobility power (from 70 to 140 kW_e). At 30 km/h the same increase in surface traction yields increases the mobility power from 153 to 526 kW_e (more than a 360% increase). At the lower value of 8.0×10^{-5} kW·h/kg·km, the mobility power required at 30 km/h is 49 kW_e. For the 100 kW_e base design, a maximum cruising speed of 30^+, 19, and 12.5 km/h can be obtained for surface traction factors of 8.0×10^{-5}, 1.6×10^{-4}, and 2.4×10^{-4} kW·h/kg·km, respectively.

3.3 **Effect of Reactor System Specific Mass**

The power system specific mass (SM_r) of 100 kg/kW_e, which is used in the base case, yields a power system total mass of 10,000 kg. This includes 3000 kg for the power system based on SP-100 technology. The remaining 7000 kg is then used for the radiation shield mass. This shield mass is required to insure the crew's safety with a dose rate from the reactor of 30 rem/y during operation (justification of this value is given in section 4.1) For the purpose of assessing the sensitivity of the total rover mass to the power system specific mass over the expected range of possible operation, the specific mass of the reactor power systems was varied from 50 to 150 kg/kW_e. A more accurate estimate of the reactor power system specific mass will be presented in

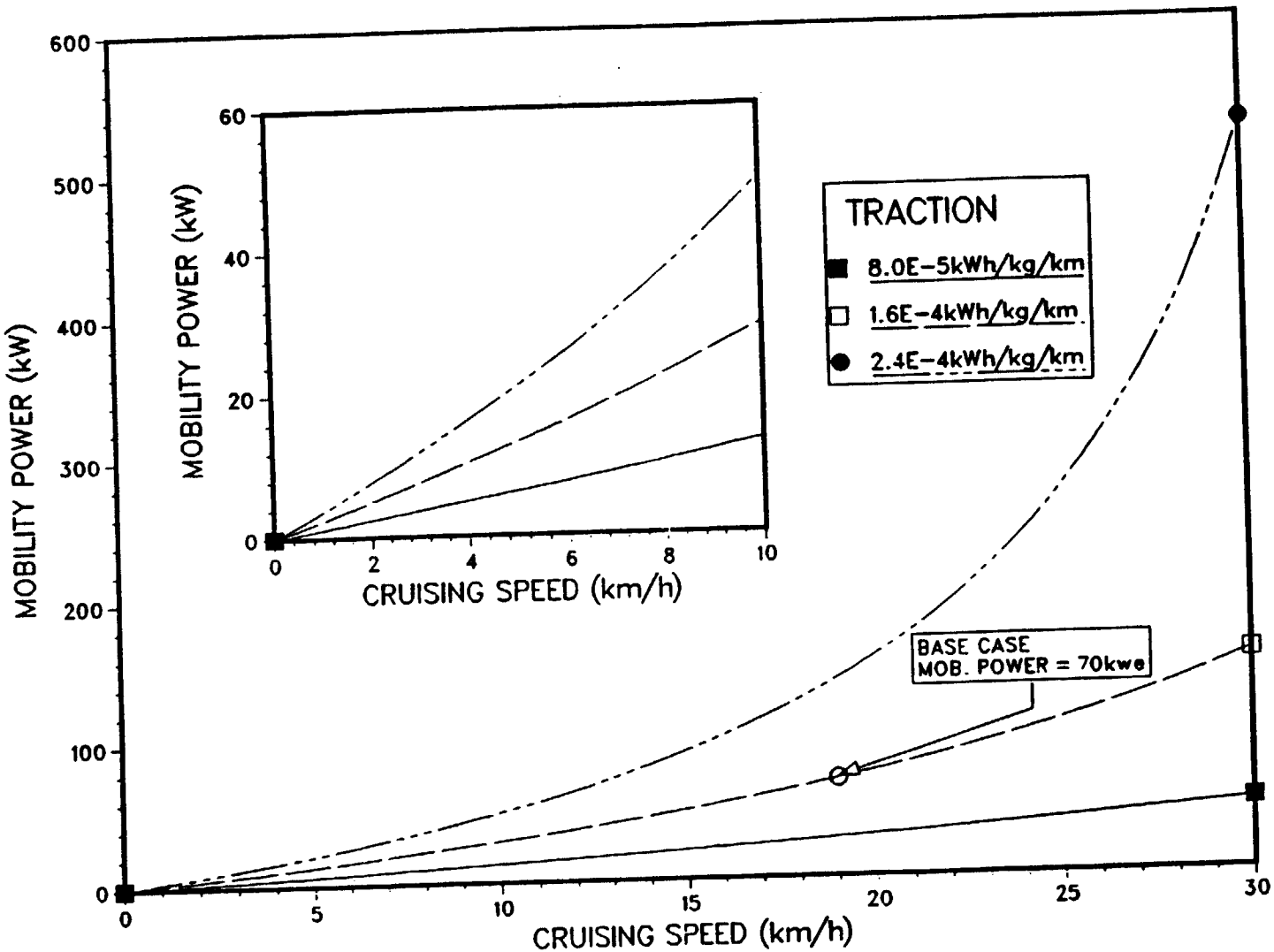

FIGURE 18: Effect of the Soil Traction Parameter on the Mobility Power

Chapters 4 though 6, when various power plant subsystems are better defined. This next phase of the project will focus on the design and integration of the radiation shield and the power system with the rover.

In Figure 19, the total power requirements as a function of cruising speed is shown for three different specific mass values (50, 100, and 150 kg/kW_e). For all three cases, the minimum power is 30 kW_e (user net power only) at 0 km/h. At low cruising speeds (< 10 km/h) the power system's specific mass has virtually no effect on the reactor power. However, once the speed begins to increase beyond 10 km/h, the specific mass begins to show a significant effect on the total reactor power requirement. For example, at 30 km/h the total power requirements double from 183 kW_e at 100 kg/kW_e to 378 kW_e at 150 kg/kW_e. Figure 19 also shows that for the base case of 100 kW_e, the maximum cruising speed attainable for the rover is 23, 19, and 16.5 km/h, for nuclear reactor system specific masses of 50, 100, and 150 kg/kW_e, respectively.

Figure 20 shows that the specific mass of the reactor power system; however, greatly impacts the total rover mass. At 100 kW_e, increasing the system's specific mass from 100 to 150 kg/kW_e only decreases the maximum cruising speed by 2.5 km/h, but increases the total rover mass from 26 to 32 metric tons. This mass increase is significant and represents an additional launch cost of approximately six billion dollars (at the cost of $1M/kg).

3.4 **Effect of the Utility Cars Mass**

The effect of varying the total mass of the three utility cars on the total rover mass and the system power was evaluated for a total RUC mass range from 15,000 to 18,000 kg. Figure 21 presents a plot of rover mass versus

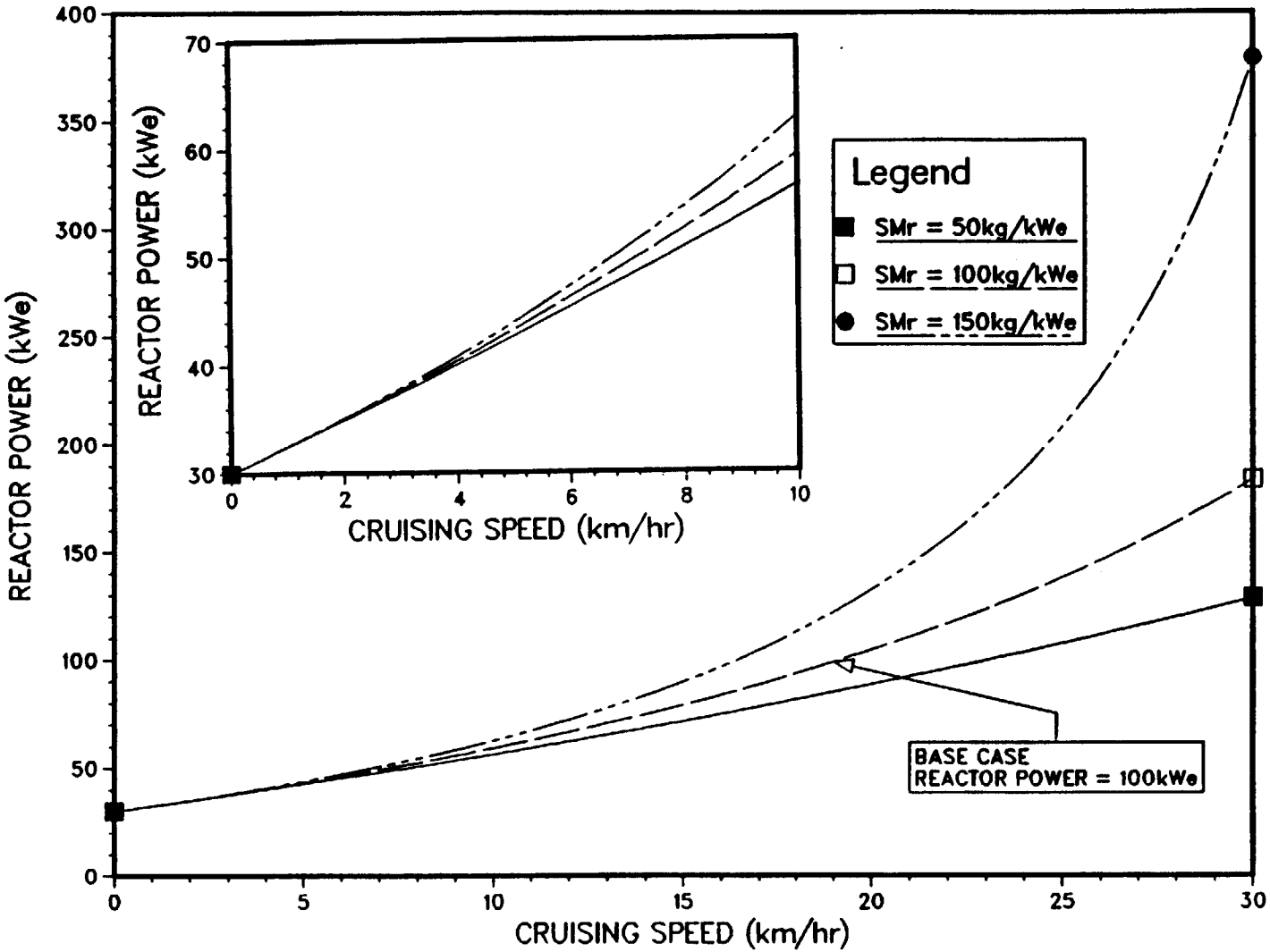

FIGURE 19: Effect of Reactor Specific Mass on Total Power Requirement

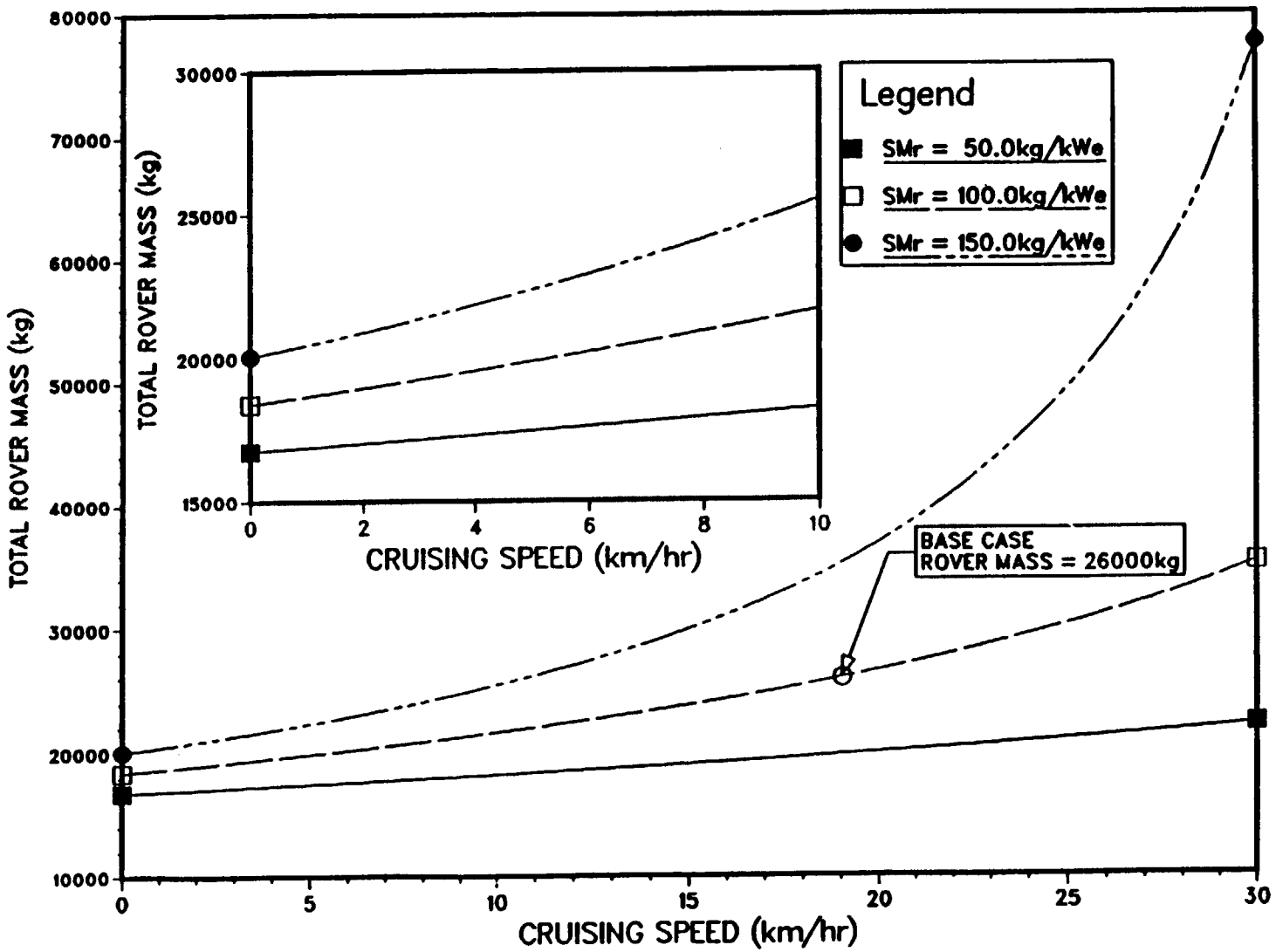

FIGURE 20: Effect of Reactor Specific Mass on Total Rover Mass

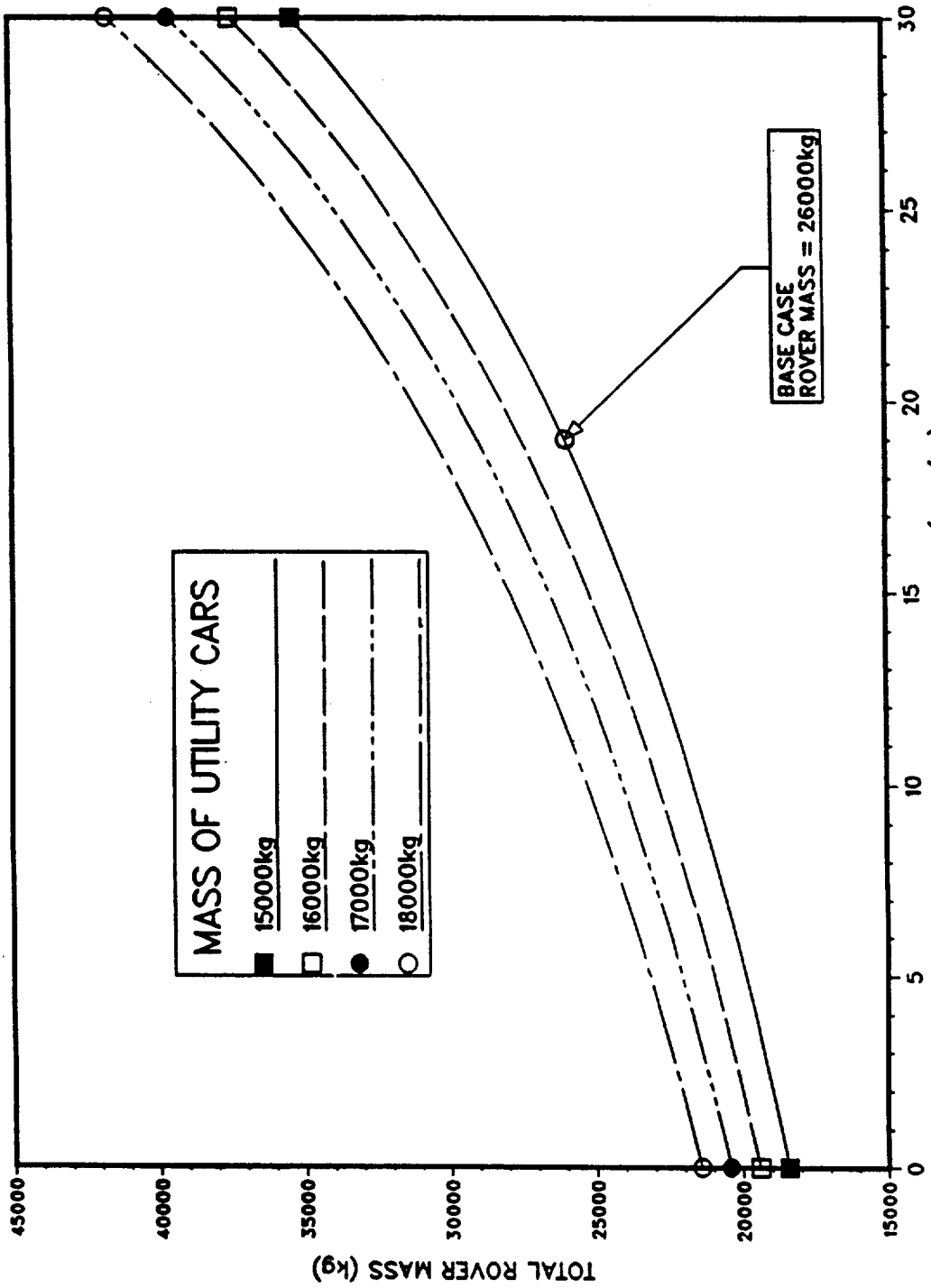

FIGURE 21: Effect of Utility Car Mass on Total Rover Mass

cruising speed for four values of RUC mass. At a speed of 0 km/h the total rover mass varies from 18,412 to 21,412 kg. This difference in total mass simply reflects the increase in RUC mass from 15,000 to 18,000 kg. At 19 km/h the same increase in the RUC mass increases the total rover mass from 26,004 to 30,511 kg, a difference of 4,507 kg. The additional 1,507 kg reflects the small increase in the PPS mass needed to meet the additional mobility power requirements. It is therefore concluded that a 300 kg variation in RUC mass is not critical in evaluating the PPS power or mass requirements.

3.5. SUMMARY OF ROVER PARAMETRIC ANALYSIS

At this point the concept of the manned Mars rover has been developed as the layout of a four car train including an auxiliary power system. As was stated earlier, the mass of the rover is a key parameter in determining the mobility power requirement, which in turn is used for determining the reactor power level. Since the total mass of the rover is strongly related to the mission scenario, it was necessary to define a reference mission prior to the start of the design. This mission, including an emergency return scenario, has been developed using the initial design goals stated in section 2 and the mass of the individual cars is given in Tables 1, 4, and 5 for the PCV, EU, and SC, respectively.

In summary, the parametric analysis showed that the total power required from a nuclear reactor primary power system and the total rover mass are strong functions of the cruising speed, specific mass of the power system, and the surface traction and drive efficiency, and to a lesser extent the mass of the rover utility cars. The use of an SP-100 reactor, generating 100 kW_e, would provide for a cruising speed of 16.5 km/h at a reactor system's specific mass of 150

kg/kW_e and 19 km/h if the system specific mass could be reduced to 100 kg/kW_e. At this power level the mass of the PPS is 32% of the total rover mass for 100 kg/kW_e and 53% at a specific mass of 150 kg/kW_e. The total mass of the rover with a 100 kW_e PPS and a specific mass of 100 kg/kW_e is approximately 26 tonnes. However, at 150 kg/kW_e the rover mass will by 23% higher at 32 tonnes.

With the mass of the PCV, EU, SC determined, the mobility power may now be addressed. In the next section, four components of the PPS will be studied in order to evaluate the system specific mass. These components include the radiation shield, the energy conversion system, the reactor, and the waste heat rejection system. The design goal is to integrate the requirements for designing the reactor power system with a nominal specific mass of 100 kg/kW_e. At a output power level of 100 kW_e the total power system mass will be 10 tonnes, of which 3 tonnes for the masses of the core, energy conversion, heat rejection, and additional subsystems and 7,000 kg in for the biological shield.

4. RADIATION SHIELD DESIGN

4.1 Shield Overview

The radiation shield for nuclear reactor, that is to be operated in the vicinity of a human crew, will makeup the largest portion of the overall system mass. Many factors must be considered in the design of any radiation shield, some of these factors include:

- size and nature of the nuclear power source,
- type of radiation produced α, β, γ, neutrons,
- configuration of the spacecraft and payload,
- length of mission,and
- total radiation dose limit that will be permitted.

Although many of the values for these unknowns have already been determined by the original mission requirements, several questions remain unanswered. For instance, it is already known that the system is to be a reactor; therefore, the primary shielding requirements will be for γ and neutrons. While the configuration of the rover has been developed, much leeway in the actual shield configuration and reactor car layout still exists. While a shadow shield is preferred for space applications, it is not as appropriate for a Mars rover . In space, vacuum conditions eliminate any significant scattering source; however, both the soil and atmosphere of Mars will contribute to an increased radiation dose rate at the crew's location if precautions are not taken. By increasing the shield angle and placing at least a moderate shield around the entire reactor, significant dose to the astronauts and prohibitive constraints on crew activities will be avoided.

The first step in designing the radiation shield is to determine the maximum allowable dose to the crew. The maximum permissible dose for the astronauts is given by the NCRP as 0.5 Sv/y (50 rem/y) from combined manmade and natural sources (i.e.cosmic radiation and solar particle events). For a three year Mars mission (1 year on the surface) a total received dose for the mission of 1.5 Sv (150 rem) can be received. The breakdown of radiation from natural sources can be seen in Table 7 [Bloomfield, 1990]. The highest annual expected dose rate of 0.2 Sv/y, while on the planet surface, is of principle value concern for the manned rover. Using the NCRP's recommendation that the maximum annual dose limit be no more than 0.5 Sv/y for astronauts undertaking exploratory missions, the dose obtained from all nuclear sources onboard the rover should not exceed 0.3 Sv/y (30 rem/y).

It is important to note that 0.2 Sv/y is the highest expected rate on the surface, while 0.1 Sv/y is the average expected rate on the surface. The dose to the crew from natural radiation sources while on the surface of the planet is significantly less than that received during transit to Mars. This is due to the shielding of cosmic and solar particle radiation by the CO_2 atmosphere (~10 g/cm^2). From this information a maximum dose rate was set at 0.3 Sv/y (0.032 mSv/h). While this dose rate coupled with the maximum surface dose of 0.2 Sv/y from natural sources gives a total rate of 0.5 Sv/y, this is again the maximum value expected. The effect of the dose rate on the required thickness of various shield materials and shield mass will be the subject of discussion later in the report.

4.2 Space Shielding History

Shielding designs have been extensively studied in the late 60's and early 70's during both the SNAP and rover Programs. With the appearance of the

SP-100 space nuclear power program in the early 1980s, again lightweight shields for space systems have become of interest.

4.2.1 SNAP-10A

To date, the only flight experience with a space reactor shield has been on the SNAP-10A. This system was launched on April 3, 1965. The reactor used a 98 kg shadow shield consisting of a cold-pressed Lithium Hydride material which was reinforced with a stainless steel honeycomb contained in a SS-316 casing [Angelo and Buden, 1985]. The design of the shield was to limit the radiation dose at the spacecraft interface to $5x10^{12}$nvt fast neutrons and $4x10^{7}$ rads of gamma radiation (the actual measured dose was significantly higher, apparently due to a higher than expected neutron flux caused by scattering from the control drums). The operating temperature of the shield was bounded between 712 and 579 K. However, the mission was experimental in nature and the shield was not designed to protect any human crew.

4.2.2 ORNL Heat Pipe Reactor Shield

Since the time of SNAP-10A many studies into the shielding for space reactor systems have been completed. One such study was performed at Oak Ridge National Laboratory (ORNL) for their stainless steel, Potassium Heat Pipe Reactor concept. This shield design, shown in Figure 22, uses a combination of tungsten (for gamma shielding) and lithium hydride (for neutron shielding). In addition, it was shown that to achieve the lowest dose rates the tungsten should be placed in two layers separated by a layer of lithium hydride. Due to tungsten's large (n,γ) cross section, it is important to limit the neutron flux within the tungsten in order to minimize production of secondary gammas. According to the ORNL report, changing the dose rate requires a change only in the

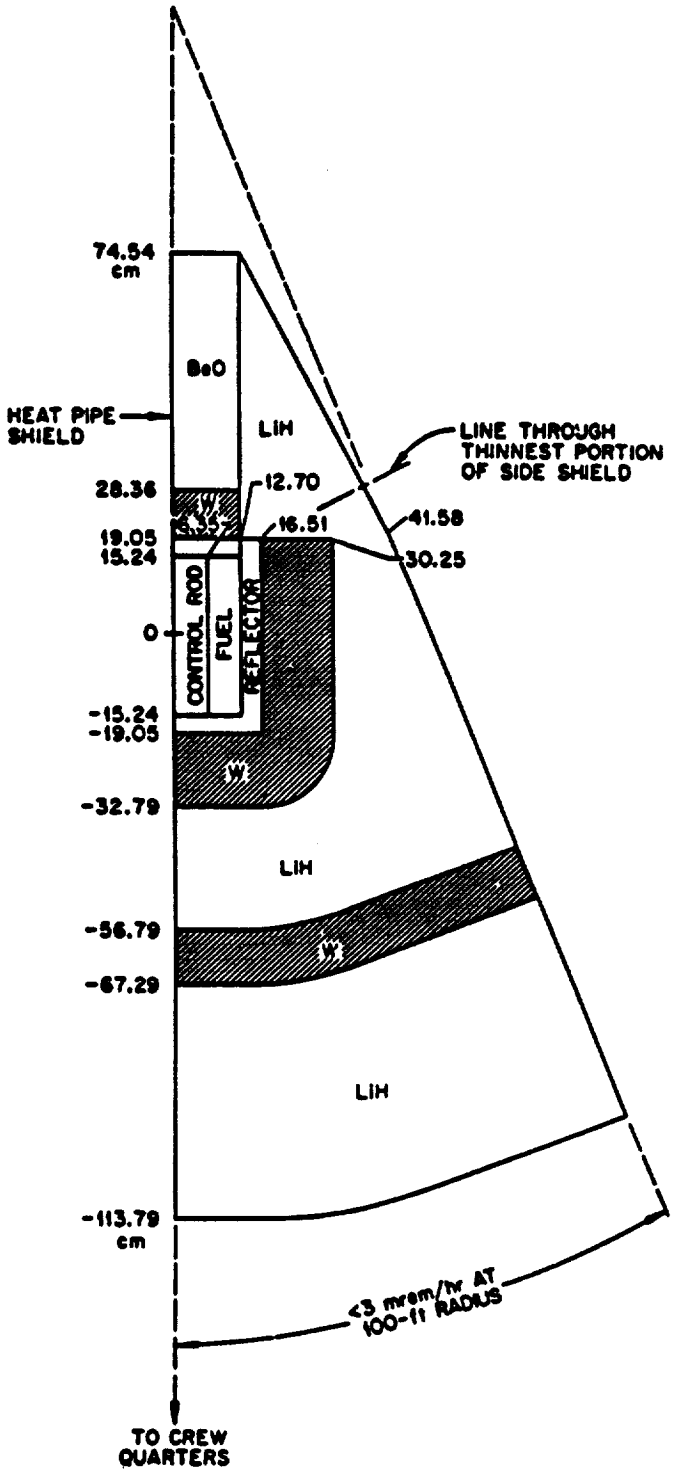

Figure 22: ORNL Heat Pipe Reactor

thickness of the first layers of tungsten and lithium hydride. The effect of various shield material thickness on the dose rate is shown in Figure 23 [Barratino,1985]. The dose constraints for the ORNL shield were .03 mSv/h within the shields shadow (45°) and 3.0 mSv/h outside the shadow at a distance of 32.81m [Engle et al., 1971].

The Oak Ridge shield study consisted of optimization analysis of both two and three cycle shields (a cycle refers to the combination of a tungsten and lithium hydride layer). The optimization of the shield was for a 45° zone of protection for the two cycle shield and a 90° cone angle for the three cycle shield. In order to perform the optimization calculations the ASOP code (ANISN Shield Optimization Program) was used.

For the two cycle shield, the reactor power was taken at 450 kW_t with dose constraints at the crew quarters of 0.0075, 0.03, and 0.12 mSv/h. The crew distance for the design was 61 m (200 ft) from the core centerline. The thickness of tungsten and lithium hydride versus the dose rate at the crew cabin is shown in Figure 24 [Engle et al., 1971]. There are two interesting points about this curve. First, in order to decrease the dose rate it is necessary to increase the thickness of the first layers of tungsten and LiH, while keeping the second layer of tungsten ~11 cm and of LiH ~42 cm. Next the total thickness of LiH required to adequately protect the crew is ~70.5 cm, which turns out to be about the same thickness as needed to protect the electronic equipment for the SP-100 reactor [Barratino,1985].

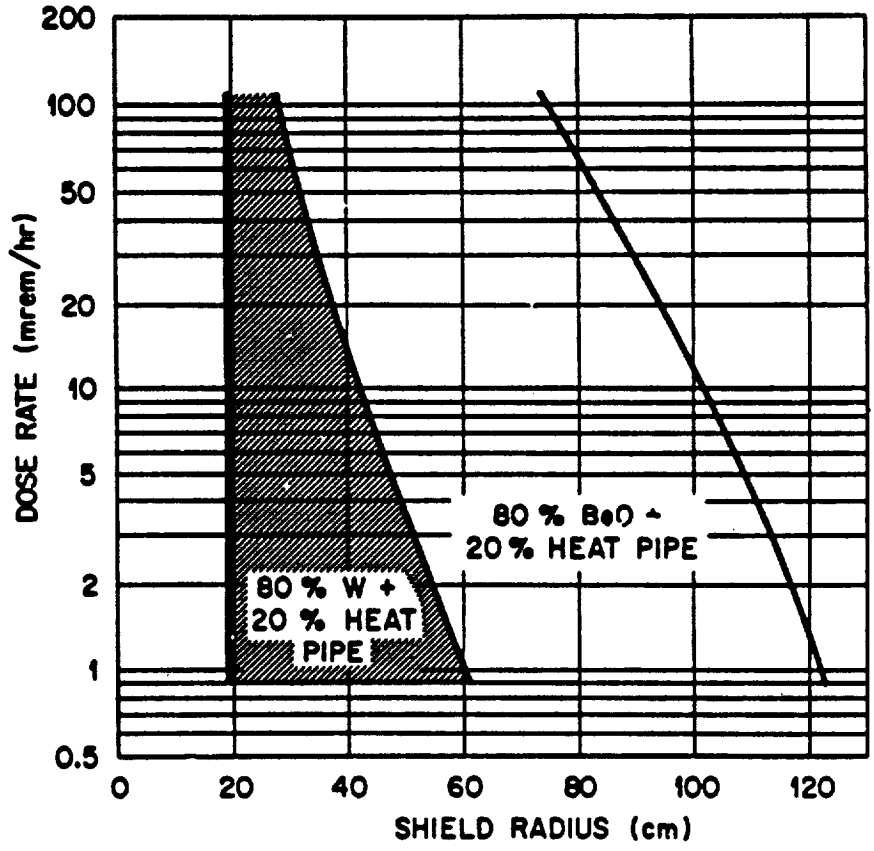

Figure 23: Shield Material Thickness vs Dose Rate

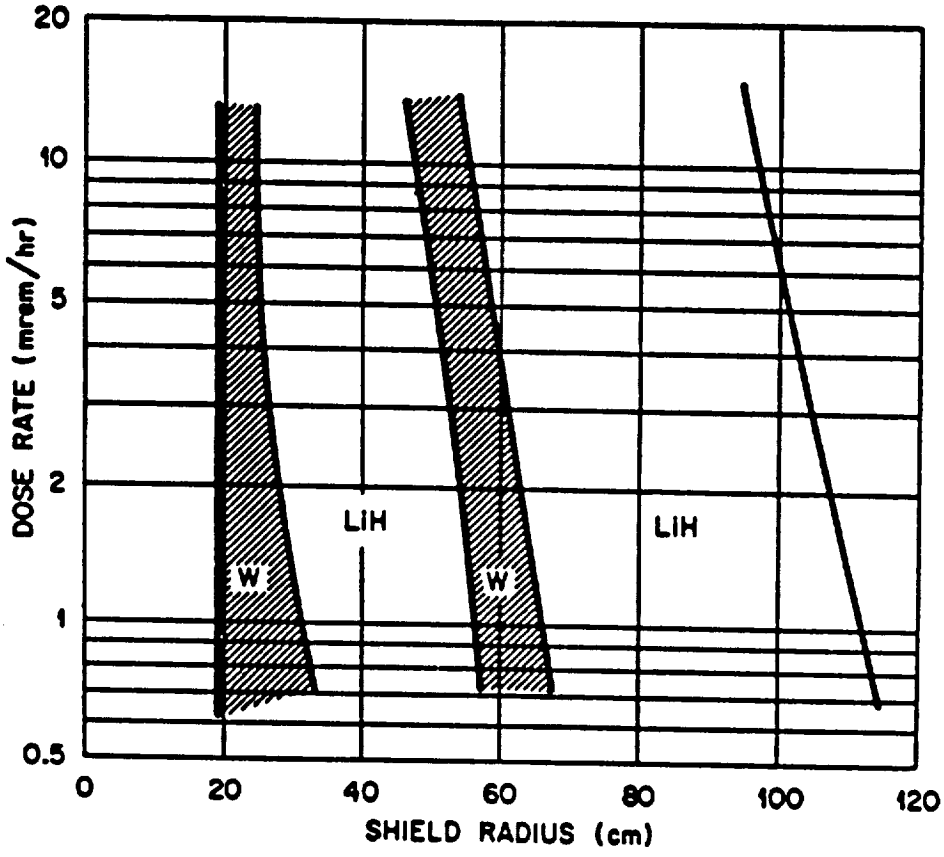

Figure 24: Thickness of W and LiH Layers in a Two-Cycle Shield as a Function of Dose Rate at a Distance of 200 ft (450 kW_t)

4.3 Shield Material Selection

One of the main objectives in any space system design is the minimization of mass. Of course the farther and faster one needs to travel the more costly it becomes to launch large heavy objects. Since man-rated shields are by definition heavy, every effort should be made to minimize its mass.

One very attractive alternative to transporting large quantities of material from earth, is the use of indigenous planetary soil materials for the shield. For Mars the estimated soil composition, as relayed by the Viking landers, is shown in Table 7 [Bloomfield]. This table shows 50% oxygen content in the soil. The oxygen is primarily found in the form of oxides. Because these estimates are based solely on the Mars Viking landing sites, considerable variation may be found at different surface locations. Also, the Viking probes only scratched the surface in their probing of the Martian soil; therefore, fluctuation may be found by excavating down several meters. Although the use of indigenous planetary

Table 7: Martian Soil Composition

Element	Percentage
O	50
Si	21
Fe	13
Mg	5
Al	3
S	3
Cl	1
Ti	0.5
K	0.2
Y	70ppm
Sr	60ppm
Rb	30ppm
Zr	30ppm

surface materials to provide radiation attenuation has been shown to be a viable shielding alternative for both Martian and Lunar base power systems, showing significant reduction in the required mass to be transported from earth [Bloomfield], it is not as attractive for a manned rover shield.

The minimum thickness of soil material needed to attenuate the radiation to acceptable levels would be ~7 m. This, in turn, would have an equivalent mass in the 10s of tonnes. While building such a shield could be accomplished with modest material handling equipment (which should be available from other planetary surface base construction) [Bloomfield,1990], such a massive shield would severely inhibit the movement of a manned surface rover. In addition to the increased mass of the operating rover, the transmutation of the soil by neutrons produced in the reactor would cause a degree of activation of the shield. Table 8 shows the activation of the soil (in curies) for given time after reactor shutdown, after 10 years of reactor operation. It should be noted that significant radionuclide buildup is present. Although the rover power system would not operate continuously for 10 years, the activation of the soil would still cause an additional radiation dose to be received by the crew. For these reasons it was decided that a rover designed with a shield constructed on earth would best suit the mission.

Table 8: Nuclide Buildup

Radionuclide	100 days curies	400 days curies	Radionuclide	100 days curies	400 days curies
P-32	587	592	Mn-56	37.9	37.9
Al-28	361	361	Si-31	87.1	87.1
Mg-27	118	118	Ar-37	43.3	50.3
Fe-55	7.9	28.3	Na-24	27.4	27.4
Mn-54	21.1	62	All others	34.2	92

4.4 Calculation Method

In order to model the core/shield configuration, the TWODANT neutral particle transport code developed at Los Alamos National Laboratories (LANL), was used [O'Dell et. al, 1989]. The first step in the shield design was to adequately model the reactor core so that an accurate source term could be developed for the shielding calculations. Since the core technology to be used is SP-100 derivative the current SP-100 design was felt to be the best possible choice for the reference model. In order to develop an adequate representation of the SP-100 core in a TWODANT input file a model of the core developed by John McGhee for helium production analysis was modified and used [McGhee, 1989]. The material zones are shown in Figure 25.

4.4.1 Neutronics Model

Since the model input file was originally developed to be run on a Cray computer at Los Alamos, the regional zones had to be simplified so that it could be run using the capabilities of a VAX-8750. The model is a two-dimensional r-z cylindrical representation of the SP-100 reactor core. Further modification was made to the core by replacing the beryllium reflector shutter panels by rotating BeO/B_4C control drums. This was done because, unlike the SP-100 reference mission which employs a shadow shield in a space environment, the rover mission will require a minimum of an oriented 4-π shield to insure adequate protection for the astronauts. Such a shield would severely limit the usefulness of a shutter control system.

4.4.2 Model Verification

In order to insure that the changes to the core model would have a minimum effect on the energy distributions, the core model was compared to the

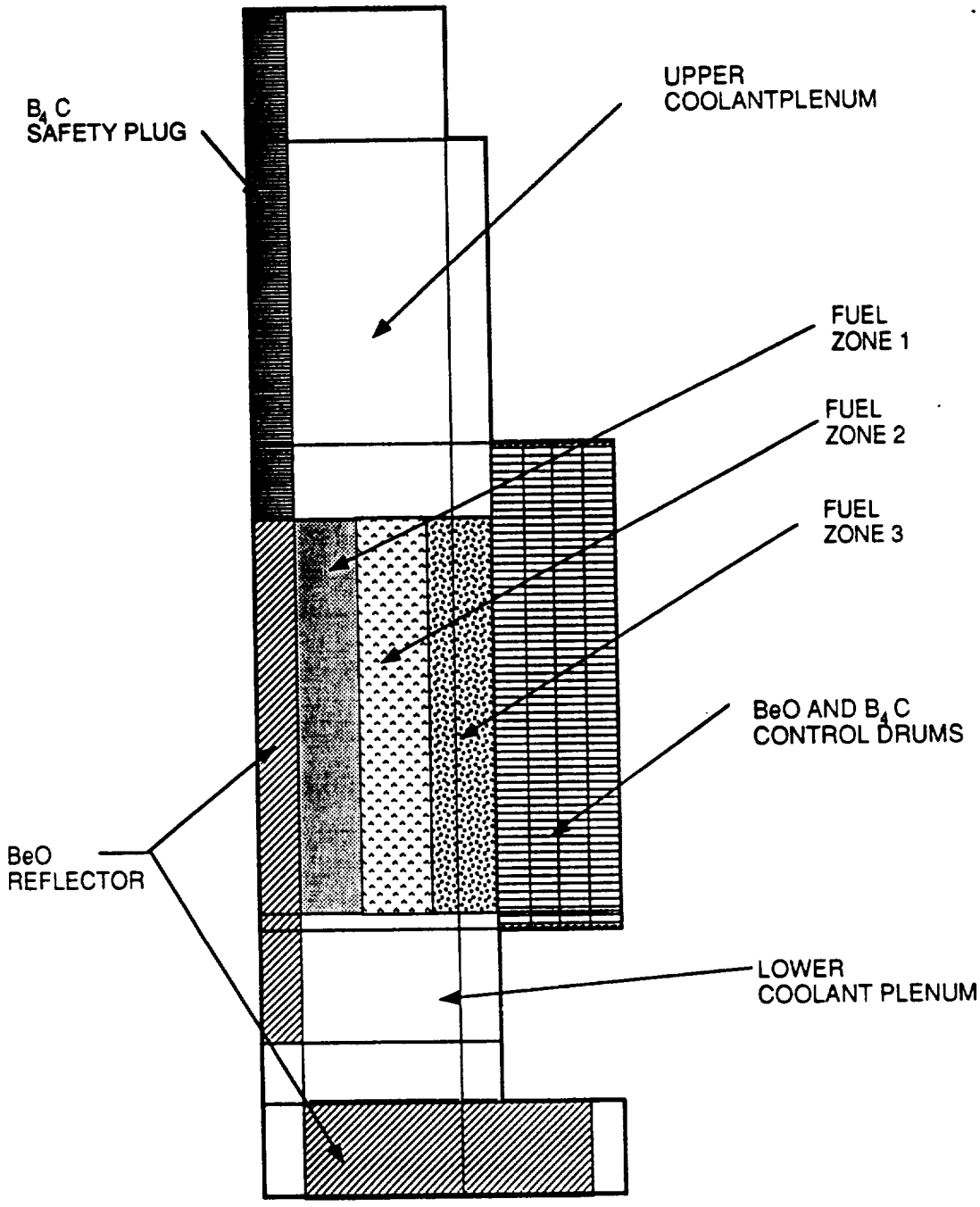

Figure 25: Material Zones For Reactor Neutronics Model

more detailed original model. The comparison of the two models is shown in Figure 26 (a&b). From the neutron energy spectrum, and Figures 27 (a &b) and 28(a&b) (the radial and axial flux distributions) it can be seen that the simplified model corresponds well with the results obtained by McGhee,although the model used a 42 group cross section library instead of the 80 neutron group library originally used. The 42-group library is a coupled neutron (30 energy groups) and gamma (12 energy groups), which allows the the gamma spectrum in addition to the neutron distributions to be plotted. Figure 29 plots the normalized gamma energy distribution at both the core centerline and the reflectors outer edge. As is expected the energy distribution, is shifted toward the lower end of the spectrum at the edge of the reflector. Figures 30 and 31 show the normalized radial and axial gamma flux distributions, respectively. Although there is no such distribution calculated for the more detailed model (it uses only a neutron cross section library), these curves can still be used to evaluate the reasonability of the model.

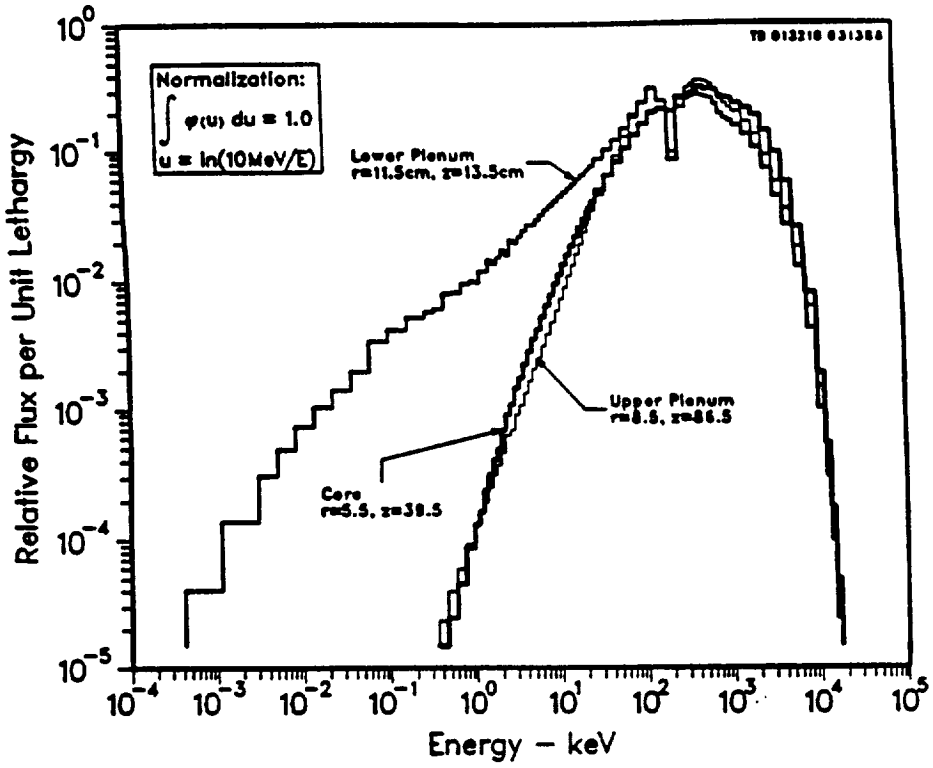

Figure 26b: Neutron Energy Distribution for Original SP-100 Core

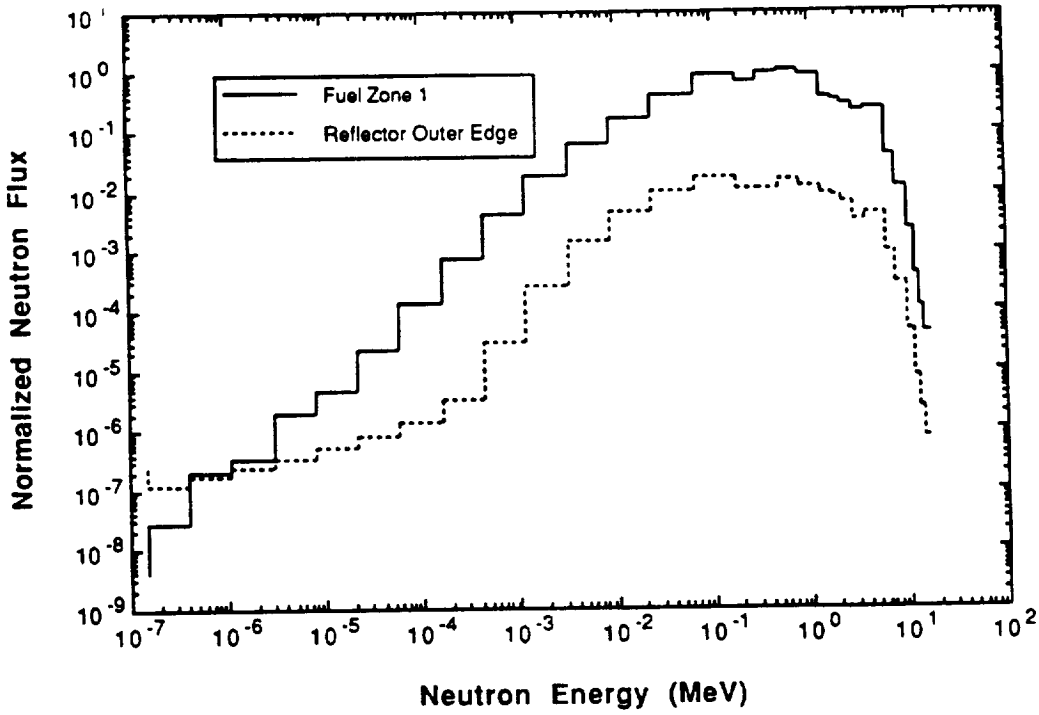

Figure 26a: Neutron Energy Distribution for Modified SP-100 Core

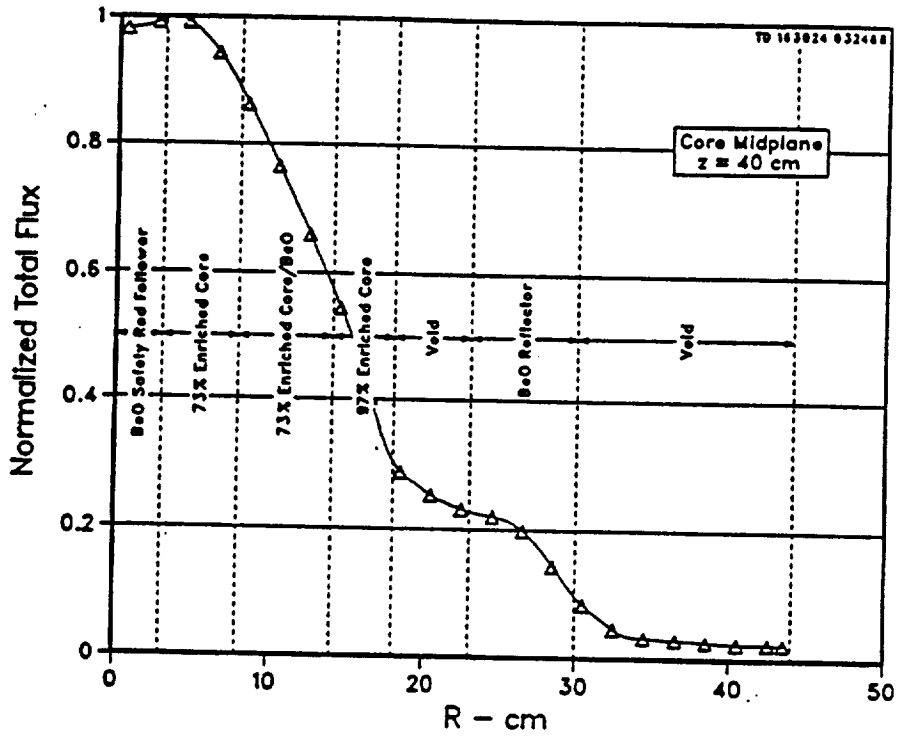

Figure 27b: Radial Neutron Flux Distribution for Original SP-100 Core

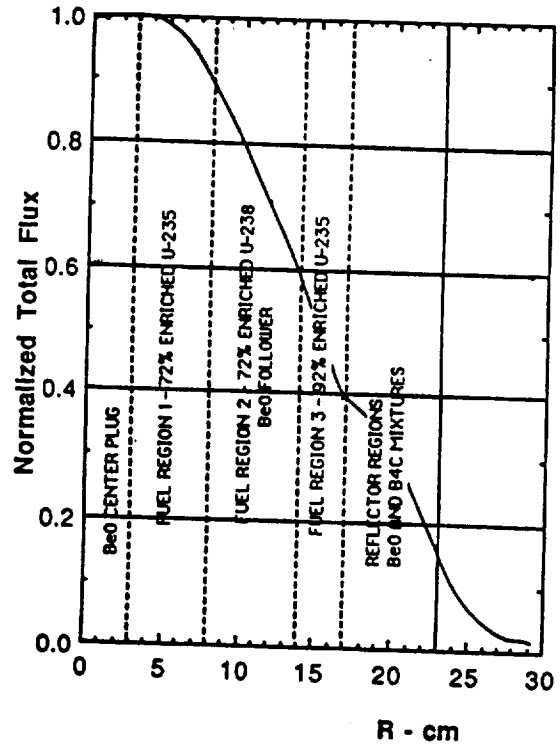

Figure 27a: Radial Neutron Flux Distribution for Modified SP-100 Core

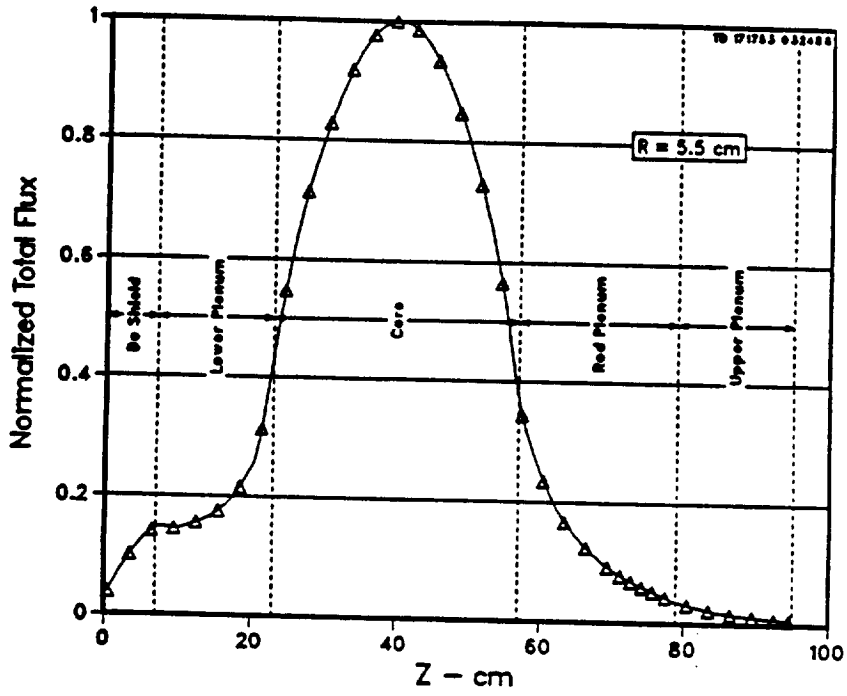

Figure 28b: Axial Neutron Flux Distribution for Original SP-100 Core

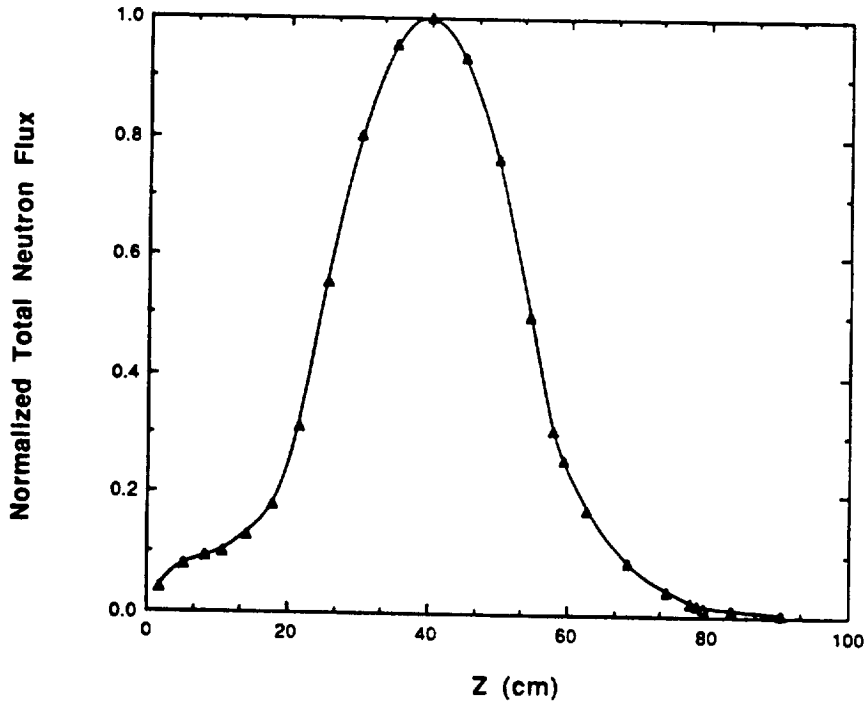

Figure 28a: Axial Neutron Flux Distribution for Modified SP-100 Core

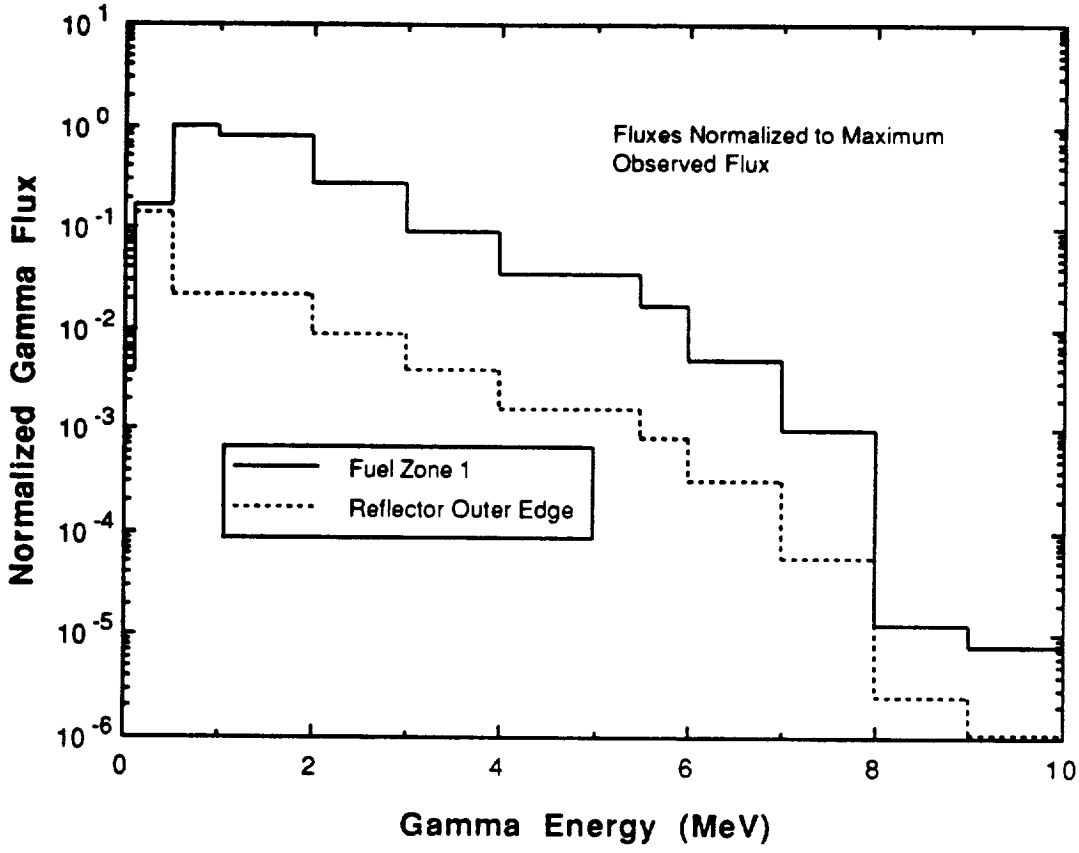

Figure 29: Normalized Gamma Energy Distribution for Modified SP-100 Core

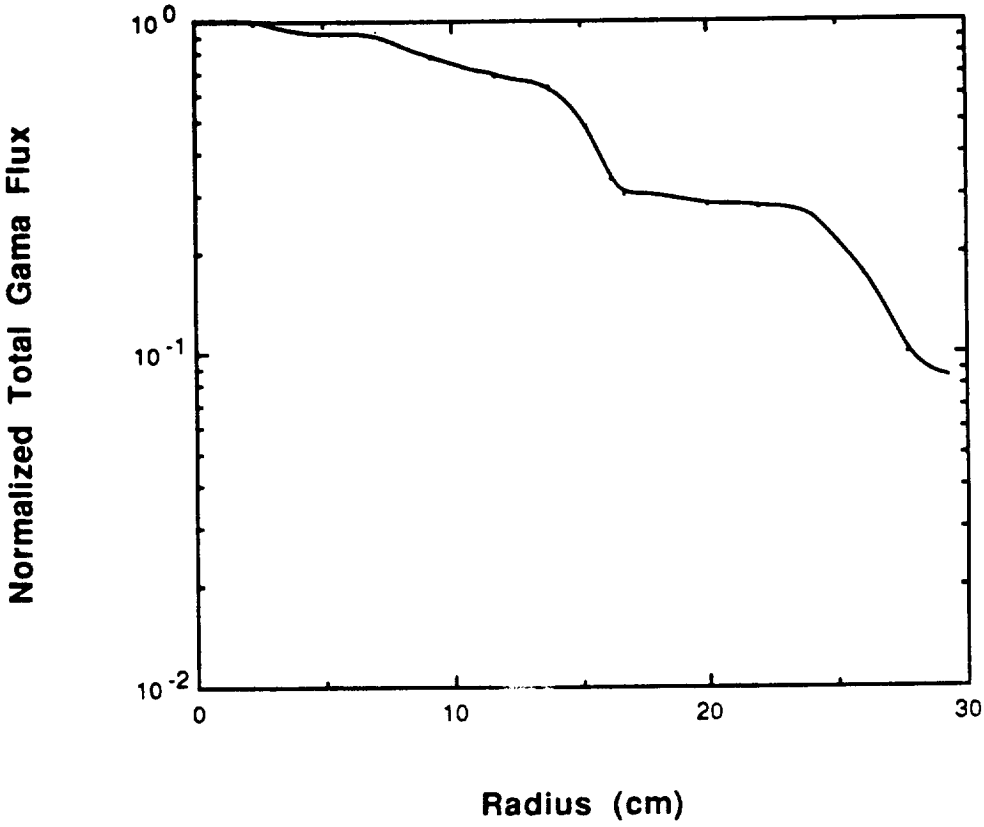

Figure 30: Radial Gamma Flux Distribution for Modified SP-100 Core

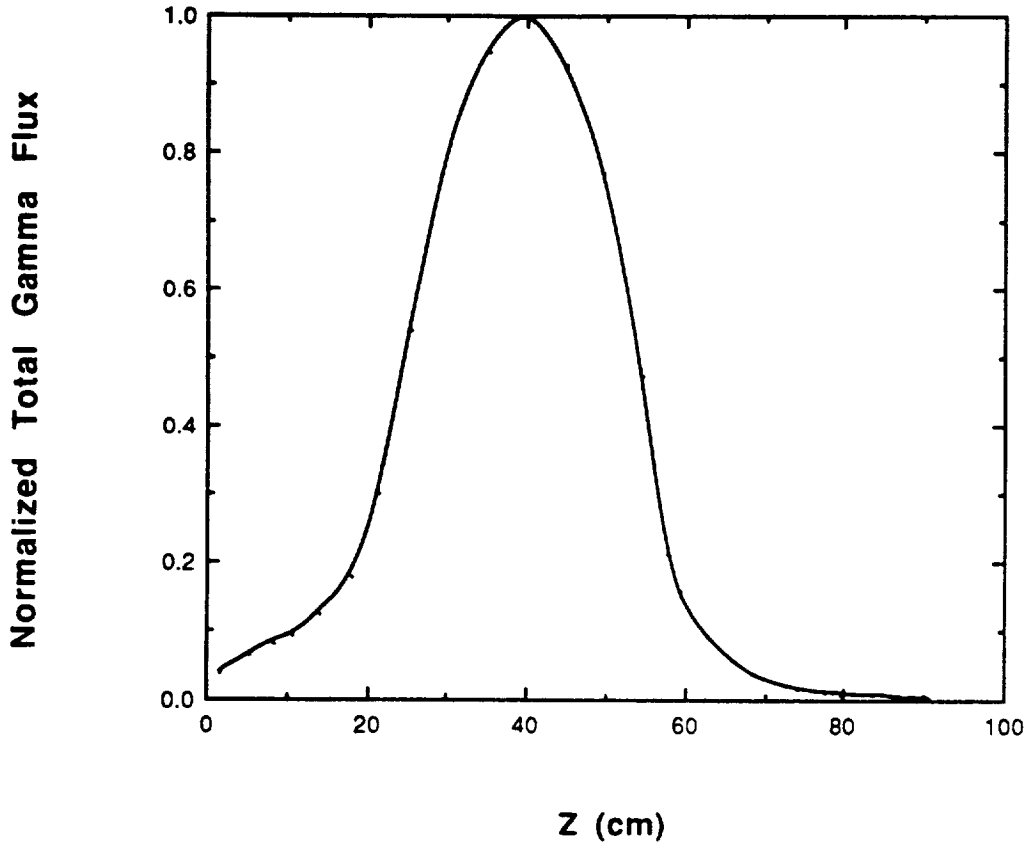

Figure 31: Axial Gamma Flux Distribution for Modified SP-100 Core

4.4.3 Dose Rate Calculation Method

Before going into the analysis of the shield, it is important to discuss the manner in which the dose rate is calculated. The output from TWODANT is in the form of fluxes at the various energy levels related to the energy groups in the cross section library. It is, therefore, necessary to convert these fluxes into equivalent dose rates at the location of interest. The calculation of the contribution to the dose rate from gammas and neutrons is carried out in two different manners.

4.4.3.1 Gamma Dose Rate

Output from TWODANT model of the SP-100 core is in the form of neutron and gamma fluxes at specified locations for each of the various energy levels related to the 42 energy groups in the cross section library. These fluxes are then converted into equivalent dose rates at the location of interest. For the gamma dose received the following equation [Lamarsh, 1983] was used:

$$\dot{D} = 5.76 \times 10^{14}\, \phi_\gamma E_\gamma (\mu_a/\rho)_{tis} Q \ \ mSv/h, \qquad (11)$$

where ϕ_γ is the gamma flux over a particular energy range, E_γ is the gamma energy, $(\mu_a/\rho)_{tis}$ is the mass absorption coefficient for tissue, and Q is the quality factor for gamma radiation (=1). The quantities for $(\mu_a/\rho)_{tis}$ are given in Appendix C.

4.4.3.2 Neutron Dose Rate

Dose computations for neutrons are more difficult than for gamma rays due to the complex way in which neutrons interact with matter. Because of this

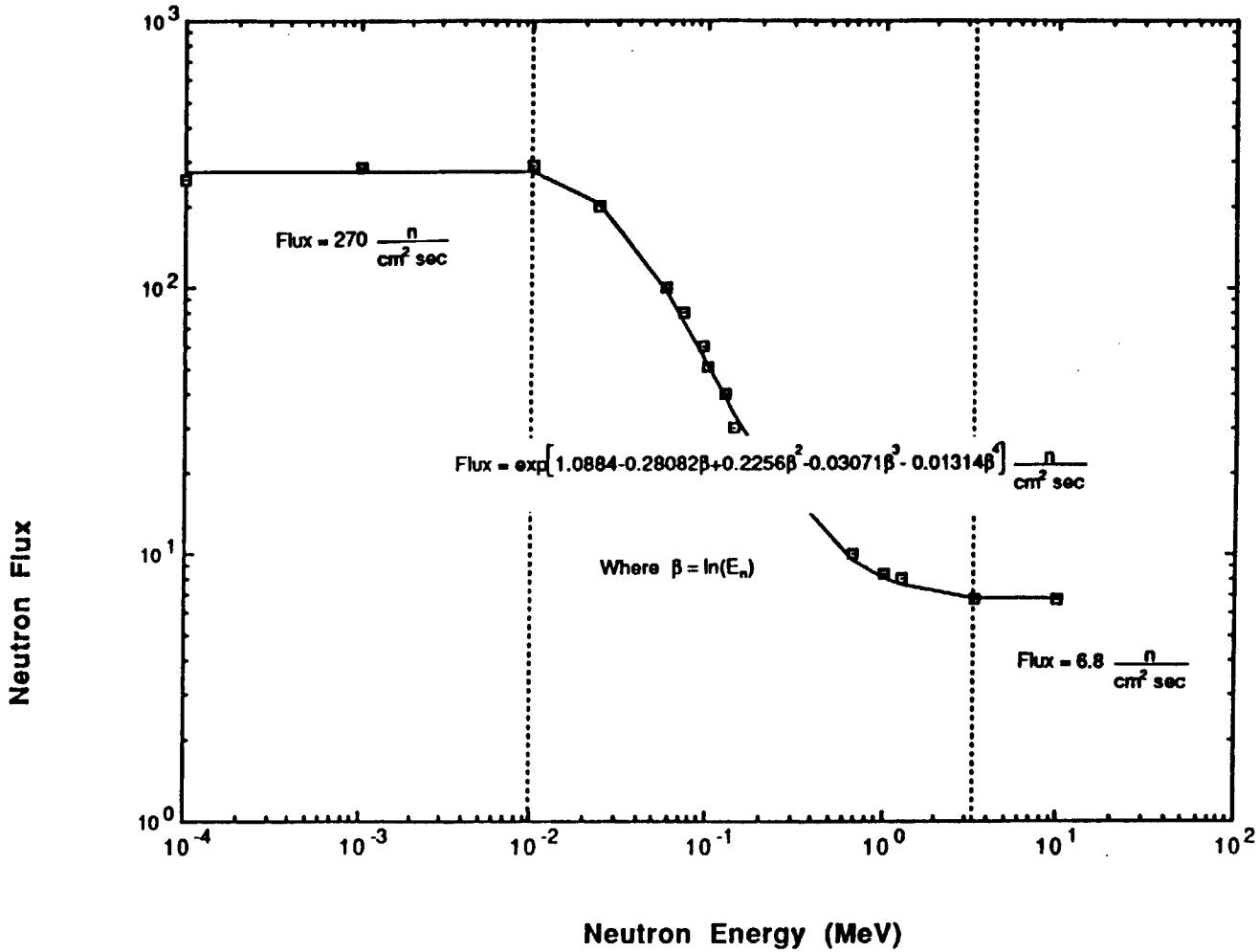

Figure 32: Neutron Flux for an Equivalent 0.01 mSv/h Dose Rate

complex interaction, the energy deposition is most conveniently computed numerically using Monte Carlo Method [Lamarsh, 1983]. From this type of calculation the curve in Figure 32 can be developed. This curve gives the neutron flux (ϕ') as a function of the neutron energy required to deliver a dose of 0.01 mSv/h. Figure 32 can then be used to compute the dose rate from a given neutron flux. To calculate the dose, the curve in Figure 32 was divided into three regions. For neutrons with energies in either region 1 and 3 the flux needed to produce 0.01 mSv/h was relatively constant at $\phi' = 270$ and $\phi' = 6.8$ n/cm^2 sec, respectively. Region 2 is approximated by the following polynomial:

$$\phi' = \exp\left[1.0884 - 0.28082\beta - 0.2256\beta^2 - 0.03071\beta^3 - 0.0131\beta^4\right], \qquad (12a)$$

and the neutron dose is given by,

$$D_n \text{ (mSv/h)} = (\phi_n/\dot{\phi_n})(100). \qquad (12b)$$

Using equations 11 and 12(a and b), along with the constant neutron fluxes for regions 1 and 2, a fortran program was developed to calculate the gamma and neutron components of the dose rate from the given fluxes generated by the TWODANT code.

4.5 **Shield Design Approach**

Now that the core model has been modified and a method for converting the fluxes into an equivalent dose rate has been developed it, is time to determine the shield geometry and composition. For the initial evaluation lithium hydride was used for neutron attenuation, while tungsten was used to reduce the gamma component of the dose rate.

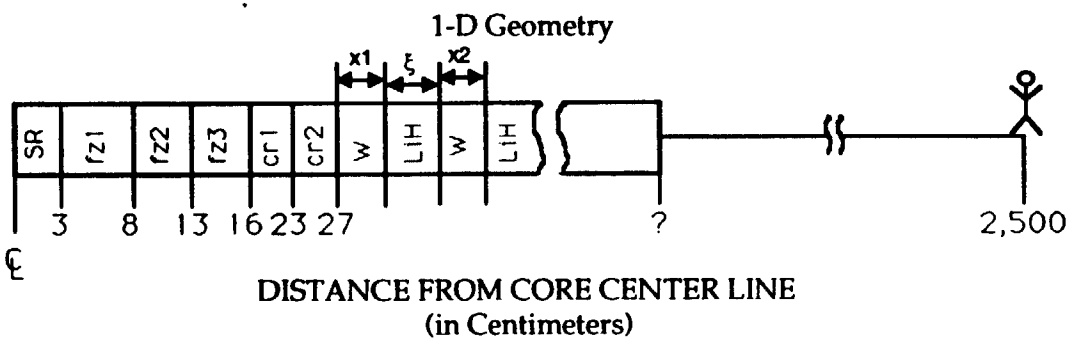

Dose Rate for Crew

DRn = ?
DRγ = ?
TOTAL = 30 rem/y

SR - Safety Rod -
fz1 - fuel zone 1 -
fz2 - fuel zone 2 -
fz3 - fuel zone 3 -
rz1 - reflector zone 1 -
rz2 - reflector zone 2 -
Lih - Lithium Hydride -
W - Tungsten -

Figure 33: One-Dimensional Shield Geometry

4.5.1 One-Dimensional Layout

The approach for the shielding design consisted of several distinct steps. First, due to the size and complexity of the two-dimension mesh, a majority of the cases were run using a one-dimensional model. The results were then adjusted to fit the 2-D cases. The one-dimensional geometry is shown in Figure 33. For all the cases a 3 cm thickness of Al and 10 cm thickness of water were placed between the reactor and the astronauts. The aluminum was used to simulate the walls of the rover and the equipment stored between the reactor and the astronauts (this includes the energy conversion equipment which will be discussed latter in the report) while the water represents the storage of consumable and waste water stored in the rover. The location or the Al was 12.5m from the core centerline and the water was placed directly in front of the Al. The 12.5m location was chosen because it is the midpoint between the reactor and the average distance of the crew. The region from the edge of the shield to the Al is filled with CO_2 to simulate the martian atmosphere. While from the edge of the water to the crew (25m) is air which simulates the atmosphere within the pressurized cars (see Figure 3).

4.5.2 Lithium Hydride Thickness

Using the one-dimensional model, the first step that was performed was to determine the effect of altering the thickness of lithium hydride. This was accomplished by first setting the tungsten thickness to zero. The shield radius (R shield) was then varied from 50-150 cm. The results from these runs are displayed in Figure 34. Both the dose rate from neutrons and gammas can be seen in Figure 34. While both components of the dose rate decrease proportionally to the log of the LiH thickness, the neutron portion decreases at a significantly greater rate. A thickness of 125 cm was chosen to be held constant

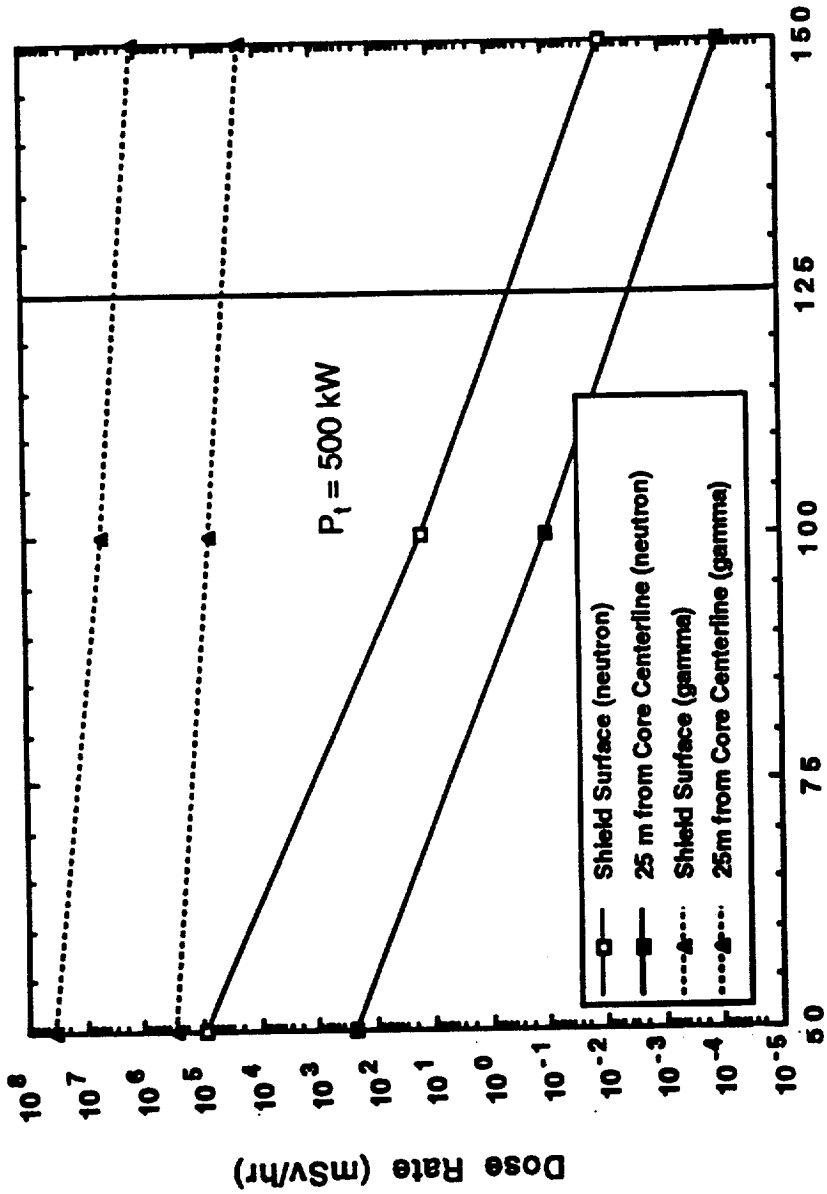

Figure 34: Dose Rate verses Lithium Hydride Thickness

for judging the effect of varying thickness of tungsten on the dose rate. 125 cm was chosen as the LiH thickness because it relates to a dose rate at the astronauts of 1/10 the total allowed rate of 0.032 mSv/h. Since the density of tungsten is 19.3g/cm^3 as compared to the 0.73g/cm^3 for lithium hydride, it is preferred to use LiH over tungsten whenever possible. An equation will be developed, in a later section, which can be used to determine the required thickness of LiH once the amount of tungsten has been determined.

4.5.3 Tungsten Thickness

By holding the LiH thickness constant the effect on both the neutron and gamma dose rates of increasing the thickness of the tungsten layer are studied. The results from varying the W layer from 0 to 40 cm are shown in Figure 35. The dose rate due to the neutrons shows a dramatic decrease, dropping six orders of magnitude. The decrease is exponential in nature which is what is expected since W-182 (26.3% W_{nat}) is a strong neutron absorber. The cross sectional data for tungsten is located in Appendix E.

While the gamma dose also decreases exponentially, this decrease is much less pronounced than for the neutrons (three orders of magnitude compared with the six for neutrons). This reduced effectiveness for γ attenuation is not due to W inability to stop the gammas produced by the core, but rather the large neutron cross section of the tungsten and secondary gammas produced in the shield by the (n,γ) reaction.

4.5.4 Effect of Separation Distance between Tungsten Layer and Core

In order to reduce the level of secondary gammas produced within the tungsten it is necessary to reduce the number of neutrons which reach the tungsten. The first step in doing this was to locate the tungsten further from the

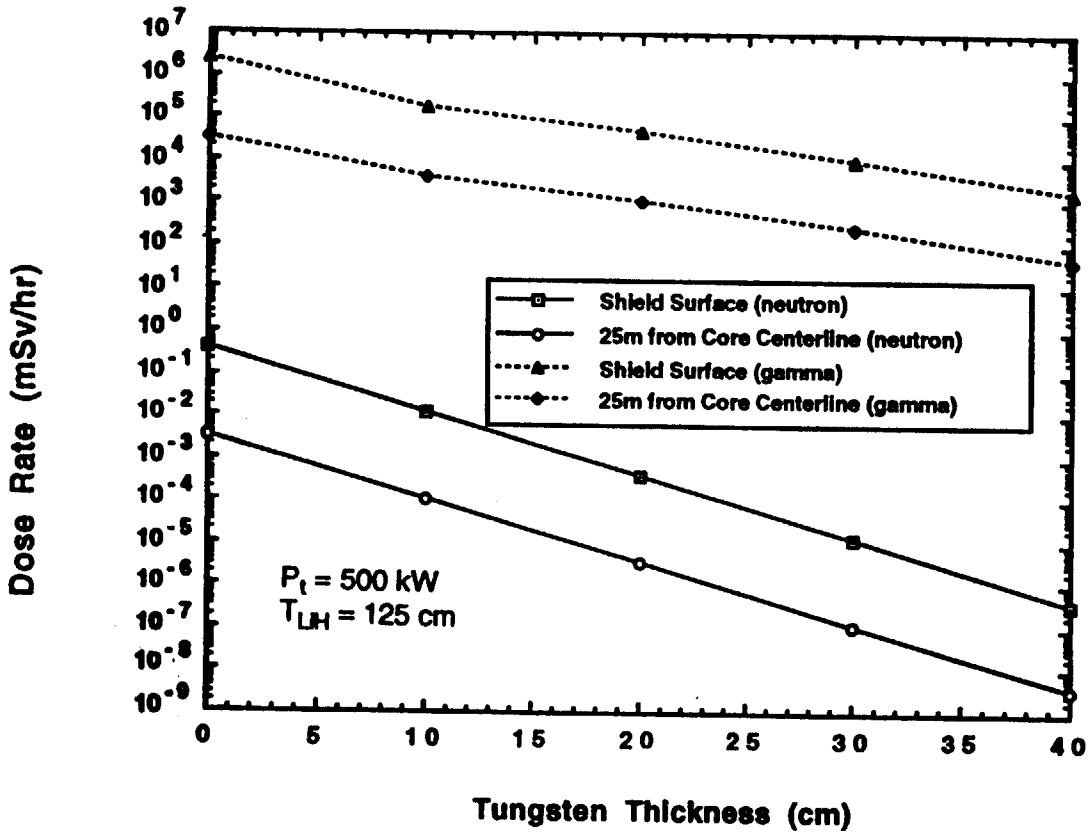

Figure 35: Dose Rate verses Tungsten Thickness

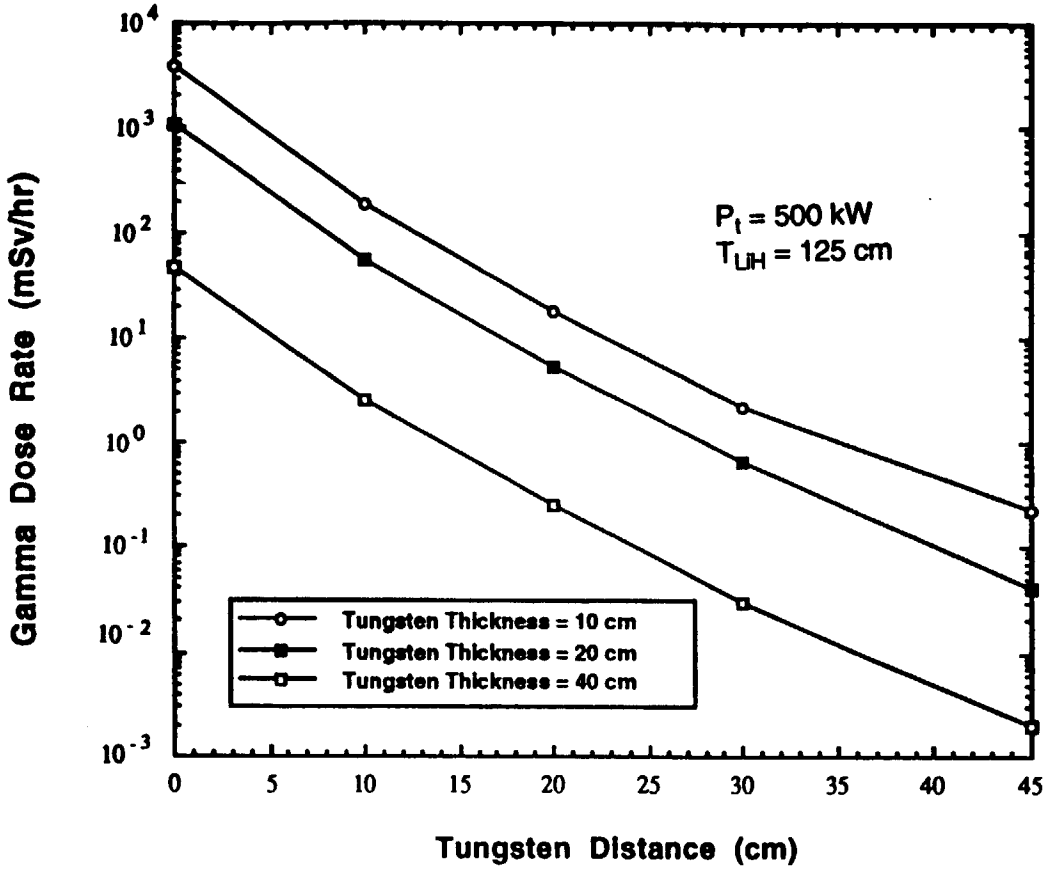

Figure 36: Dose Rate verses Tungsten Distance from the Core

reactor and inserting a layer of LiH within the gap. Doing this has the advantage of decreasing the neutrons by neutron attenuation within the LiH. By increasing the distance from the core edge, as expected, the gamma component of the dose rate was dramatically reduced. Placing 45 of the 125 cm of lithium hydride between the reactor and the tungsten lowered the gamma dose rate by over four orders of magnitude independent of the tungsten thickness. This result is shown in Figure 36 for a tungsten thickness of 10 cm, 20 cm, and 40 cm. While the use of 40 cm of tungsten placed directly adjacent to this reactor resulted in a gamma dose of ~ 0.045 Sv/h (this would surpass the 0.3 Sv/y limit in < 8 h and would prove fatal to the crew in ~ 9 days), a distance of 45 cm was enough to bring the dose down below the limit of 0.03 mSv/h. In fact, at this separation distance,a thickness of just over 20 cm of tungsten would be sufficient for a gamma shield. The problem here is that while placing the tungsten further from the core reduces the thickness needed, the mass of the tungsten for such a shield would be over 30 tonnes.

4.5.5 Multilayers of Tungsten

The next step in reducing the shield mass was to divide the tungsten gamma shield into 2 layers, similar to the ORNL shield discussed earlier. By doing this, the mass of the tungsten may be reduced further. In this case the first layer of tungsten was placed adjacent to the BeO reflector outside the reactor (22 cm from the core centerline). The separation distance between the first and second tungsten layers (ξ in Figure 33) was then varied from 0 to 45 cm. In all cases the total LiH thickness was 125 cm and the total tungsten thickness ($x_1 + x_2$) was 30 cm. The results of four cases are shown in Figure 37. These four cases represent a second tungsten layer thickness (x_2) equal to 30 cm, 20 cm, 10 cm, and 5 cm. The curves of Figure 37 show some interesting

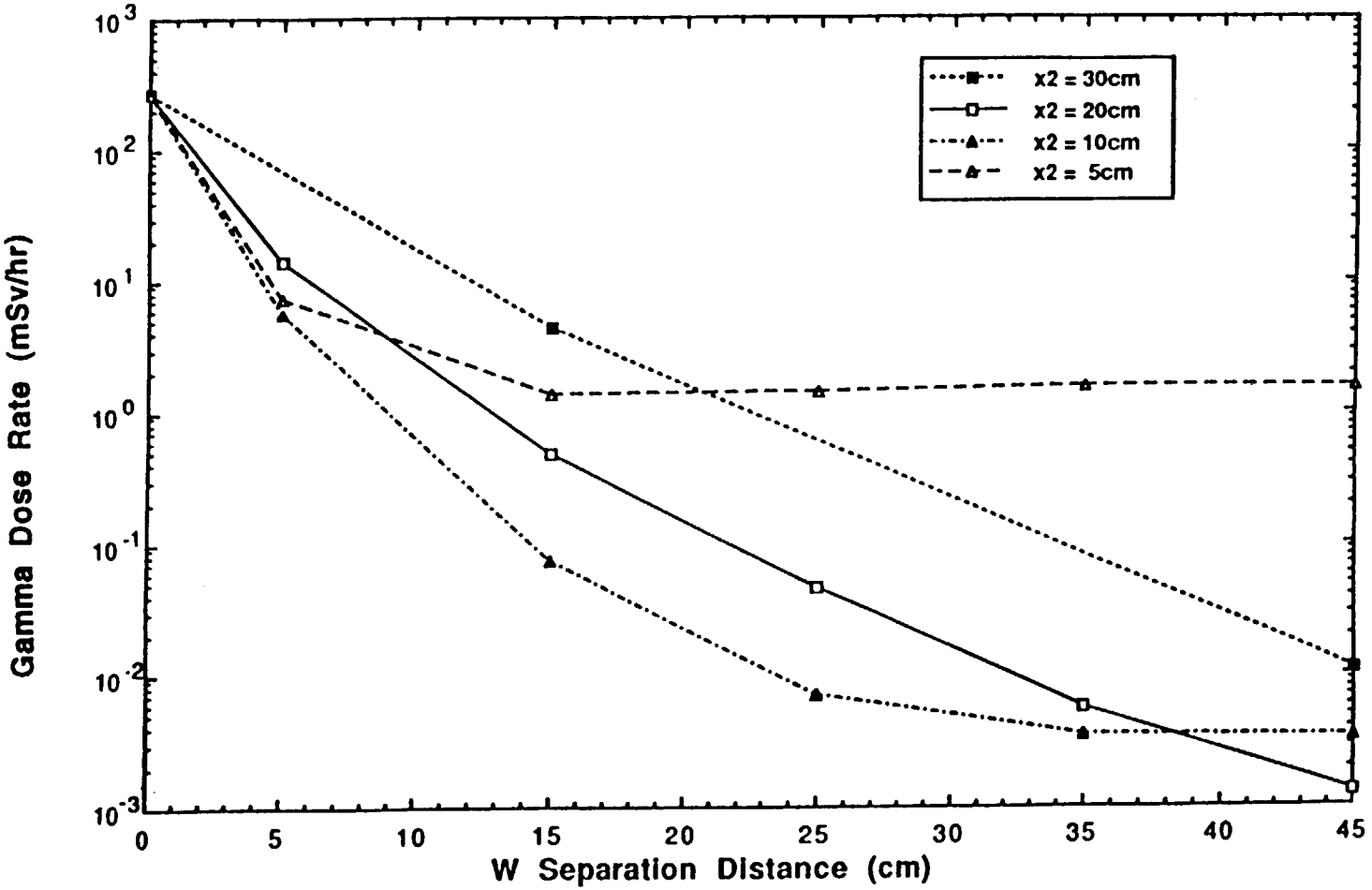

Figure 37: Dose Rate verses Tungsten Layer Seperation Distance

characteristic behaviors of the tungsten portion of the shield. First at $\xi = 0$ all four curves converge to the same dose rate. This is expected since the point simply represents a single layer 30 cm thick layer of tungsten placed against the BeO reflector.

As the separation distance begins to increase the three split tungsten shields show much smaller dose rates than single 30 cm layer of tungsten. The smaller dose rate is due to the fact that the first layer of tungsten, while producing many secondary gammas, also removes (through absorption) many of the neutrons produced in the core. In addition many more neutrons are removed by the LiH section separating the two W layers. The second layer of tungsten then absorbs many of the secondary gammas while producing few additional secondary gammas due to the lower neutron flux.

As the separation distance (ξ) between the W layers is increased beyond 10 cm the curve for x_2=5 cm levels out at a constant 1.5 mSv/h while beyond 30 cm the x_2=10 cm curve levels out at 0.003 mSv/h. This is because as ξ is increased a point is reached where the neutron flux is at a point where secondary gammas produced in the second layer becomes negligible. When the thickness of the second layer becomes larger, the separation distance at which the neutron interaction becomes negligible also increases. This is not only because the neutrons have a higher probability to interact within the larger thickness, but more importantly because the first layer is smaller; therefore, the flux is greater at the front of the second layer of tungsten. As seen in Figure 37, the combination of a 20 cm first layer and a 10 cm second layer gives the lowest dose rate up to ξ =38 cm where it crosses the x_2=20 cm line. This is preferred because not only is the dose rate lower, but the mass is also lower since a larger fraction of the tungsten is at a smaller radius.

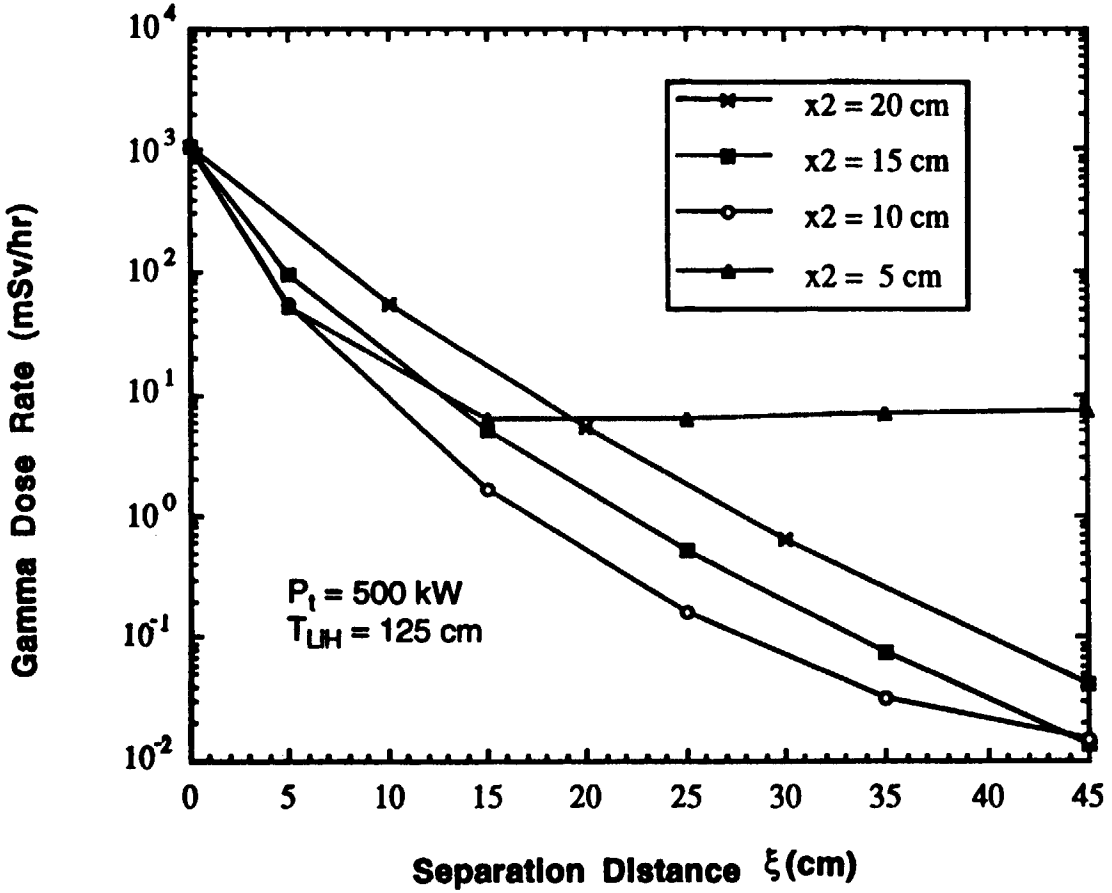

Figure 38: Effect on Dose Rate of Reduced Thickness W Multilayers

4.5.6 Dose Rate Results for Reduced Tungsten Thickness

Since the dose rate for the x_2=10 cm shield is 8.5 times smaller than the maximum dose rate, the shield mass can be reduced by eliminating a portion of the tungsten. In Figure 39 data, similar to that in Figure 38 is plotted; however, in this case, the sum of both tungsten layers is 20 cm. Here the dose rate to the astronauts is 0.03 mSv/h due to gammas when x_1=10 cm, x_2=10 cm, and ξ =35 cm. Using these dimensions will yield a substantial weight savings over the previous 30 cm thick tungsten shield.

4.5.7 Multilayer Tungsten/ Depleted Uranium Shield

The final step in order to evaluate a minimum shield mass is to replace the second layer of tungsten with depleted uranium (U-238). In this stage, the second layer of tungsten in the x_1=20 cm x_2=10 cm shield was replaced by depleted uranium. A layer of U-238 is chosen to compare to tungsten because of its excellent gamma attenuating abilities [Lamarsh, 1983] and its lower density (18.5 g/cm^3 compared to 19.3 g/cm^3)[Walker, et.al, 1984]. The disadvantage with U-238 is that if it is exposed to fast neutrons ($E_n \geq 0.6$ MeV), the atom can undergo fission, causing an increased dose rate to the astronauts by both secondary gammas and neutrons. In addition, the fissioning of U-238 will increase the heat generated in the radiation shield, which may cause severe deterioration the shields ability to attenuate the oncoming radiation may occur if the shields temperature becomes too high [Barratino, 1985]. For these two reasons only the second layer of the shield used U-238. Being placed outside a layers of tungsten and two layers of lithium hydride the neutron flux (especially fast neutrons) is significantly lower.

When the second layer of tungsten is replaced by depleted uranium the W-W shield showed a slightly lower dose rate. The results of the W-U shield

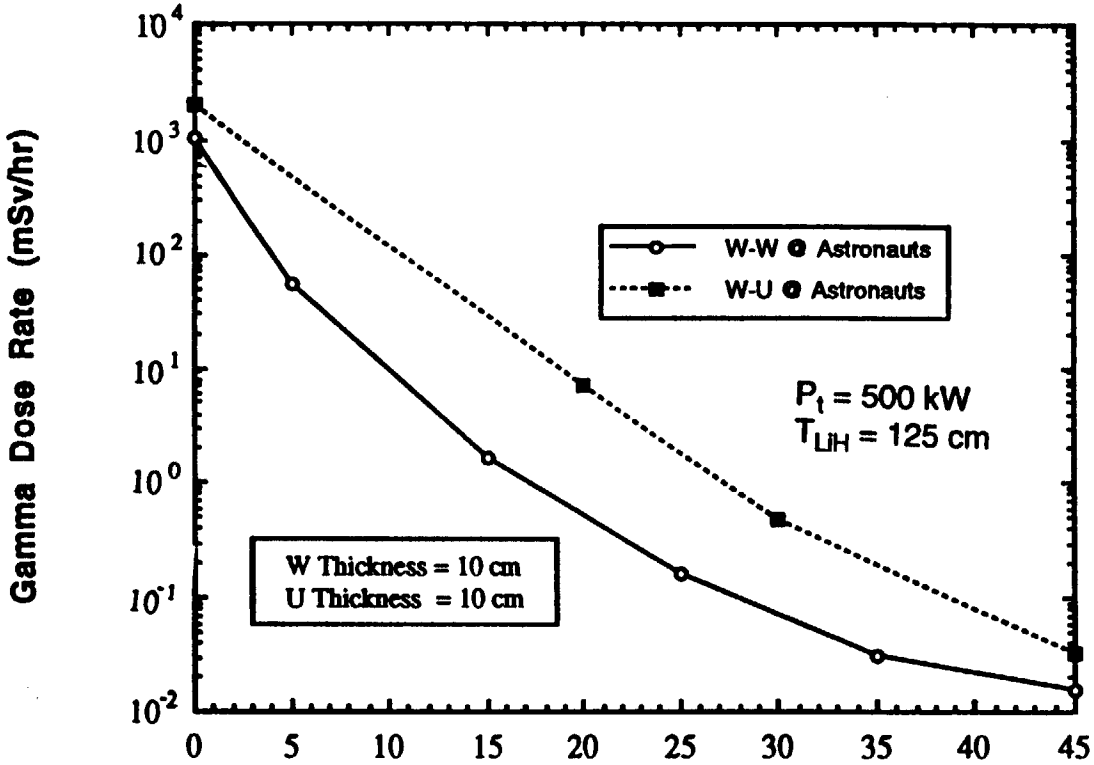

Figure 39: Comparison of Astronaut Dose Rate W/W and W/dep. U

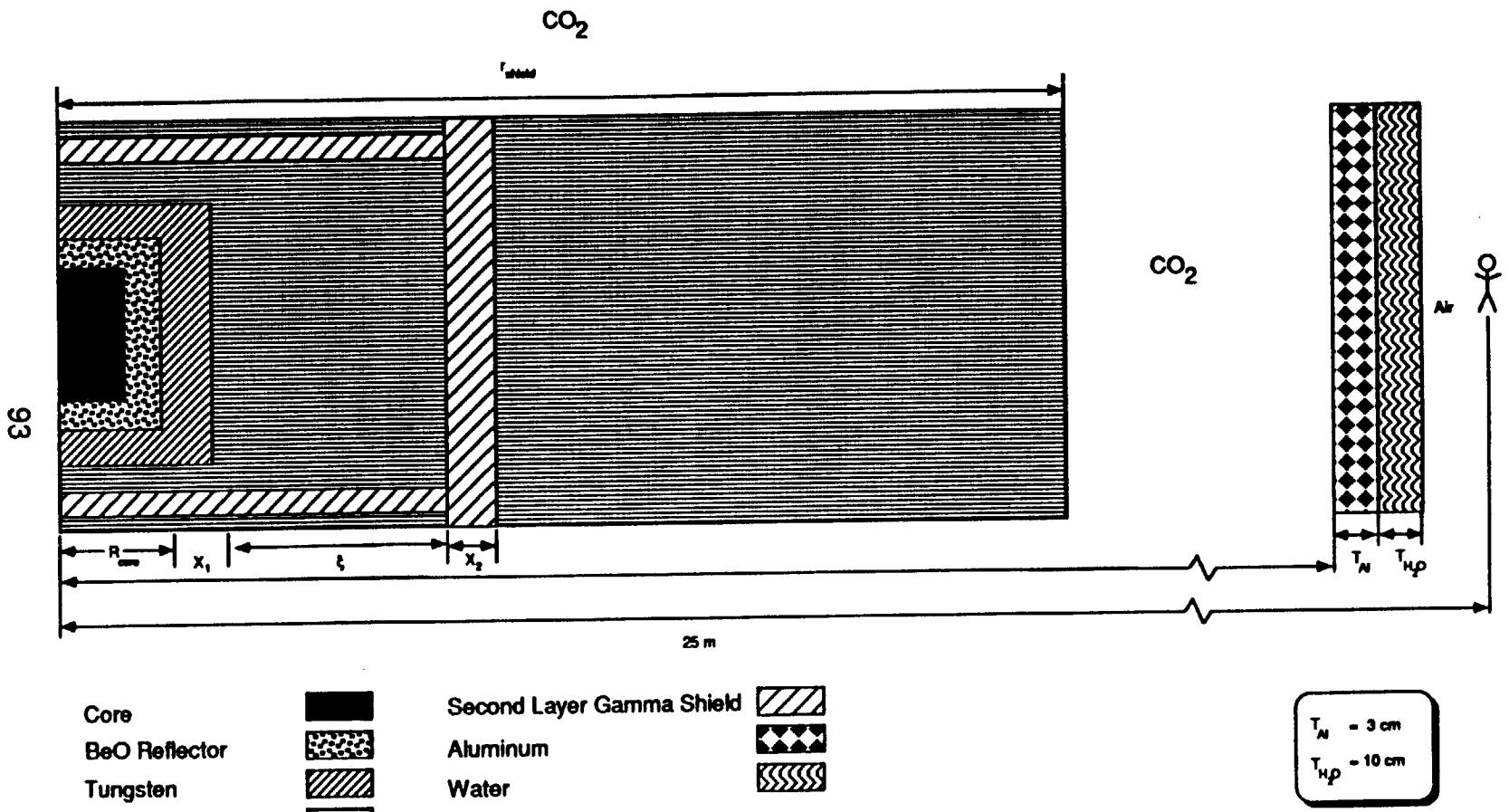

Figure 40: Two-Dimensional Core Shield Configuration

analysis are compared with those from the previous W-W shield in Figure 39 (a and b). While the curve shows that a combined tungsten-uranium shield is superior for a x_1=20 cm and x_2=10 cm, when x_1 is reduced to 10 cm the W-W shield yields a significantly lower dose rate, therefore, a W-W shield was chosen for lower shield mass.

4.6 **Two Dimensional Verification**

For the two dimensional verification of the shield layer thicknesses, the core shield configuration shown in Figure 40 was used. For all the runs the r direction is identical to that used in the one-dimensional case. The core model previously described was inserted as the source generator, and a secondary layer of tungsten was placed above and below the reactor. The first tungsten layers above and below the reactor are smaller that x_1. The justification for this is twofold. First, as can be seen by the flux curve in Figures 28 and 30 the radiation levels from both neutrons and gammas are lower at the ends than at the sides. Secondly, a higher dose rate at the edge of the shields may be allowed, with only sufficient shielding needed to protect the astronauts from radiation scattered from the CO_2 atmosphere or the Martian soil. The results of the two-dimensional runs are shown against the 1-D results in Figure 41. It can be seen that going to the two dimensional geometry reduces the calculated dose to the astronauts by ~15%. This helps to confirm that the 1-D dimensions calculated for the shield are more than sufficient to protect the astronauts.

4.7 **Shield Design**

From the results in the previous sections it can bee seen that a cylindrical shield consisting of 63 cm of lithium hydride, and two layers of tungsten, the first being 11 cm thick while the second is 9 cm thick will sufficiently protect a group

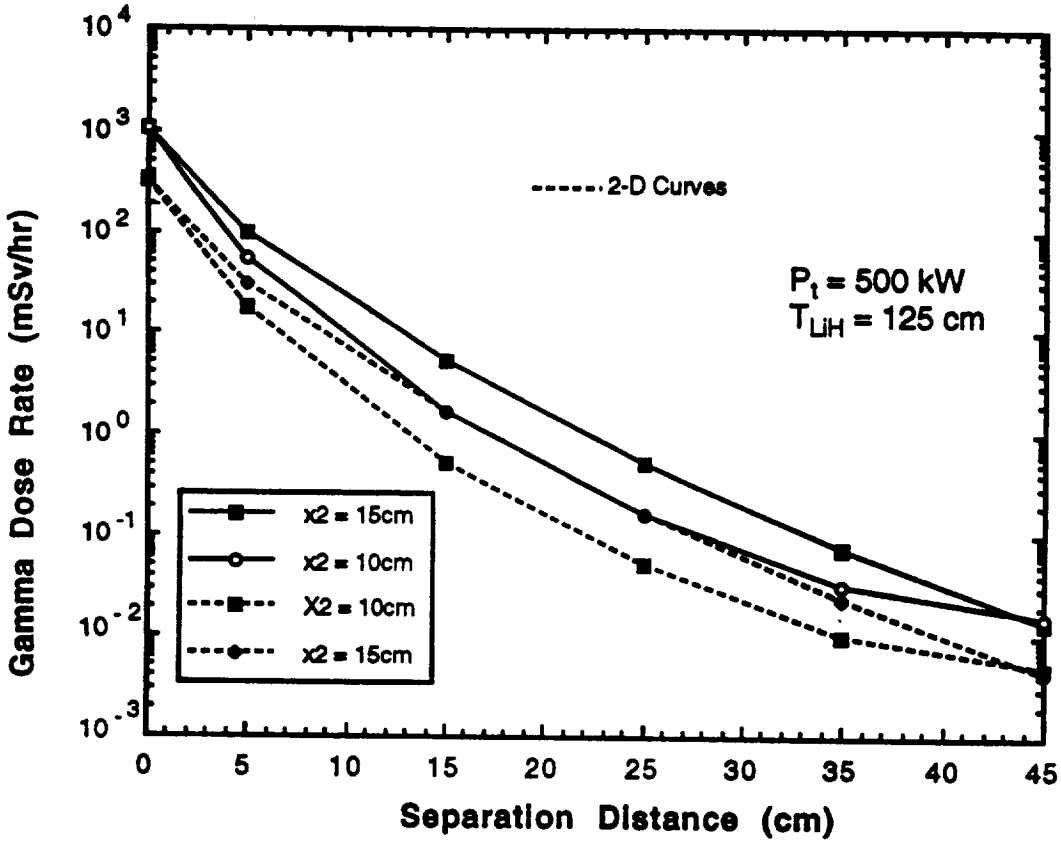

Figure 41: Comparison of 1-d to 2-D Results

of astronauts at a distance of 25m. However, while this shield reduces the radiation from the reactor to a sufficiently low level for the crew, it is be extremely massive and protects a larger area than needed.

For the train rover it is anticipated that a majority of the astronaut's time will be spent within the rover. Therefore, it is of primary concern to protect this area. If the shield is designed so that some of its mass on the sides not directly facing the astronauts is trimmed away, then a large mass saving may be incurred. Because of the vacuum of space removing large portions of a shield (leaving only a shadow of protection) mearly limits the area which is usable by equipment and crew. However, on Mars scattering off of both the soil and atmosphere can increase the dose rate. For this reason, along with the need for limited access around the reactor car, the shielding on the side of the reactor cannot be completely eliminated.

In addition to the thickness of the side shielding is the forward angle which will get the maximum protection from the shield. Figure 42 shows the layout of the rover along with the 25m radius from the reactor and several forward angles. The minimum shield angle is determined by the smallest possible angle needed to completely cover the PCV and EU. Of course, if any significant amount of work is to be completed outside the rover, then a larger forward angle will be required.

Besides protecting the astronauts during any work outside the rover, the vehicle must be protected while turning, Figure 43 shows the turning protection. With the minimum angle (8.6%) primary control vehicle leaves the zone of maximum protection (ZMP) with only a few degree turn. While a 90° forward angle on the shield would give protection for even the most severe turns, it is felt that such a small fraction of the transit time would be dedicated to high degree turn that this would be too conservative. In addition, by taking proper

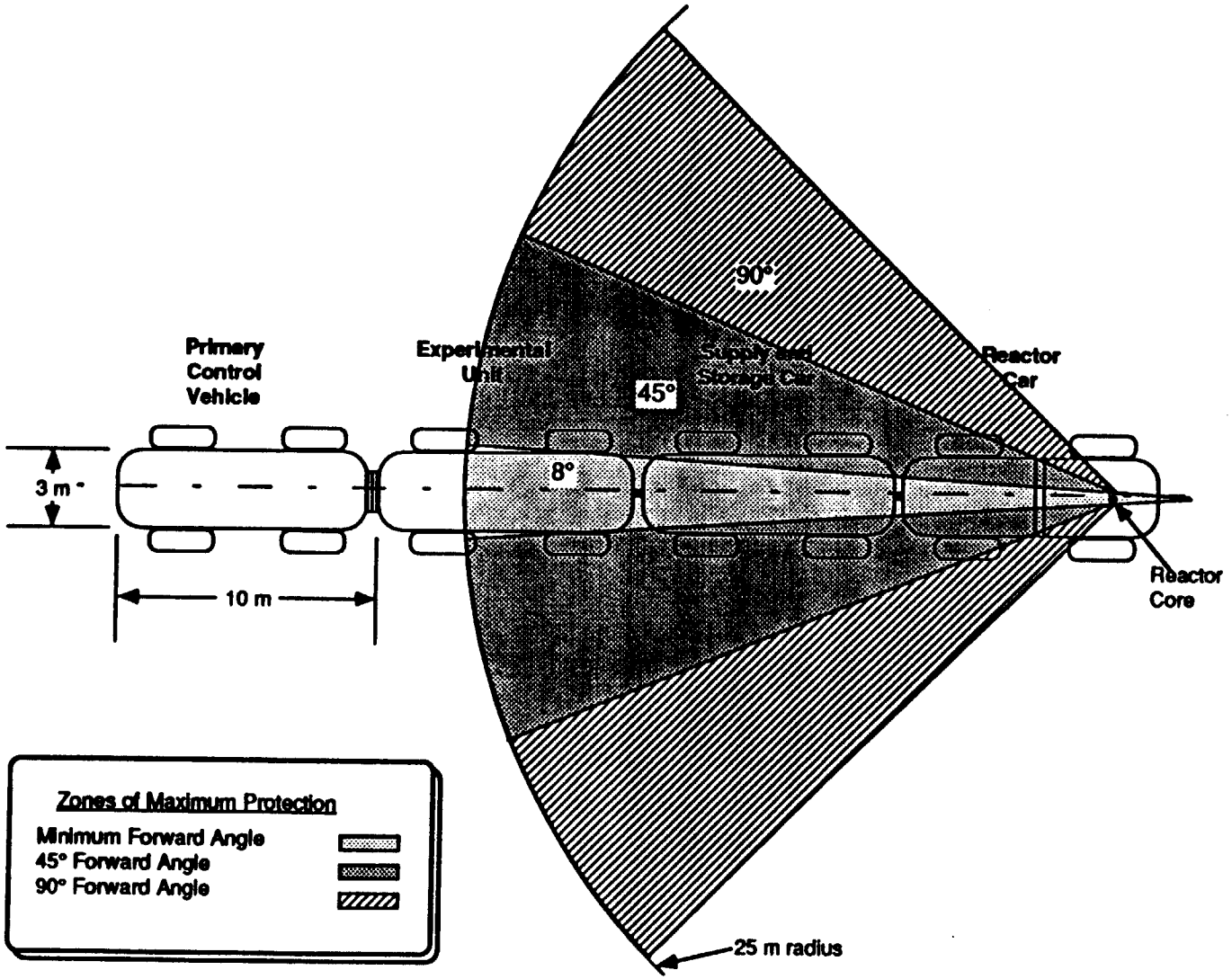

Figure 42: Area of Protection For Various Shield Forward Angles

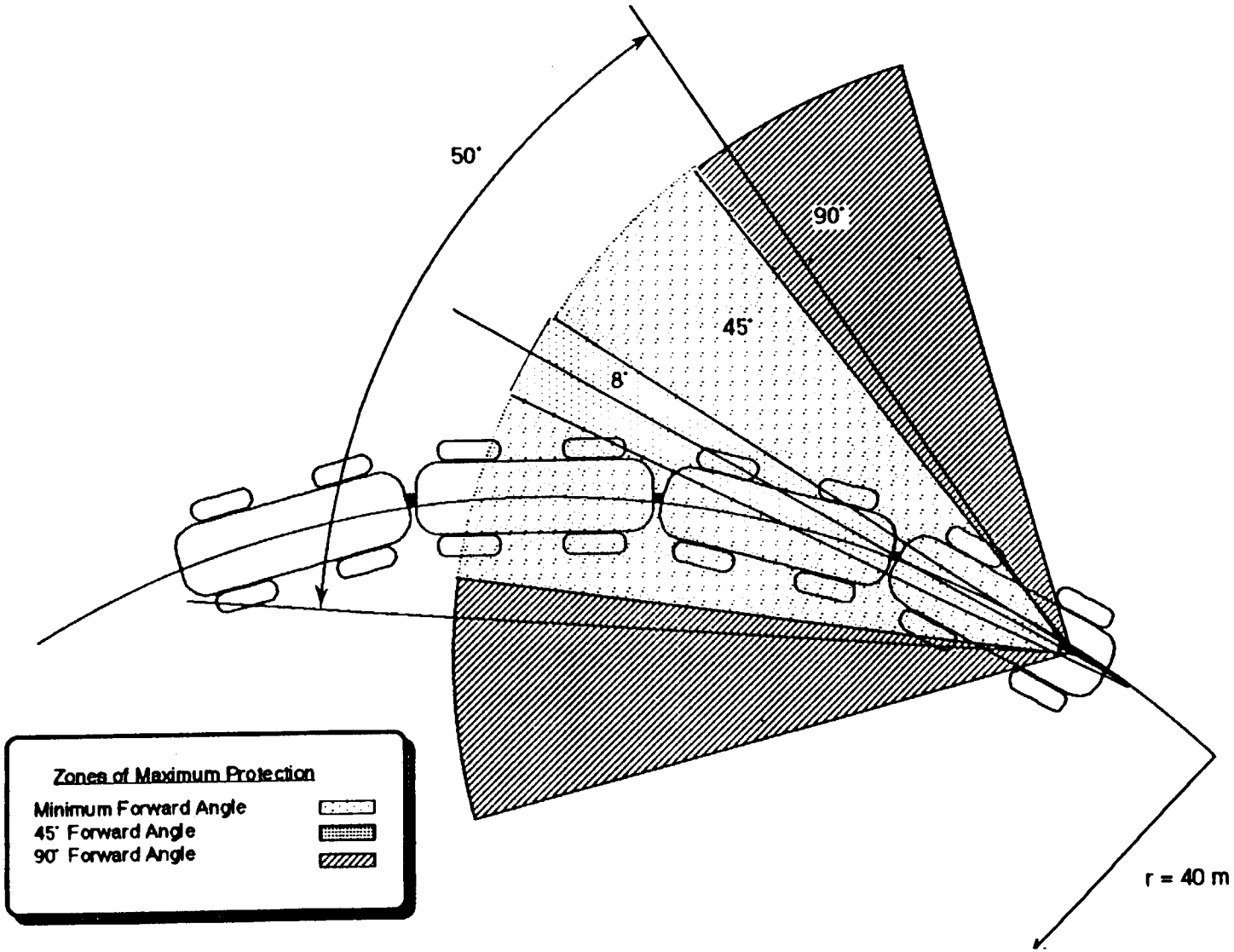

Figure 43: Turn Protection for Various Shield Forward Angles.

precaution, a majority of the severe turns may be avoided. A forward shield angle of 50° was selected. This will allow the rover to have a turning radius of 40 m while remaining in the ZMP, although sharper turns should be avoided if possible, they can be made as long as their time of execution is kept small.

With the information in the previous curve, the shield configuration and dimensions can now be determined. From Figures 34 and 35 an estimate of the required lithium hydride thickness may be determined given the total tungsten thickness used. The equation is as follows:

$$D.R.(LiH) = C \exp(T_w) \exp(T_{LiH}) \tag{13a}$$

or solving for the LiH thickness and rearranging,

$$T_{LiH} = \left[\frac{D.R.(LiH)}{C \exp(T_w)}\right] . \tag{13b}$$

Of course in order to use these equations for the lithium hydride thickness, it is first required that the tungsten thickness is known. Also, equation 13b is no longer valid if the separation distance ξ is less than the LiH thickness.

To determine the required W thickness and the separation distance, ξ, curves similar to Figures 35 and 36 were used. The typical shield layout is shown in Figure 44 and 45. For the base case of a 500kW$_t$ reactor we have x_1=11 cm, x_2=10 cm, ξ =40 cm, and T_{LiH}=65 cm for the forward direction. For the sides dimensions are slightly smaller due to the higher allowed flux at the surface of the shield. Here the dimensions are:

x_1 = 7 cm
x_2 = 9 cm
ξ = 30 cm
T_{LiH} = 41cm

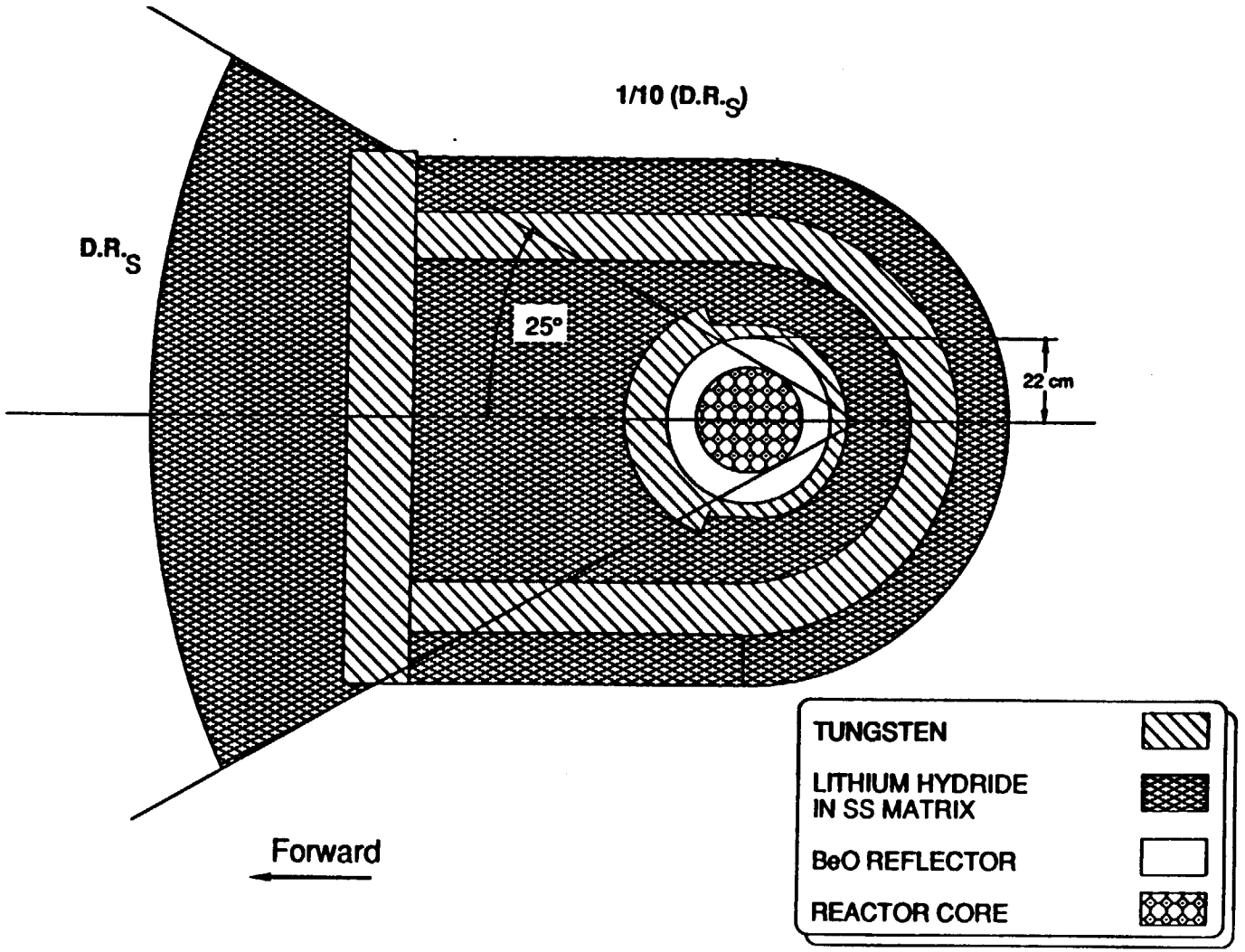

Figure 44: Reference Shield Layout for Manned Mars Rover (top view)

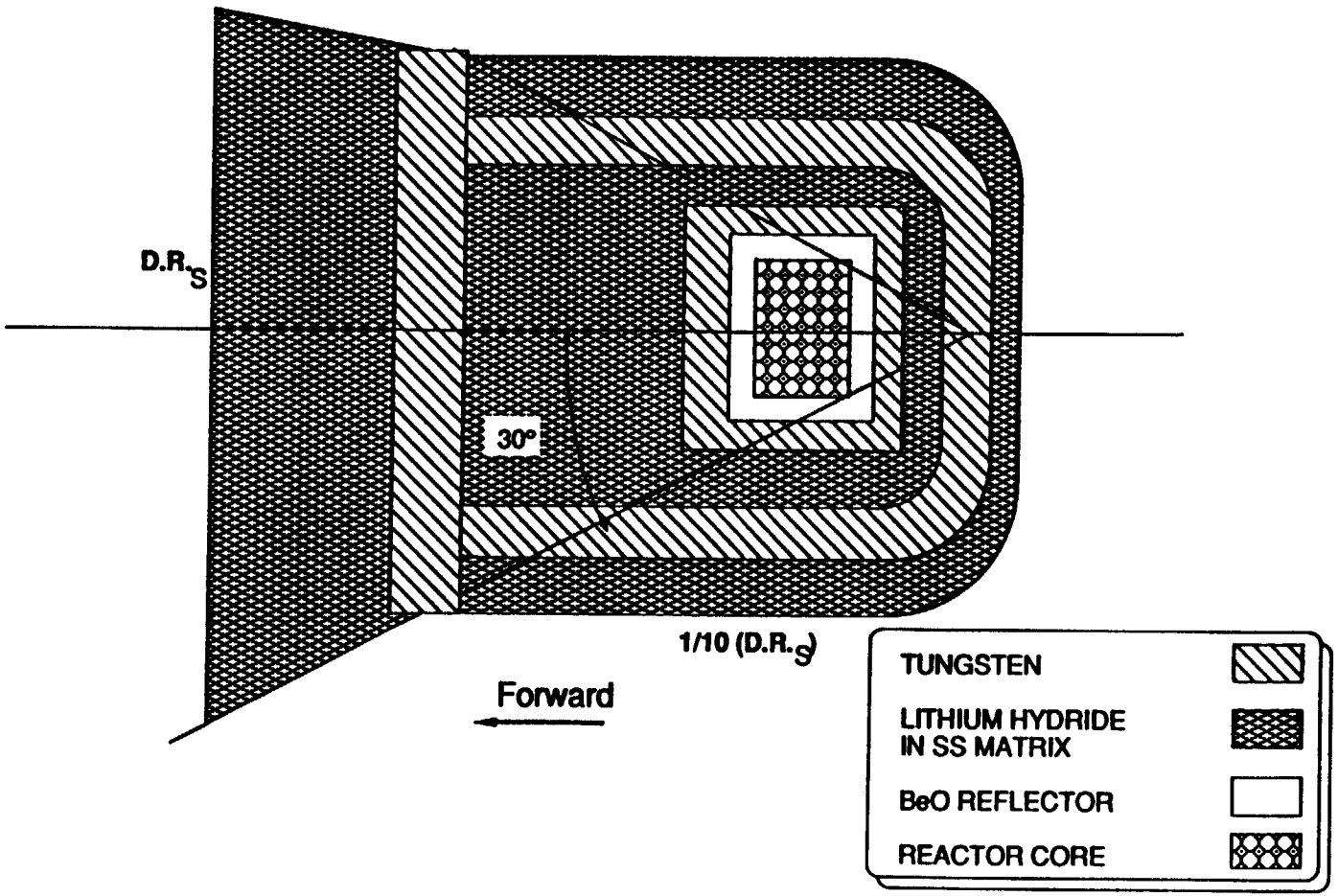

Figure 45: Reference Shield Layout for Manned Mars Rover (side view)

The total shield mass is 16,567 kg. In order to develop an approximation for the shield mass, an analysis was performed at four additional power levels (100, 200, 300, and 1000 kW_t). The mass versus power level is shown in Figure 46. By fitting an equation to the curve the following formula was generated:

$$SM_{shield} = 1494\ (P_{th})^{-0.6203} \tag{14}$$

where SM_{shield} is the shield specific mass in kg/kW_t and P_{th} is the reactor thermal power in kW_t. While this equation seems rather simplistic, it should be remembered that shield are quite reactor specific and much more than a rough estimate can give a false sense of finality to a conceptual design. By comparing masses calculated by this equation to designed man-rated shield masses [Bloomfield et. al,1989; Engle et. al, 1971], the results appear to be reasonable (in a general sense) to within 1000 kg. This equation will be used later once the reactor thermal power is determined from the energy conversion system efficiency.

A source of conservatism, that will be seen in the results of the total PPS mass, is the assumption that the reactor will be operating at its nominal thermal power all the time and assuming constant core dimensions, regardless of the reactor thermal power level. In reality, it is expected that the reactor power at night will be reduced by more than 50% when mobility power is not needed (life support power and user power are only 30 kWe). When a thermal power of 0.75 of nominal is used in equation (14) to account for a 50% reduction in reactor power during the non-driving periods, the shield mass can be reduced by 10 percent without exceeding the maximum permissible dose rate of 0.032 mSv/h to the crew on board the rover vehicle.

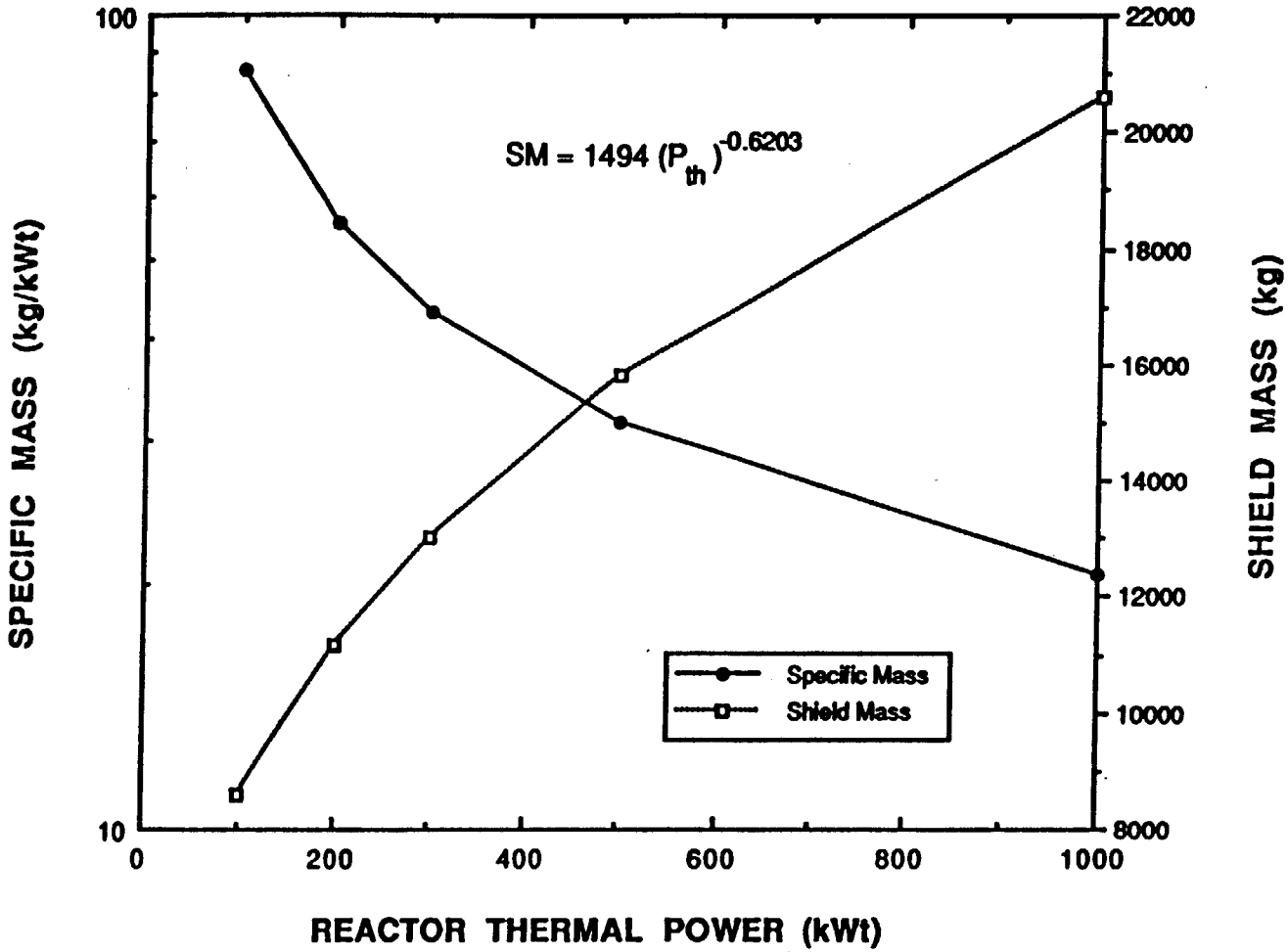

Figure 46: Shield Mass verses Reactor Thermal Power for a Manned Mars Rover

5. REACTOR AND RADIATOR

5.1 Reactor Specific Mass

It will be shown that the selection of the conversion system will strongly influence the mass the other three main system components; namely, the reactor, radiation shield, and waste heat radiator. An equation for the effect of the thermal power on the mass of the shield has already been developed; however, it is also necessary to have the relationship for the reactor mass versus the thermal power of the reactor. Increased power requires a larger reactor mass and size. The following equation is developed from a curve fit of past and present space reactor designs (see Figure 47) and is used to calculate the reactor specific mass as:

$$SM_{reactor} = 66.54\ (P_{th})^{-0.7189} \qquad (15)$$

Although equation 15 is not an exact relationship, it does give a reasonable estimate of the reactor specific mass. The maximum deviation from the mass of the reactor system used was 15%, which yields an error in the calculated mass of 50 - 150 kg. This deviation is only a small fraction of the overall reactor system mass; therefore, this difference will yield less than a 2% error in the calculation of the total system mass.

5.2 Radiator Specific Mass

For three of the four energy conversion systems considered in the next section the waste heat is rejected by means a thermal radiator. Both the surface area and the mass are very sensitive to the rejection temperature, with higher rejection temperature corresponding to lower radiator mass. It will be seen;

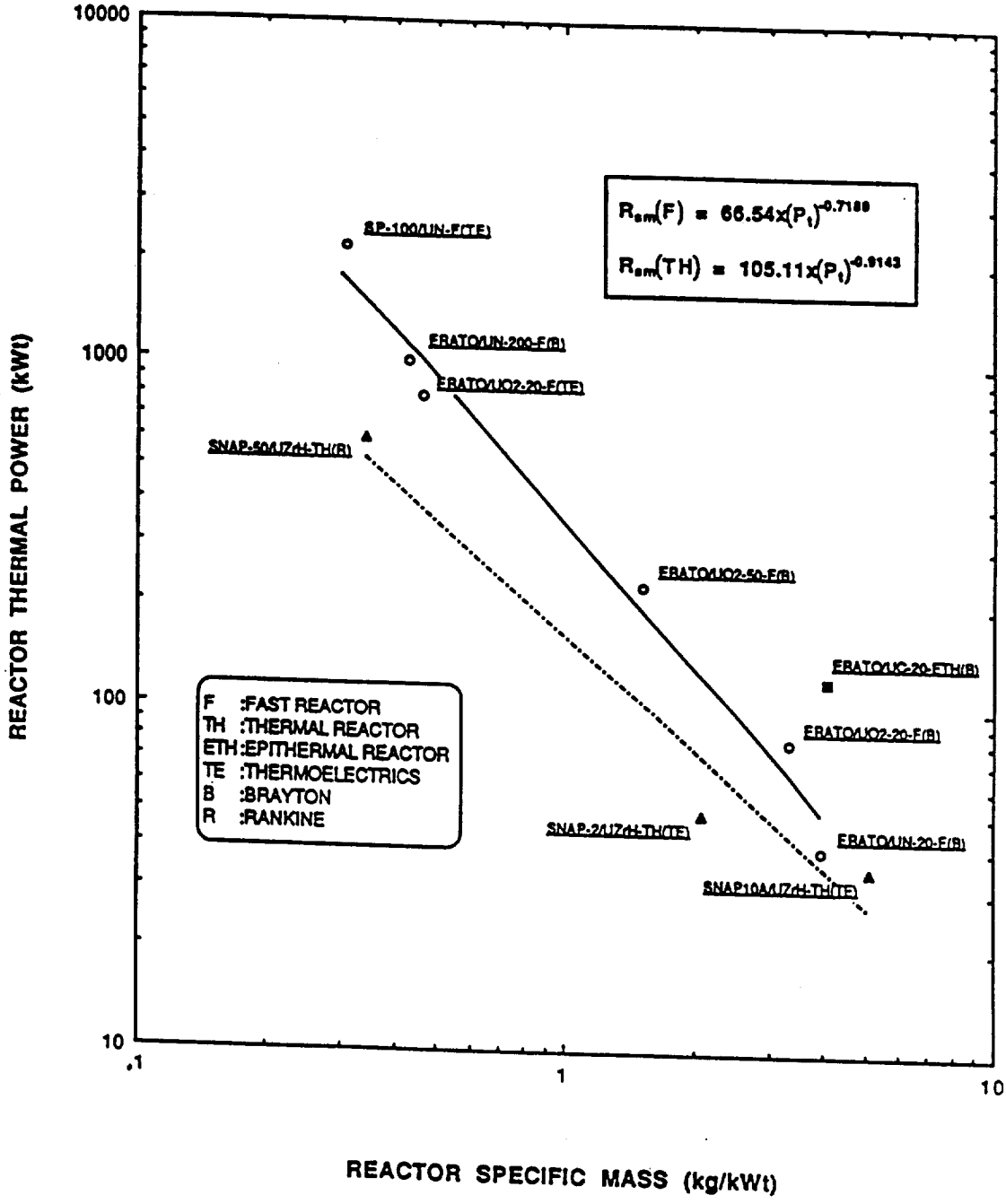

Figure 47: Reactor Specific Mass Curve.

however, in the next section that this high radiator temperature will decrease the conversion efficiency which increase the shield mass [Angelo and Buden, 1985]. The manned rover offers both advantages and limitations for a radiator heat rejection system.

In order to maintain simplicity and allow the reactor to operate continuously the area of the radiator panels is limited to the surface area of the reactor car, <100 m^2. While this will restrict the lower temperature end of the energy conversion system, it will allow the reactor car to remain a single self contained unit, without large awkward fins. The radiator material selector for use in the rover should exhibit the following qualities:

1) high strength to mass ratio,
2) high thermal conductivity,
3) compatibility with working fluid or coolant,
4) compatibility with Mars atmosphere,
5) high emissivity, and
6) good structural integrity.

The material considered for the radiator will eventually be dependent on the power conversion system, since the correct choice can only be made once the operating temperature is known [Angelo and Buden, 1985]. Although the material selection cannot be made without a better understanding of the operating conditions currently space radiator designs range in a mass per area from 1 to 10 kg/m^2 depending upon the amount of armor included. On the surface of Mars micrometers (a major concern in space) are not a concern, therefore, a large amount of armor is not necessary. A conservative 5 kg/m^2 was selected to be used as the radiator mass.

The radiator area can be calculated as a function of the radiator temperature and the ambient temperature raised to the 4th power [Bennett and Myers, 1982]. For the radiator calculations the following equation is used:

$$A = \frac{P_{rej}}{\sigma F\left(\varepsilon T_{rad}^4 - \alpha T_{am}^4\right)}, \qquad (16)$$

where A is the radiator area (m^2), P_{rej} is the thermal power rejected (kW_t), σ is the Stefan-Boltzmann Constant, F is the view factor, ε is the radiator surface emissivity, α is the radiator absorptivity, and T_{rad} and T_{am} are the radiator and ambient temperatures, respectively. Using values of radiator materials currently available [Angelo and Buden, 1985] and information on Mars [Kaplan, 1988], the radiator variable are selected as follows: $\varepsilon = 0.85$, $\alpha = 0.2$, and $T_{am} = 250$ K. The view factor F is taken as 0.8 to allow for reflection off the planet's surface. The Specific Area of the radiator versus the radiator temp is shown in Figure 48, where the importance of maintaining as high a temperature as possible can be seen.

The specific mass equations for the radiator, reactor, and shield may now be used to evaluate the mass benefits obtained from various energy conversion systems. This comparison will be carried out in the following chapter.

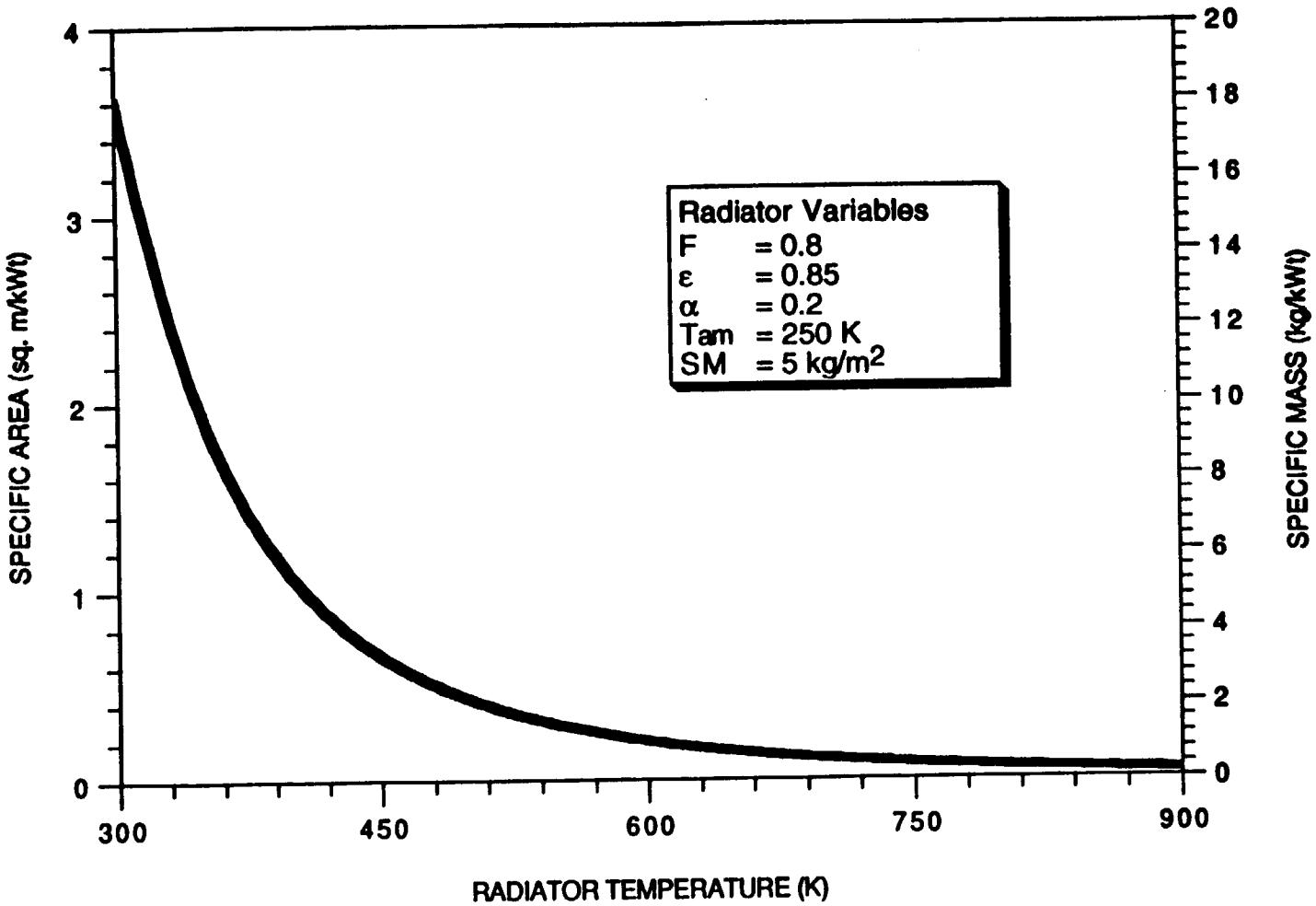

Figure 48: Radiator Area and Specific Mass verses Surface Temperature

6. ENERGY CONVERSION SYSTEM

As we have seen in the last sections, the mass of the radiation shield, reactor, and waste heat radiator are all dependent on the thermal power of the reactor. The reactor thermal power is controlled by two main factors: 1) the electrical power required by the rover, and 2) the efficiency of the energy conversion system. In order to minimize the shield mass and overall system mass, an efficient energy conversion scheme is required. In this section four energy conversion systems are assessed for use with an SP-100 type nuclear reactor system in a manned mars rover. The conversion systems under investigation are: 1) SiGe/GaP Thermoelectrics (TE), 2) CO_2 Open Brayton Cycle (OBC), 3) He/Xe Closed Brayton Cycle (CBC), 4) Free Piston Stirling Engine (FPSE). Each of these four systems display certain advantages and disadvantages which will now be discussed.

6.1 **Thermoelectric Conversion**

Thermoelectric (TE) conversion is a way to directly convert thermal energy into electrical energy based upon the Seebeck effect. While this effect was originally noticed through the junction of two dissimilar metals, the appearance of specially tailored semiconductors has increased the conversion efficiency. Modern TE devices use the junction of doped p-type and n-type semiconductor [Angrist, 1976]. The electrical output of the TE device depends on the temperature drop across the TE, the properties of the semiconductor (electrical resistance, thermal conductivity, and Seebeck coefficient), and the specific design of the converter element. Figure 49 the layout of an idealized converter [Angelo and Buden, 1985].

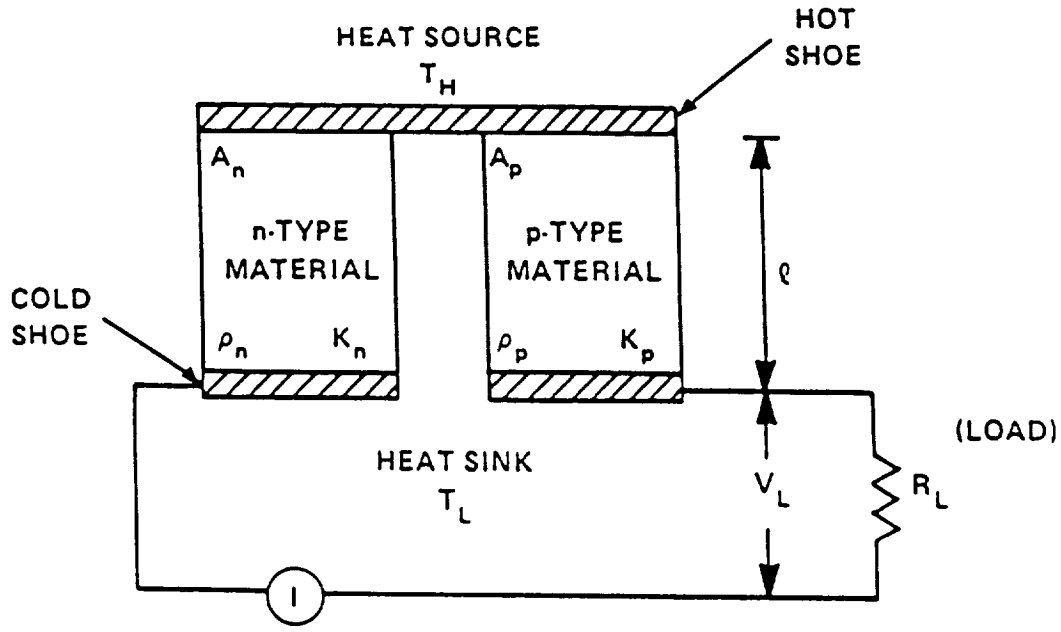

Figure 49: Idealized Thermoelectric Converter.

TE converters have been flown in space by the U.S. since 1961 with the launch of the of the Transit 4a and 4b satilites. Since then TEs have amassed an impressive flight history, having been flown on all of NASA's most exciting missions to the outer edges of the Solar System. TEs have demonstrated both a high degree of reliability and predictability throughout their lifetime [Angelo and Buden, 1985].

The use of TE conversion in the area of space nuclear power has, however, been primarily limited to RTG systems. The only flight experience with TE conversion on a space reactor was on the SNAP-10A system in 1965. The TE material used was a Silicon/Germanium (SiGe) mix. While the TEs performed as expected, the reactor was accidentally shutdown after only 42 days of operation. The SP-100 Space Nuclear Power System, currently under design by General Electric, will also use TE conversion. While the standard TE element used in the past has been the unicouple design (see in Figure 50), the SP-100 TEs are designed in the form of multicouple cells. The layout for these cells are shown in Figure 51. Unlike the Unicouple which contains a single TE element per couple, the Multicouple contains 32 elements per cell. The total SP-100 power conversion system design calls for a total of 4320 multicouples to be used.

Because power conversion system of the SP-100 has already been designed to deliver 100 kW_e, the same design parameters are used for the evaluation of TE conversion in the rover power system. These Parameters include: T_{rad} = 800K, number of cell = 4320, conversion efficiency = 5.4%, reactor thermal power = 2331 kW_{th}, rejected power = 2131 kW_{th}, and converter mass = 370 kg [General Electric,1988]. From these values the component mass for thermoelectric conversion on a manned rover may be calculated from the

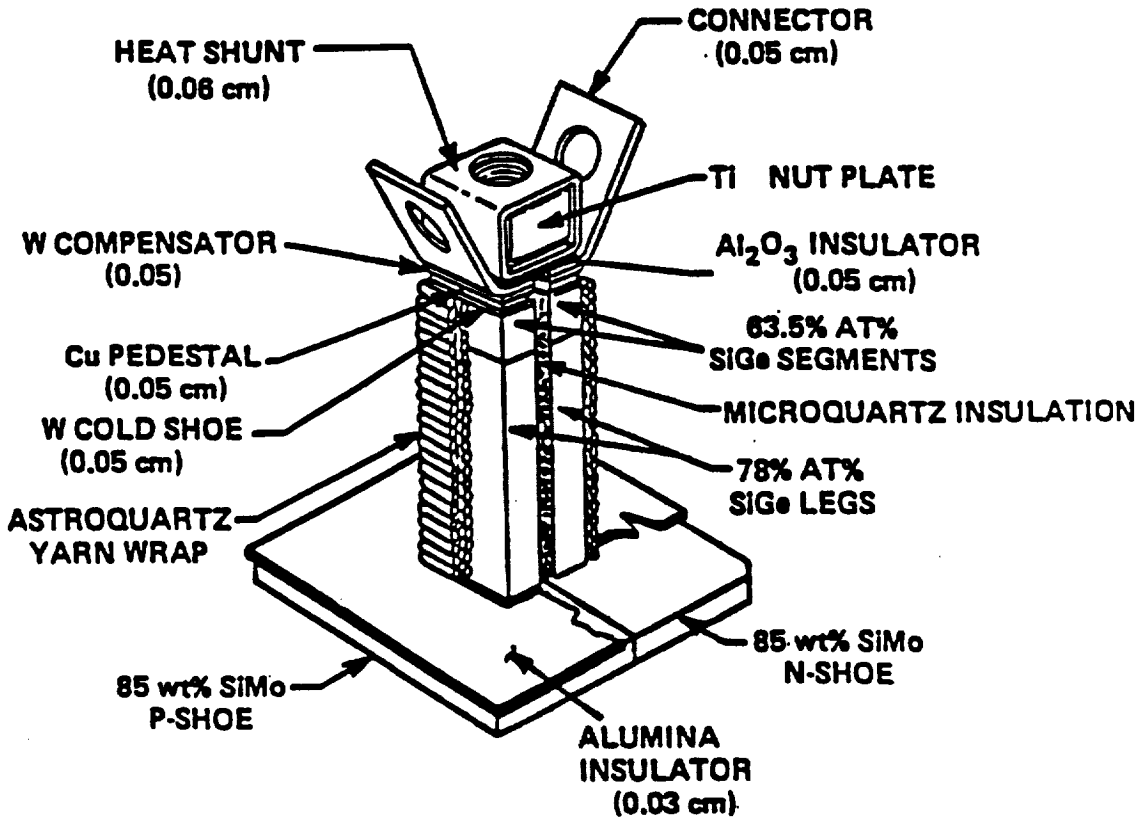

Figure 50: Thermoelectric Unicouple Element

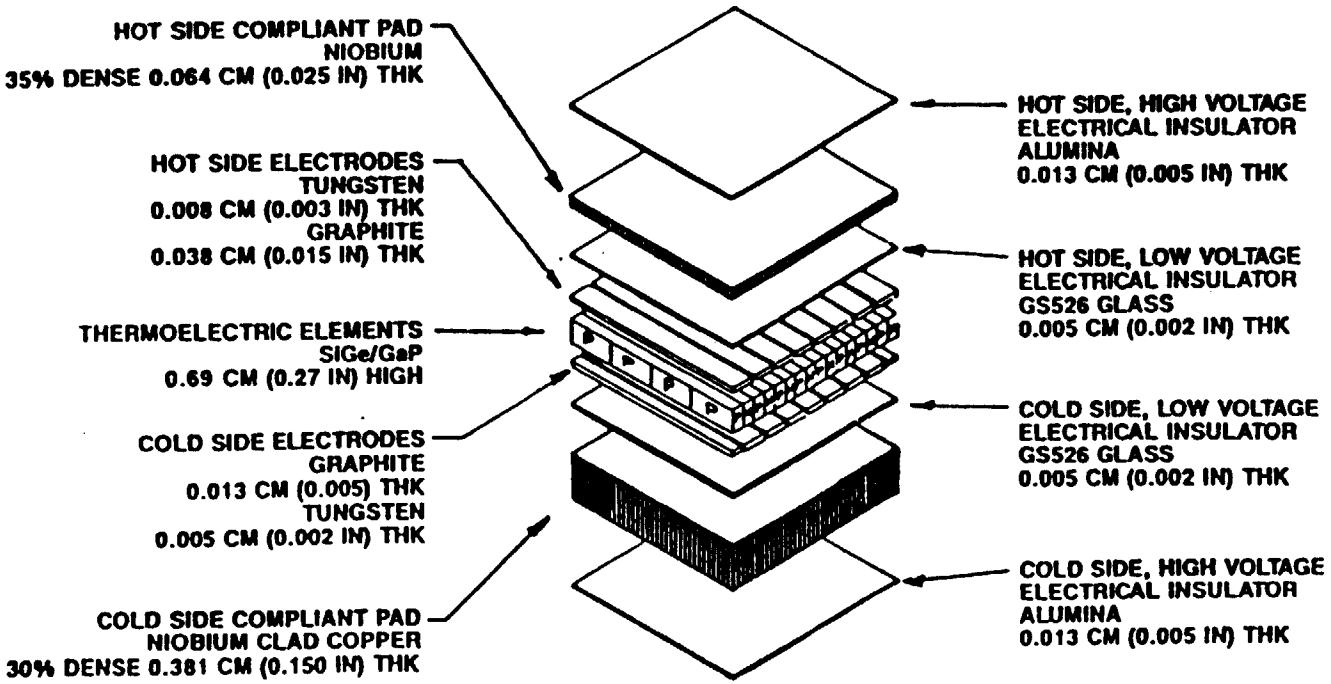

Figure 51: Multicouple Element For SP-100

equations developed earlier. The results of these calculations are given in Table 9.

Table 9. Mass Breakdown of TE Conversion System for Manned Rover.

Reactor	Shield	Converter	Radiator
563 kg	27600 kg	1300 kg	430 kg

While Thermoelectric systems have shown a high degree of reliability in past use from the component mass breakdown it is seen that the mass of a rover powered by a nuclear reactor with a thermoelectric conversion system comes nowhere near the design goal of 100 kg/kW$_e$. For this reason a Thermoelectric system is ruled out as a choice for the rover energy conversion system.

6.2 CO_2 Open Brayton Cycle

The use of a CO_2 Open Brayton Cycle (OBC) in a Mars rover eliminates the Thermoelectrics problem of large shield mass due to low conversion efficiency. By using the atmospheric CO_2 as the working fluid the system has the potential to operate at extremely high efficiencies (>50%), due to the low ambient temperature (t_{ave}~230 K).

The OBC operates according to the P-v and T-s diagrams shown in Figures 52 a and b. Figure 53 shows a system layout for OBC with a regenerator. The cycle consists of intake of atmospheric CO_2, isentropic compression, isobaric heat addition, isentropic expansion, and finally expulsion of the gas back to the atmosphere. The efficiency of the a simple OBC can be

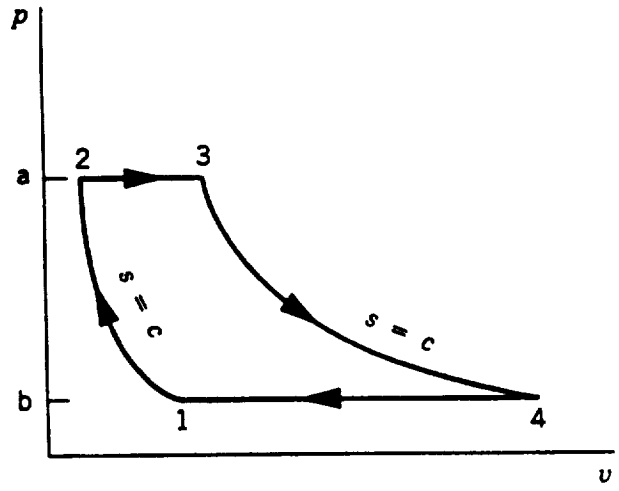

Figure 52a: P-v Diagram For Open Brayton Cycle

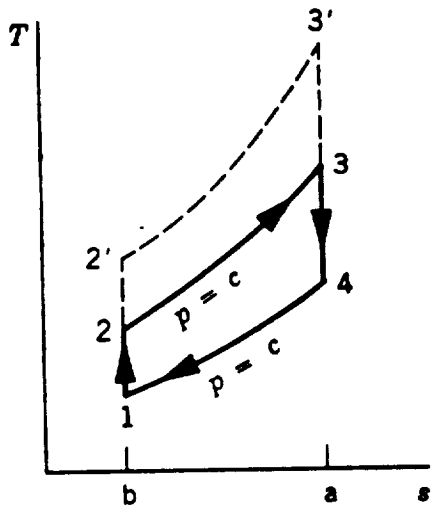

Figure 52b: T-s Diagram for Open Brayton Cycle

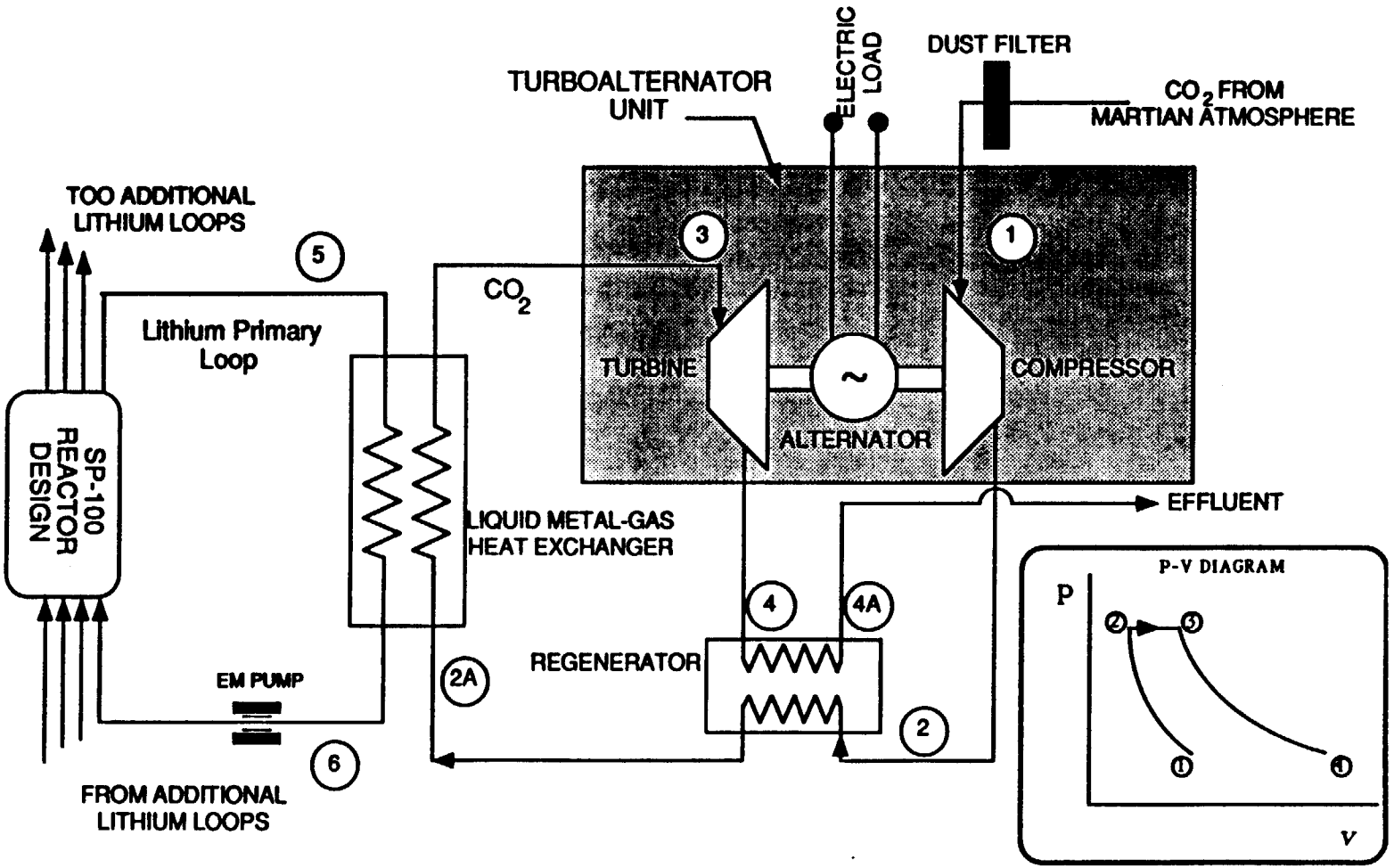

Figure 53: System Diagram for Open Brayton Cycle

calculated as :

$$\eta_{th} = 1 - \frac{1}{(P_2 - P_1)^{(k-1/k)}} \qquad (17)$$

where η_{th} is the thermal efficiency, P_1 if the inlet pressure, P_2 is the compressor outlet pressure and k is the ratio specific heat at constant volume to specific heat at constant pressure. This equation shows that the efficiency is a function of the isentropic pressure ratio [Van Wylen and Sonntag, 1985]. The efficiency versus pressure ratio is shown in Figure 53. From this curve the the OBC is attractive because the high efficiency will yield a lower reactor thermal power and lower shield mass. In addition since the OBC is an open system there will be no need for a waste heat radiator, again decreasing the mass of the entire system.

For the CO_2 Open Brayton Cycle a simplified axial flow turbine model was used for calculating the mass and size of the converter. The axial flow turbine model determines the blade length and disk radius for each stage of a turbine by calculating (1) the energy transfer from the working fluid to the rotating blades for each stage of the turbine; (2) the flow area required by the working fluid as it exits each stage; and (3) the limiting stage blade speed due to material strength considerations. The process is done in an iterative fashion due to the interdependence of these calculations.

The model can accommodate various working fluids (including CO_2 and turbine structural materials. A nickel super alloy was used as the turbine material along with the CO_2 working fluid. However, CO_2 OBC was rejected, because at the low atmospheric pressure on Mars (~10 mbar) the compression ratio required to achieve the high efficiencies become large(50 to 100) and the the converter becomes the dominant mass component. Table 10 lists the mass Breakdown for the OBC. The large converter mass again pushes the system specific mass far above the design goal of 100 kg/kW_e.

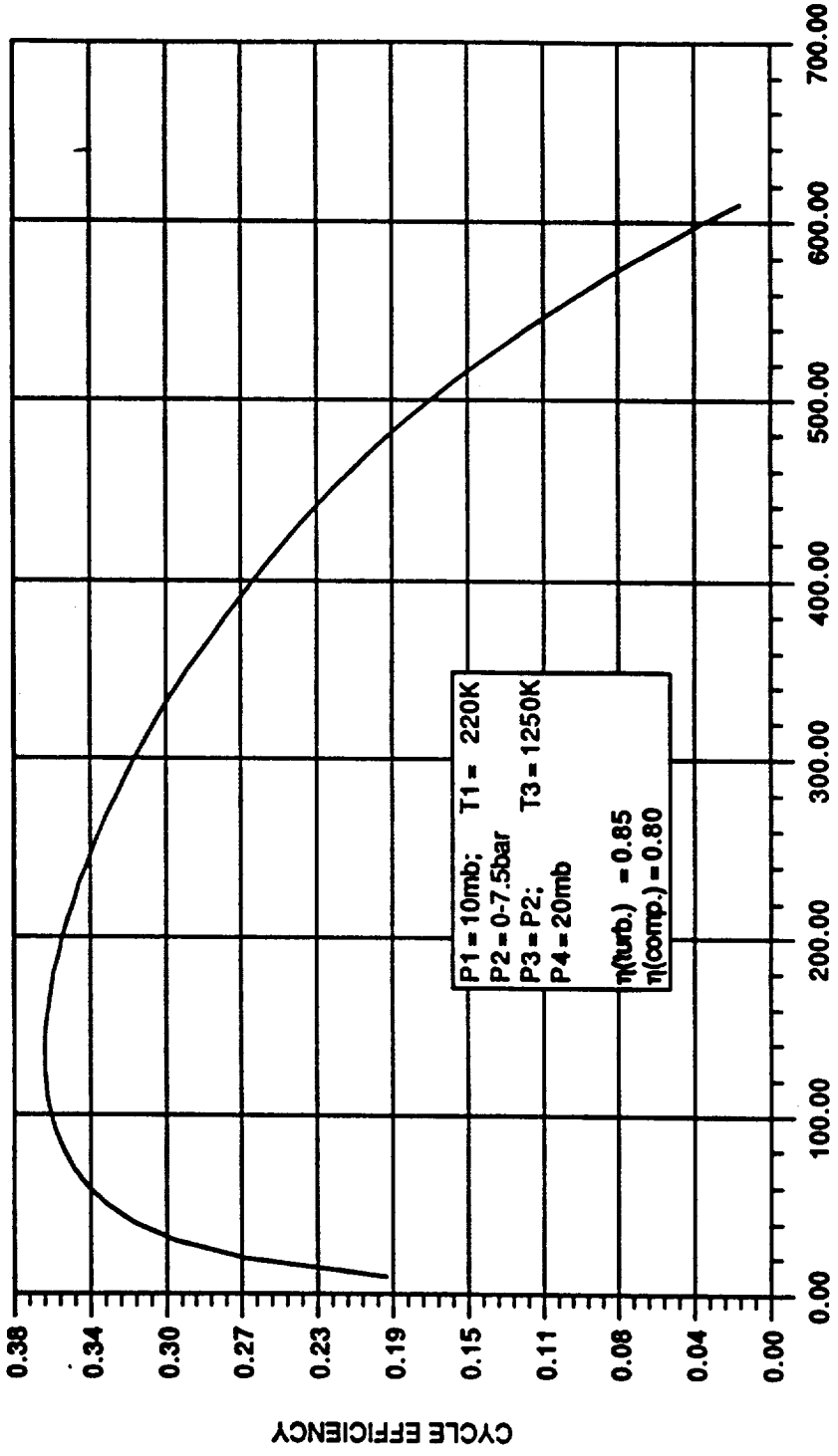

Figure 54: Efficiency verses Temperature for Open Brayton Cycle

Table 10. Mass Breakdown for Open Brayton Cycle.

Reactor	Shield	Converter	Radiator
302 kg	11725 kg	10580 kg	0

6.3 **He/Xe Closed Brayton Cycle**

The He/Xe Closed Brayton Cycle is the standard Brayton Cycle discussed with use as a dynamic space energy conversion cycle. The P-v and T-s are similar to those in Figure 52 a and b for the Open Brayton Cycle; However, because it is a closed system, instead of expelling the effluent back to the atmosphere, there is an isobaric heat rejection from 4 to 1. The system diagram for the CBC is shown in Figure 55. By adding a regenerator to the system the overall efficiency may be increased above that of a simple CBC. Figure 56 shows the T-s diagram for a CBC with regenerator. For a CBC with a regenerator the efficiency is given by the following equation:

$$\eta_{th} = 1 - \frac{T_1}{T_3}\left(\frac{P_2}{P_1}\right)^{(k-1/k)}, \qquad (18)$$

Here T_1/T_3 is the ratio of minimum to maximum temperature.

Two different size engines were used for the evaluation of the CBC. In order to maintain a degree of redundancy each of the two system contained an additional conversion unit. The mass breakdown for the systems studied is given in Table 11. As in the case of the Thermoelectric system the largest mass component is the shield. While the mass of each of the two systems is significantly lower than the TE system, both still have a specific mass of almost twice the design goal of 100 kg/kW$_e$.

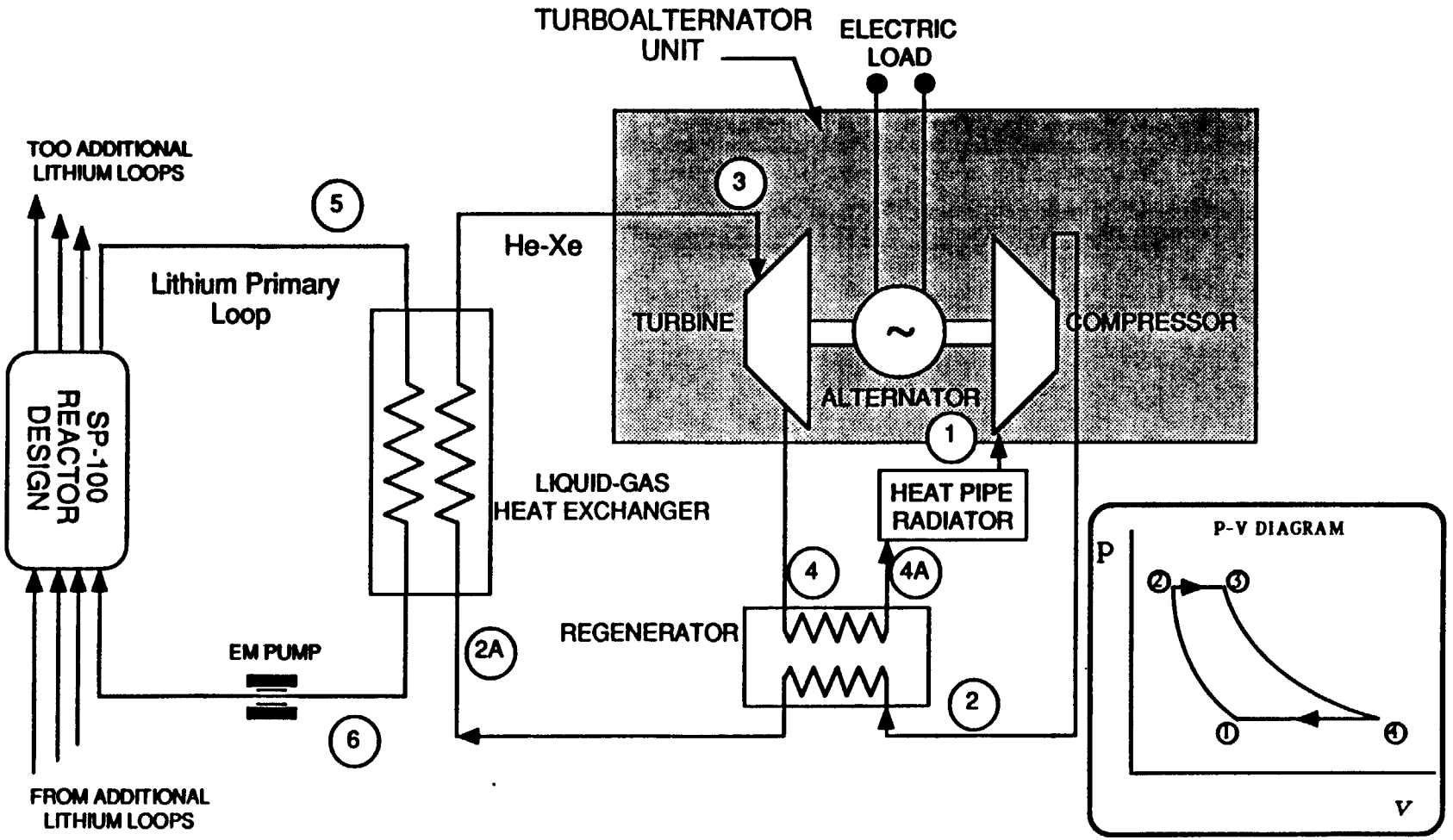

Figure 55: System Diagram for Closed Brayton Cycle

Table 11: Mass Breakdown of CBC Conversion System for Manned Rover

	Reactor	Shield	Converter	Radiator
3x50 kW_e	325 kg	12900 kg	4362 kg	492 kg
2x100 kW_e	320 kg	12507 kg	5133 kg	491 kg

6.4 **Free Piston Stirling Engine**

The P-v and T-s diagrams for the Stirling Cycle are shown in Figure 56 a and b. Heat is transferred to the the working fluid during a constant volume process (2-3) and during a isothermal expansion (3-4), while heat is rejected during (4-1) and (1-2). The Free Piston Stirling Engine technology is currently being developed under the guidance of NASA Lewis Research Center. The FPSE is a reciprocating engine that contains only two moving parts. The converter uses gas bearings for low friction and wear, along with a unique mechanically balance design for low vibration. Figure 57 shows some of the features of the FPSE. The system diagram for a FPSE coupled with an SP-100 reactor core can be seen in Figure 58. Again multiple converter units would be used in the system. The efficiency versus radiator temperature is seen in Figure 59 for different sized 50 kW_e engines.

For calculating the mass and efficiency for the FPSE an empirical correlation of the conversion efficiency and the temperature ratio (TR), specific mass of the converter (SM_c), and the electrical Power (P_e) was used. The correlation was a third degree polynomial with respect to both TR, SM_c, and P_e determined from a preliminary test conducted at Lewis Research Center (LeRC).

The equation was then used with a SMC of 6-kg/kW_e over a range of

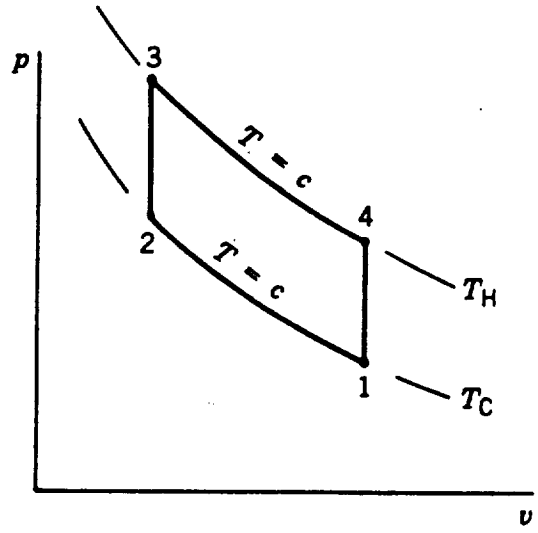

Figure 56a: P-v Diagram for Ideal Stirling Cycle

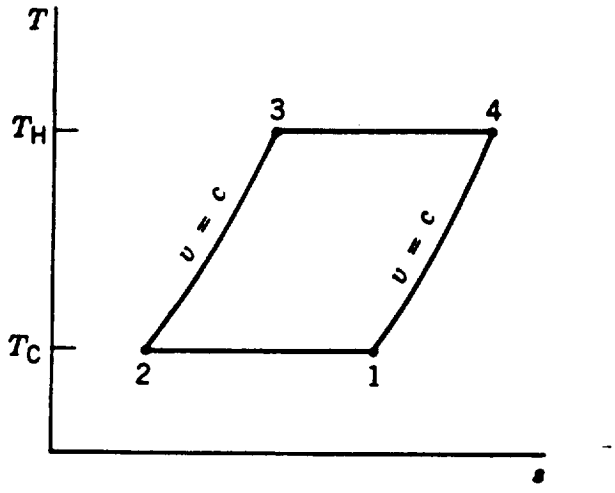

Figure 56b: T-s Diagram for Ideal Stirling Cycle

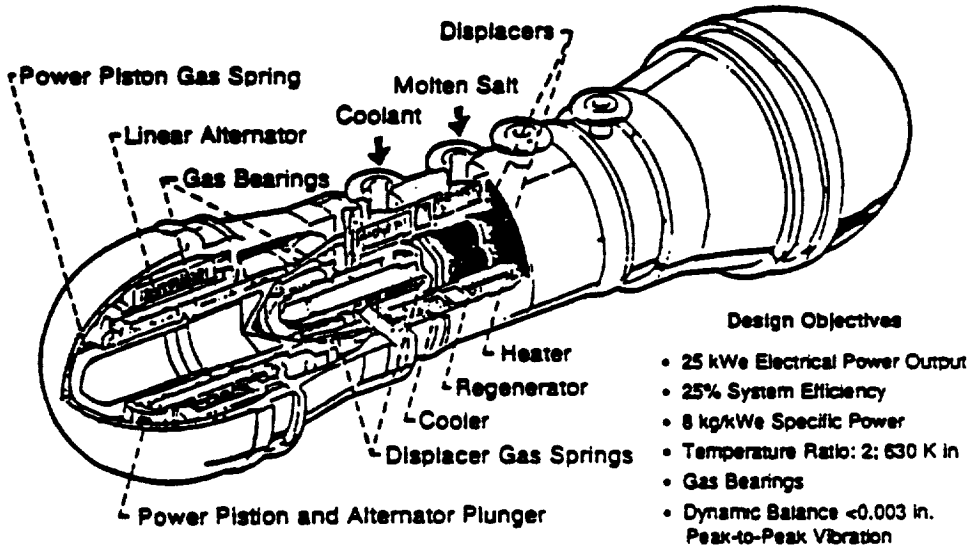

Figure 57: Free Piston Stirling Engine

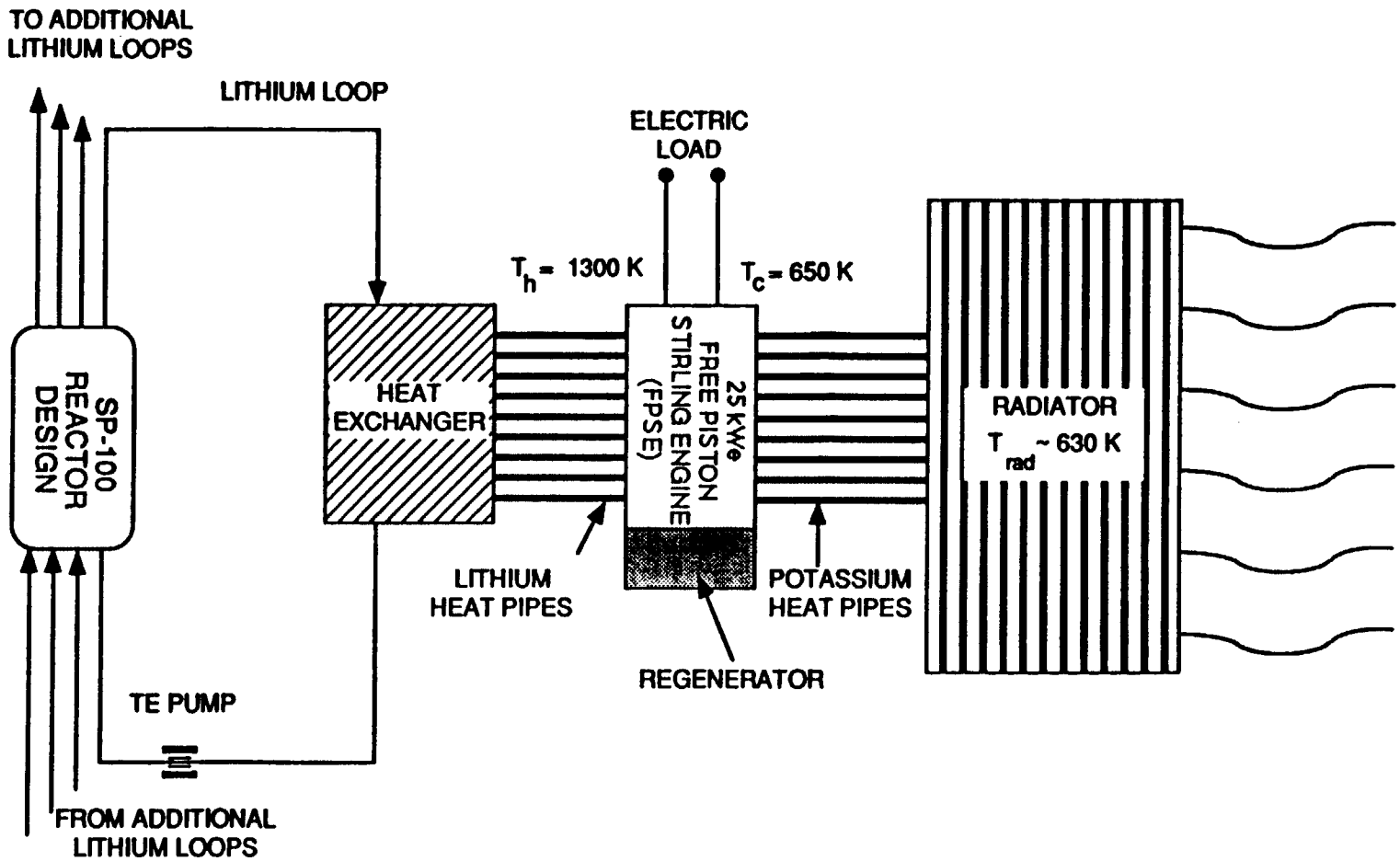

Figure 58: System Diagram for Free Piston Stirling Engine

temperature ratios from 1.5 to 3.0. The determined efficiency is in terms of fraction of ideal (Carnot) efficiency. From the electric power and specific mass of the FPSE, the total conversion system mass may be calculated along with the efficiency. Subsequently, the reactor thermal power and the heat rejected from the radiator are calculated, and have the mass of the entire primary power system may be calculated. The results for both 25 kW_e and 50 kW_e engines are given in Table 12. In each case an additional 50 kW_e potential is used for redundancy.

Table 12: Mass Breakdown of FPSE Conversion System for Manned Rover

	Reactor	Shield	Converter	Radiator
6x25kW_e	314 kg	12200 kg	2914 kg	500 kg
3x50kW_e	309 kg	12025 kg	2693 kg	476 kg

Once again the specific mass of the system is significantly higher than the design goal. The uses of FPSE technology will; however, allow the lowest specific mass (150-160 kg/kW_e) of the four systems studied.

6.5 **Parametric Analysis of FPSE and CBC**

In the previous sections the mass was seen to be lowest for the FPSE and CBC systems. Because these masses were calculated using projected values for the cycle efficiency, the effect of the efficiency on the overall system mass was examined. Here the efficiency of the FPSE was taken to be 29% while that of the CBC system was 25%, which represent current design capabilities. For both systems the converter mass given in Tables 11 and 12 were used. While the mass of each system increased, due to the lower system efficiency, they

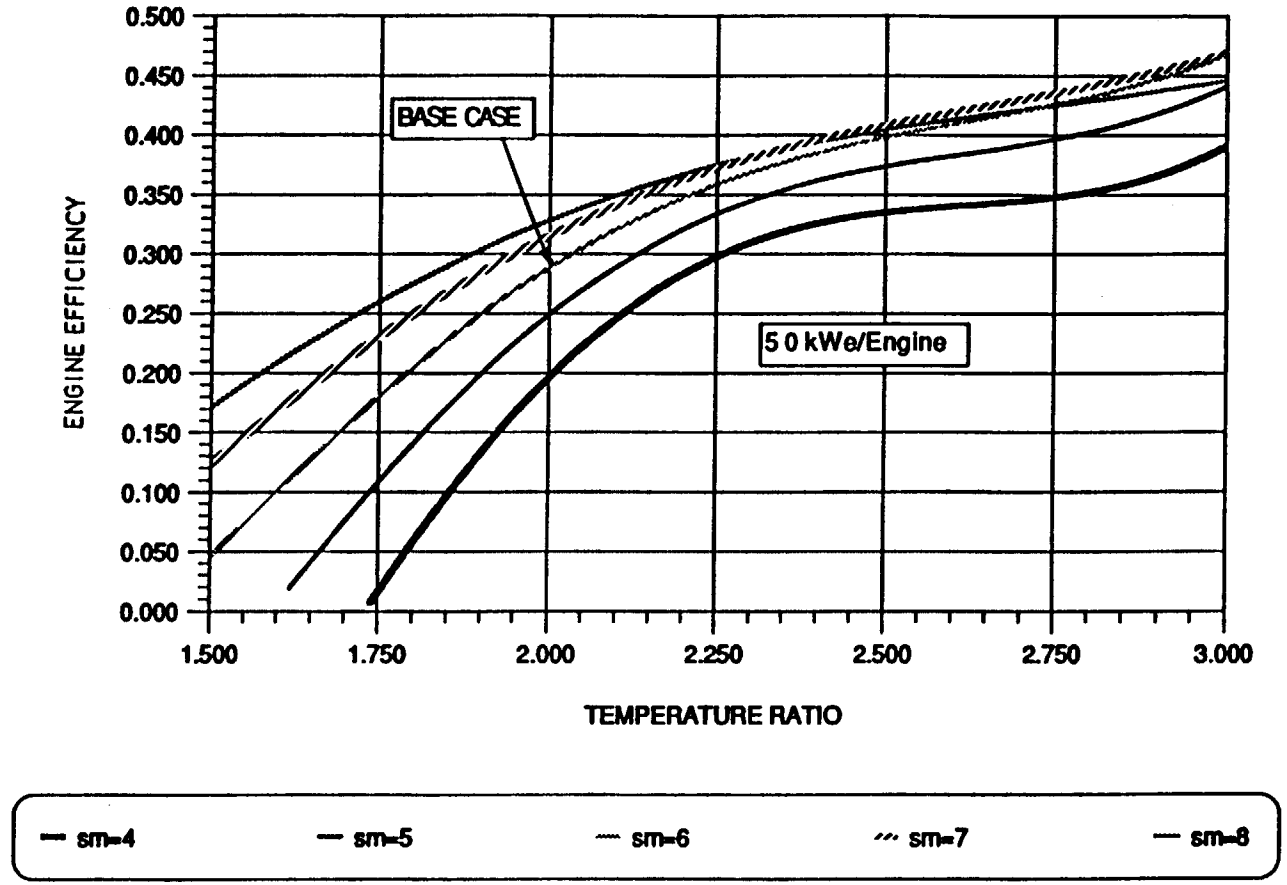

Figure 59: Cycle Efficiency for FPSE

both had a lower mass than the CO_2-OBC or the TE systems. The 3x50 kW_e FPSE showed the lowest mass of 17.6 tonnes with the 6x25 kW_e at 17.8 tonnes. The CBC systems had a slightly higher calculated mass at 20.1 tonnes for the 3x50 kW_e system and 20.9 tonnes for the 2x100 kW_e system. The rover mass breakdown for each of the power system options investigated are shown in Table 13.

6.6 Converter Summary

None of the four systems considered (TE, OBC, CBC, FPSE) was able to meet the design goal, set in Chapter 3, of 100 kg/kW_e. At this point the best alternative from a mass standpoint appears to be the Free Piston Stirling Engine, with a specific mass of 150- 160 kg/kW_e. While the Closed Brayton Cycle power system has a larger specific mass (185-190 kg/kW_e), it should be noted that the technology needed to implement this system is much further along in its development. The parametric analysis of the FPSE and CBC system showed that even at reduced efficiencies, these systems still required a lower mass than the CO_2-OBC and the TE systems.

The overall rover mass breakdowns for the conversion systems (excluding the OBC) are shown in Figure 60 with the operating parameters for each system listed in Table 14. As stated before it is seen that the radiation shield is the largest mass component for each system. Although the layout of the reactor car will vary from component to component Figure 60 shows the layout for 3x50 kW_e CBC system. From the analysis in Chapters 4,5 and 6, a new range for the specific mass of the system was set at 150-190 kg/kW_e. The rover mass over this range is shown versus the cruising speed in Figure 61. By reducing the maximum rover speed, from the base case value of 19 km/h, the mass and power requirements of the rover will be kept to within a reasonable level.

Table 13: Rover Mass Breakdown for Different Power Conversion System Options

CONVERSION SYSTEM OPTION	MASS BREAKDOWN OF POWER CONVERSION SYSTEM (kg)										MASS BREAKDOWN OF ROVER VEHICLE (tonne)						
	REACTOR		RADIATION SHIELD		CONVERTER UNITS		RADIATOR		TOTAL		PCV	EU	SC	RC(c)		TOTAL	
	(a)	(b)	(a)	(b)	(a)	(b)	(a)	(b)	(a)	(b)	(a)	(a)	(a)	(a)	(b)	(a)	(b)
6 x 25 kWe FBSE	314	344	12200	13736	2914	2914	500	841	15928	17835	6.53	5.50	3.13	17.52	19.60	32.68	34.76
3 x 50 kWe FBSE	309	344	12025	13736	2693	2693	476	841	15503	17614	6.53	5.50	3.13	17.05	19.40	32.21	34.56
3 x 50 kWe CBC	325	359	12900	14533	4362	4362	492	833	18079	20087	6.53	5.50	3.13	19.89	22.10	35.05	37.26
2 x 100 kWe CBC	320	359	12507	14533	5133	5133	491	833	18451	20858	6.53	5.50	3.13	20.29	22.90	35.45	38.06
CO2 - OBC	303	–	11725	–	10580	–	–	–	22608	–	6.53	5.50	3.13	24.86	–	40.02	–
SiGe - Graph TES	–	563	–	27600	–	1300	–	430	–	29893	6.53	5.50	3.13	–	32.90	–	48.06

(a) Based on calculated cycle efficiency in Table 2.
(b) Based on projected cycle efficiency in Table 2.
(c) RC = Reactor car, includes power conversion system (reactor, radiation shield, radiator and conversion).

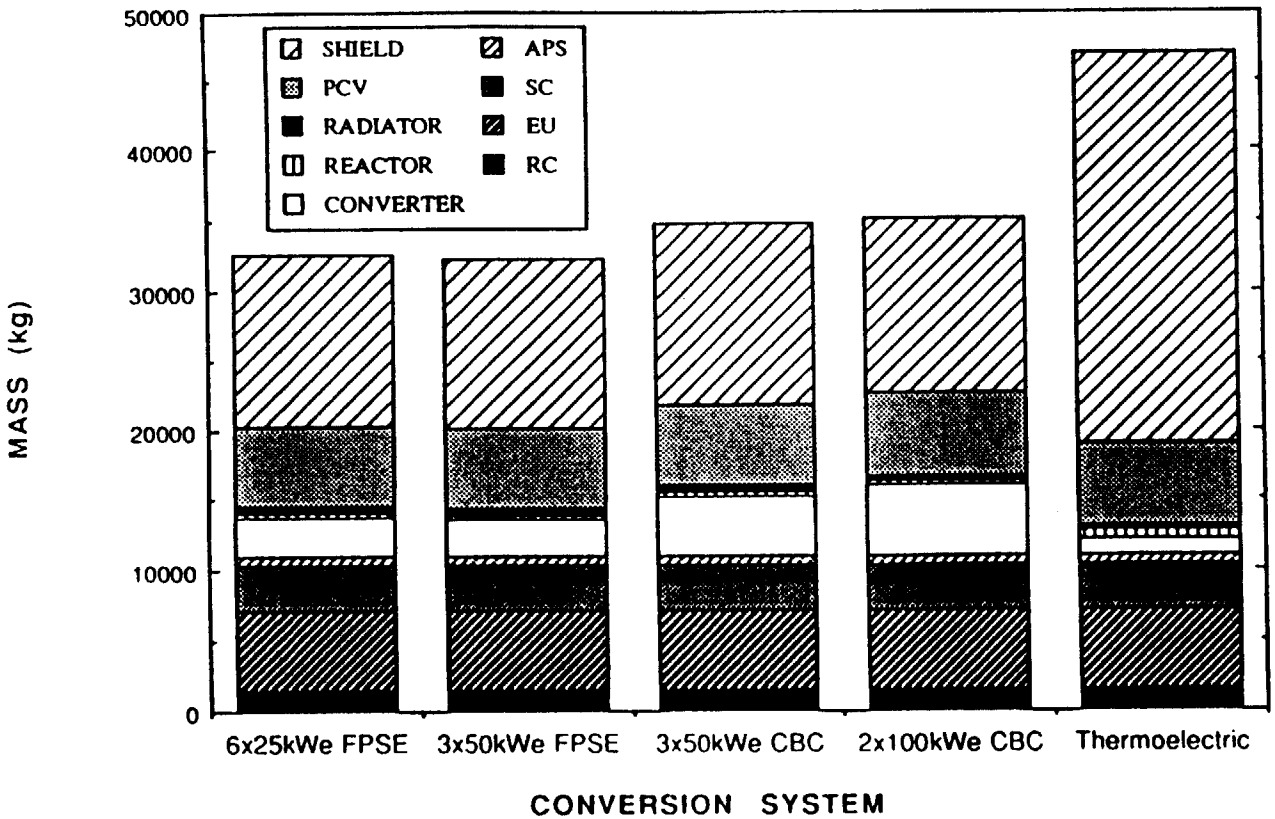

Figure 60: Rover Mass Breakdown for Various Energy Conversion Options

Table 14: Operating Parameters and Calculated and Projected Efficiencies for Various Energy Conversion Systems.

Converter	Number of Units	Temp. Ratio	Radiator Temp. K	Pressure Ratio	Cycle Efficiency %	Projected Efficiency %
25-kWe FPSE	6	2.7	500	-	40	25
50-kWe FPSE	3	2.7	500	-	42	27
50-kWe CBC	3	3.16	395	1.667	36.1	23
100-kWe CBC	2	3.21	389	1.662	37.1	25
TE[(a)]	4320	1.5	800	-	>5	5
CO_2-OBC	2	3.5	-	2	43	28-30

[(a)]Number of Thermoelectric Conversion Assemblies (TCA), each contains a total of 32 SiGe/GaP Thermoelectric unicouples.

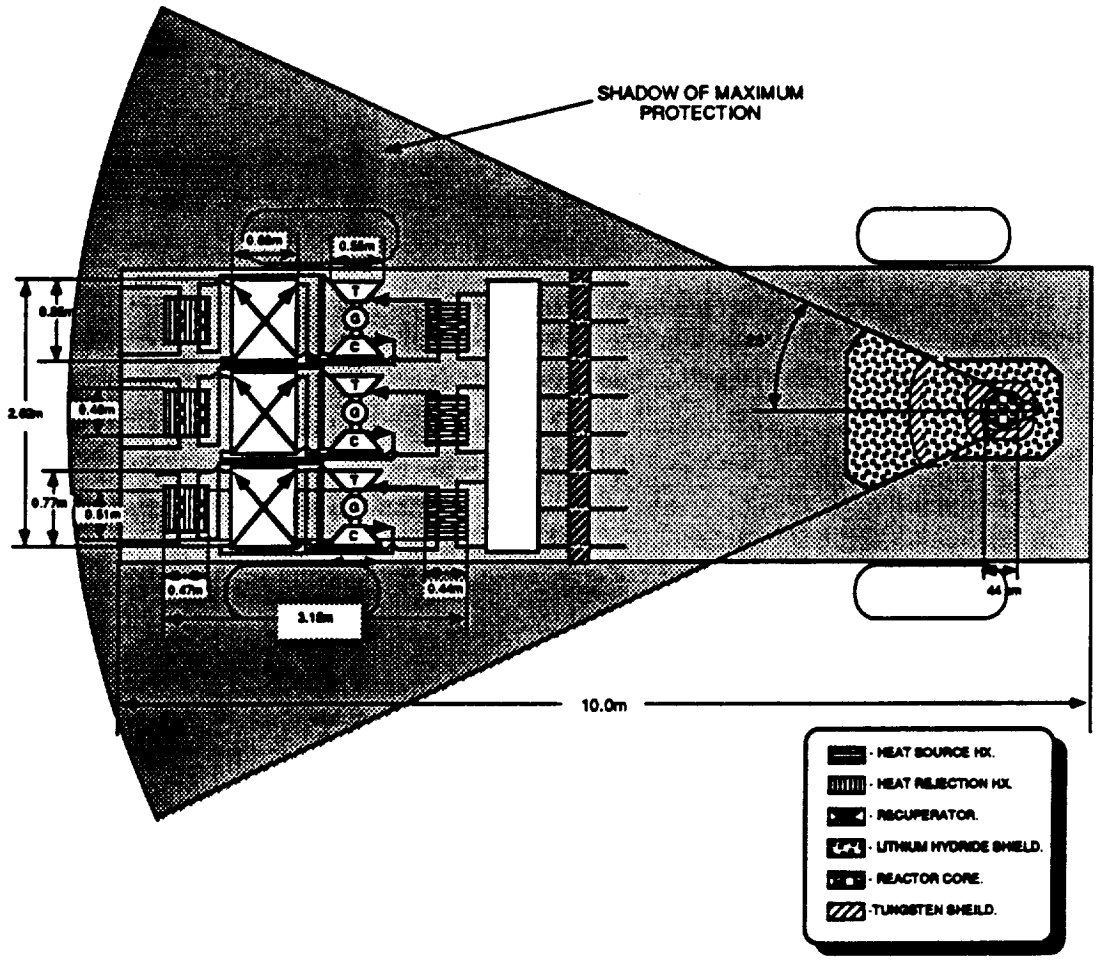

Figure 61: Reactor Car Layout for CBC using 3x50 kW_e Turboaltinators

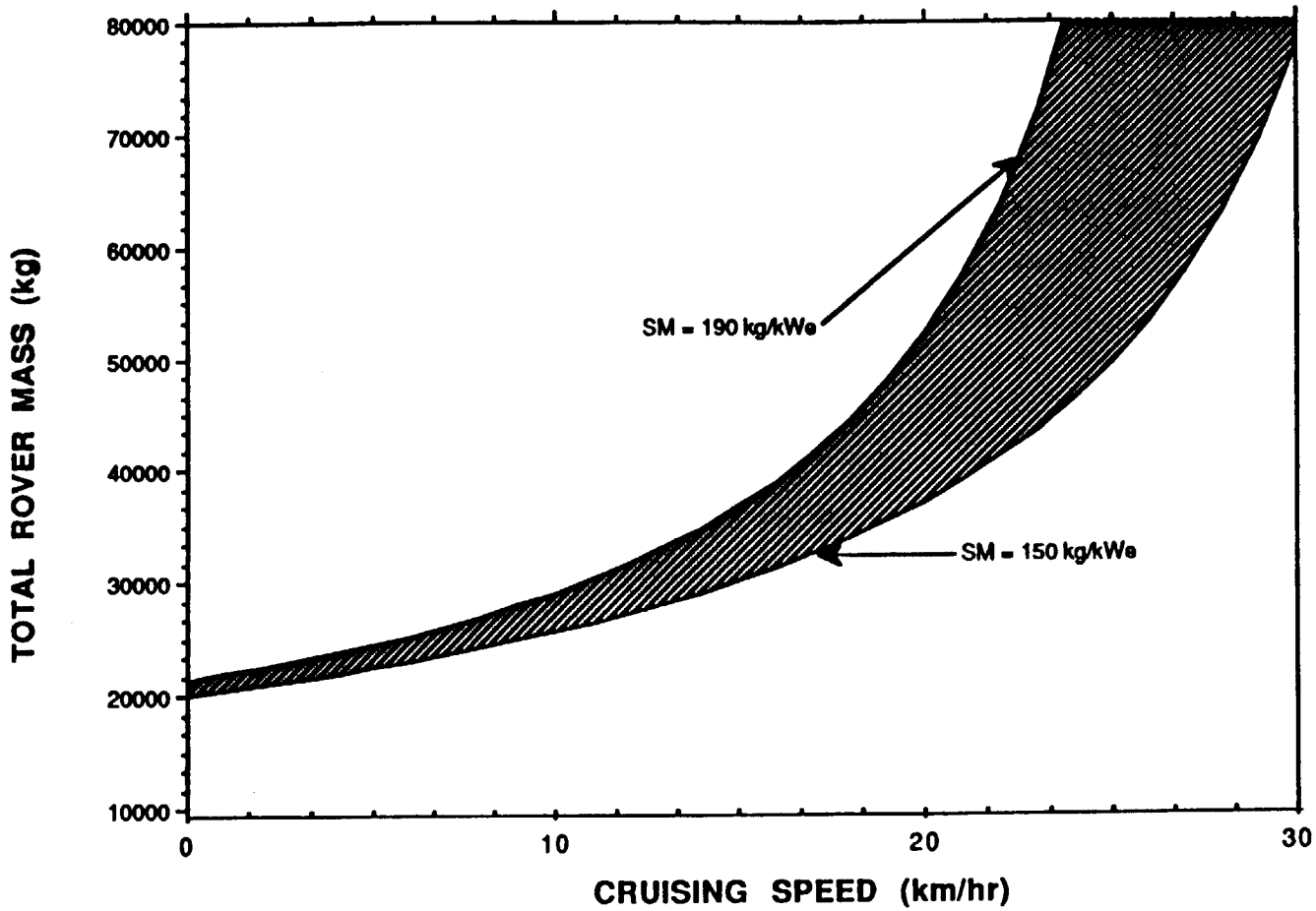

Figure 62: Mass Range for System Specific Mass

7. SUMMARY AND CONCLUSIONS

The study found that the life support power requirement per astronaut strongly affects the mass and size of the PV panels for the auxiliary power system. Therefore, a careful assessment of life support power requirements is strongly recommended. The mass and the size of the PV panels depends on parameters such as the emergency cruising speed, the surface density and efficiency of the PV panels, and the number of astronauts on board the rover. Results show that in order to minimize the size and mass of the PV panels, traversing during emergency return should be made at night and day time travel should be limited.

The primary power requirement of 100 kWe was met using an SP-100 type nuclear reactor coupled to a dynamic conversion system and a man-rated radiation shield. The masses of the shield, reactor,and the radiator were directly dependent on the reactor power, while this power was dictated by the electrical output and the conversion system parameters. The following four conversion systems were investigated for use in the PPS: Free Piston Stirling Engine (FPSE), He/Xe Closed Brayton Cycle (CBC), CO_2 Open Brayton Cycle (OBC), and Thermoelectric conversion. Of the systems studied, the FPSE and CBC systems yield the lowest overall PPS mass, with the Stirling system (15-16 tonnes) giving slightly lower system mass than the Brayton system (18-19.5 tonnes). Because the shield was such a large portion of the overall system mass, its size must be kept as low as possible. Therefore the system with of the highest conversion efficiency has the lowest overall mass. This associated mass of the 150 to 190 kg/kW_e range for specific mass is shown in Figure 61. The overall rover mass for such a system could range from 30 to 34 tonnes.

Since the efficiencies calculated for both the Stirling and Brayton cycles were projected upper limits a parametric analysis was completed to see what

effect lower efficiencies would have on the total rover mass. The analysis show that while the masses of each system increased by reducing the efficiencies to 29% for the Stirling and 25% for the Brayton, both systems still had a total mass less than the thermoelectric and the open Brayton systems.

It was seen that major mass component for the PPS was the radiation shield. While it was possible to design an effective man-rated radiation shield (satisfying the dose rate limit of 0.3 Sv/y to the rover crew) for a manned Mars rover using a single layer each of tungsten and lithium hydride, the shield would not be mass efficient. A double layered W and LiH shield was more effective and significantly lighter. The thickness and positions of the tungsten layers, within the shield, were varied to determine the impact of secondary gammas produced in the W on the dose rate and total shield mass.

The combined shield of LiH and W/depleted U was slightly heavier than a double layered W-LiH shield. The mass of the optimized man-rated W-LiH shield for the Mars rover vehicle powered by a nuclear reactor system increases with the thermal power of the reactor raised to the 0.3797 power, and varies from 8600 to 20580 kg over the power range of 100 to 1000 kW_{th}, respectively. These shield masses were based on a conservative design correlation developed based on the results of 1-D neutronics analysis. Results show that shield mass estimates could be as much as 15 percent higher than those based on 2-D neutronics calculations. A manned Mars rover can easily be designed with a SP-100 type reactor power system; however, the astronauts would be limited in their freedom by the forward angle of the shield.

8. AREAS OF FUTURE WORK

Since this project was a conceptual design there is still considerable work that needs to be done in order to finalize any one for the systems considered. Both structural analysis and component integration need to be addressed in great detail. In addition much work is still needed in the area of shielding. No thermal analysis was performed on the shield and it may be necessary to design an active cooling system to keep the maximum shield temperature within an acceptable level.

In this study it was assumed that the power system components could be sufficiently isolated from the Martian atmosphere (either by coatings or sealing off the reactor car) that corrosion would not affect them over the rover lifetime It may be also necessary to investigate the compatibility of any such isolating materials and the effect of high temperature upon them. In addition the adaptation the Mars rover for lunar applications may show new advantages in applicability and economy.

REFERENCES

1. AeroVirnment Inc, Mars Solar Rover Technical Note, MSR TN4, May 1, 1989.

2. Andrews, D. G., "Near-Term Nuclear Space Missions", Space Power, vol. 8, No. 3, IAF International Conference on Space Power, 1989.

3. Angelo, J. A., and D. Buden, Space Nuclear Power, Orbit Book Company, Inc., Malabar, Fl., 1985.

4. Angrist, S. W., Direct Energy Conversion 3rd ed., Allyn and Bacon, Boston, 1976.

5. Appelbaum, D., and D. J. Flood, "The Mars Climate for a Photovoltaic System", Space Power, vol. 8, No. 3, IAF International Conference on Space Power 1989.

6. Barattino W.J., M.S. El-Genk, and S.S. Voss, "Review of Previous Shield Analysis for Space Reactors", Space Nuclear Power Systems 1984, Orbit Company, Malabar, Fl., 1985.

7. Bekker, M.G., Introduction to Terrain-Vehicle Systems, The University of Michigan Press, Ann Arbor, 1969.

8 Bennett, C.O. and J.E. Myers, Momentum, Heat, and Mass Transfer 3rd ed., McGraw-Hill Book Company, New York,1982.

9. Bennett, G., J. Lombardo, R. Hemler, and J. Peterson, "The General Purpose Heat Source Radioisotope Thermoelectric Generator: Power for the Galileo and Ulysses Missions", 21st Intersociety Energy Conversion Engineering Conference, vol. 3, pp. 1999-2011, San Diego, Ca., Aug 25-29, 1986.

10. Bennett, G. L., J. A. Janzen, J. J. Lombardo, and A. S. Mehner, "The Dynamic Isotope Power System Technology Program", Proc. 23rd Intersociety Energy Conversion Engineering Conference, vol. 3, pp. 131-136, NY, 1988.

11. Bents, D. J., "Preliminary Assessment of Rover Power Systems for the Mars Rover Sample Return Mission", Space Power, vol. 8, No. 3, IAF International Conference on Space Power, pp. 319-332, 1989.

12. Bloomfield, H.S., "Overview of NASA Radiation Exposure Limit Guidelines for Space Flight Crewmembers ", Proc. 7th Symposium on Space Nuclear Power Systems, Albuquerque, NM, January, 1990.

13. Bloomfield, H.S., Small Reactor Power Systems for Manned Planetary Surface Bases, NASA Lewis Research Center, NASA Technical Memorandum 100223, Cleveland, Oh., December, 1987.

14. Cataldo, Robert, Personal phone conversation, NASA Lewis Research Center, Cleveland, Oh., April 21, 1989.

15. Eagle Engineering, Inc., Lunar Surface Transportation Systems Conceptual Design, Lunar Base Systems Study Task 5.2, EEI report 88-188, July 1988.

16. El-Genk, M.S., N.J. Morley, R. Cataldo, and H. Bloomfield, "A Comparison of Energy Conversion Systems for Meeting The Power Requirements of Manned Rover for Mars Mission" , Proc. 23rd Intersociety Energy Conversion Engineering Conference, Reno, NV., August, 1990.

17. Engle, W.W., R.L. Childs, F.R.Mynatt, and L.S.Abott, Optimization of a Shield for a Heat-Pipe-Cooled Fast Reactor Designed as a Nuclear Electric Space Power Plant, Oak Ridge National Laboratory, ORNL-TM-3449, Oak Ridge, Tenn., June, 1971.

18. Ezell, E. C., and L. N. Ezell, On Mars - Exploration of the Red Planet 1958-1978, National Aeronautics and Space Administration, Washington, DC, 1984.

19. General Electric Company, Materials Presented at SP-100 Project Integration Meeting (PIM), Long Beach, California, 19-21, July, 1988

20 Hartman, Robert F., "Current Status of Mod-RTG Program", Proc. 23rd Intersociety Energy Conversion Engineering Conference, vol. 3, pp. 153 to 158, NY, 1988.

21. Juhasz, Albert., NASA Lewis Research Center, Personal Communication, May 1989.

22. Kaplan, D., Environment of Mars, 1988, NASA technical Memorandum 100470, Lyndon B. Johnson Space Flight Center, Houston, Texas, 1988.

23. Kelly,C.," MHW RTG Performance During Les 8/9 and Voyager Missions", Transactions of the Fourth Symposium on Space Nuclear Power Systems, CONF-870102-SUMMS. pp. 197-200, Albuquerque,New Mexico, January 12-16, 1987.

24. Keshishian, L.J., et al., Radiation Shielding for Zirconium Hydride Reactor Systems, Ai-AEC-13081, Atomics International Division, 1973.

25. Landis, G. A., S. G. Bailey, and J. J. Flood, "Advances in Thin-Film Solar Cells for Lightweight Space PV Power", Space Power, vol. 8, No. 1 and 2, IAF International Conference on Space Power, pp. 31-50, 1989.

26. Lamarsh, J.R., Introduction to Nuclear Engineering, Addison-Wesley Publishing Company, Reading, Mass.,1983.

27. National Council on Radiation Protection and Measurements, Guidance on Radiation Received in Space Activities, NCRP Report No. 98, NCRP, Bethesda, MD., July, 1989.

28. O'Dell, R.D., F.W. Brinkley Jr., and D.R. Marr, User's Manual for ONEDANT: A Code Package for One-Dimensional Diffusion-Accelerated, Neutral-P:article Transport, Los Alamos National Laboratory, Los Alamos, NM, LA-9184-M, 1982.

29. Pearson, Richard J., "Dynamic Isotope Power System Component Demonstrations", Proc. 23rd Intersociety Energy Conversion Engineering Conference, vol. 3, pp. 137-144, NY, 1988.

30. Ralph, E. L., "PV Space Power History and Perspective", Space Power, vol. 8, No. 1 and 2, IAF International Conference on Space Power, pp. 3-10, 1989.

31. Shock, A., et. al., Mars Rover RTG Study, Fairchild Space Co., Germantown, Md., August 10, 1989, FSC-ESD-217/89/449.

32. Van Wylen, G.J., and R.E. Sonntag, Fundamentals of Classical Thermodynamics 3rd Ed., John Wiley and Sons, New York, 1985.

APPENDIX A

MODEL DESCRIPTION AND FLOW CHARTS FOR ROVER MASS PROGRAM

MANNED ROVER POWER/MASS MODEL

Flow Chart

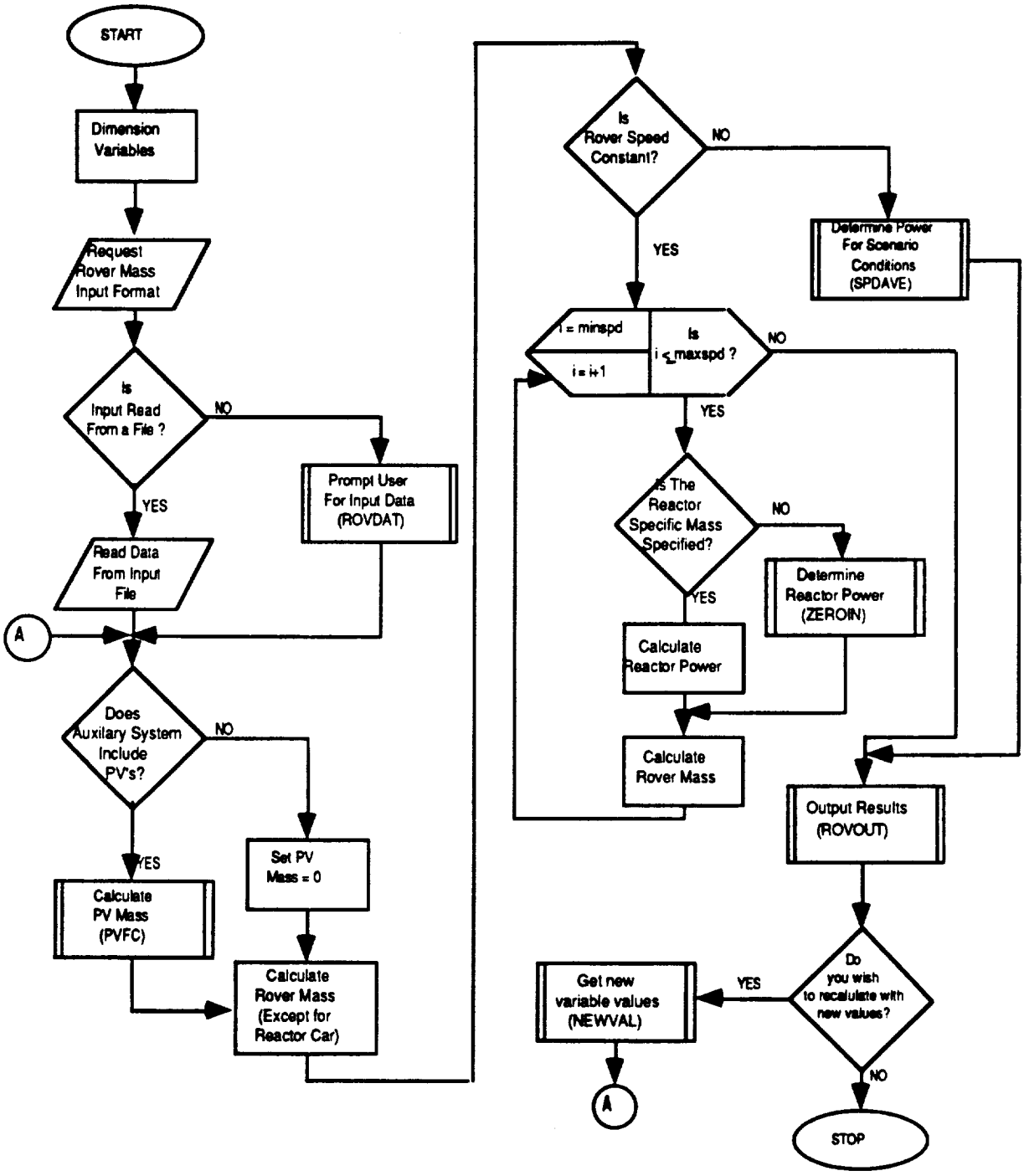

SUBROUTINE INPUT

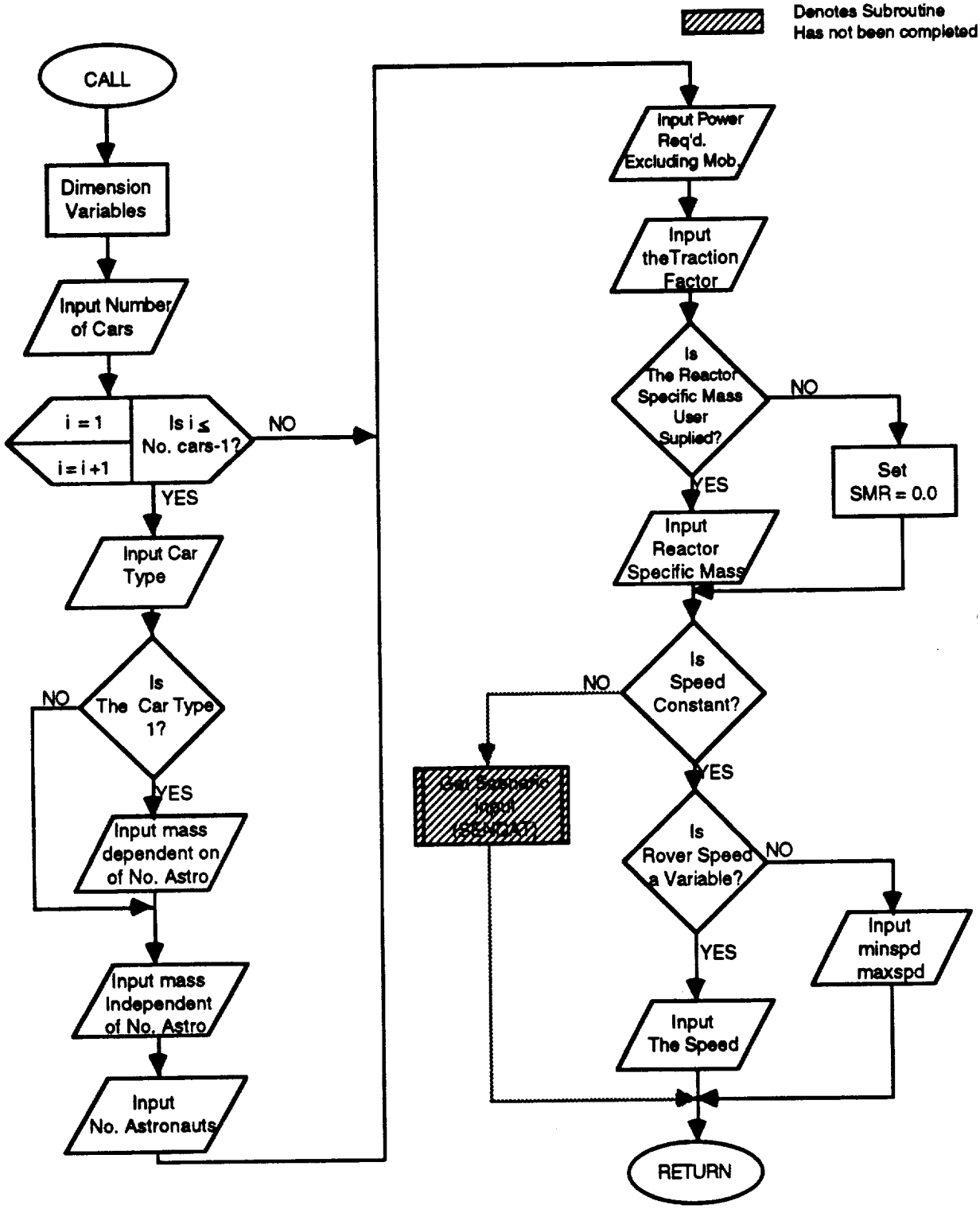

PVFC SUBROUTINE

Flow Chart

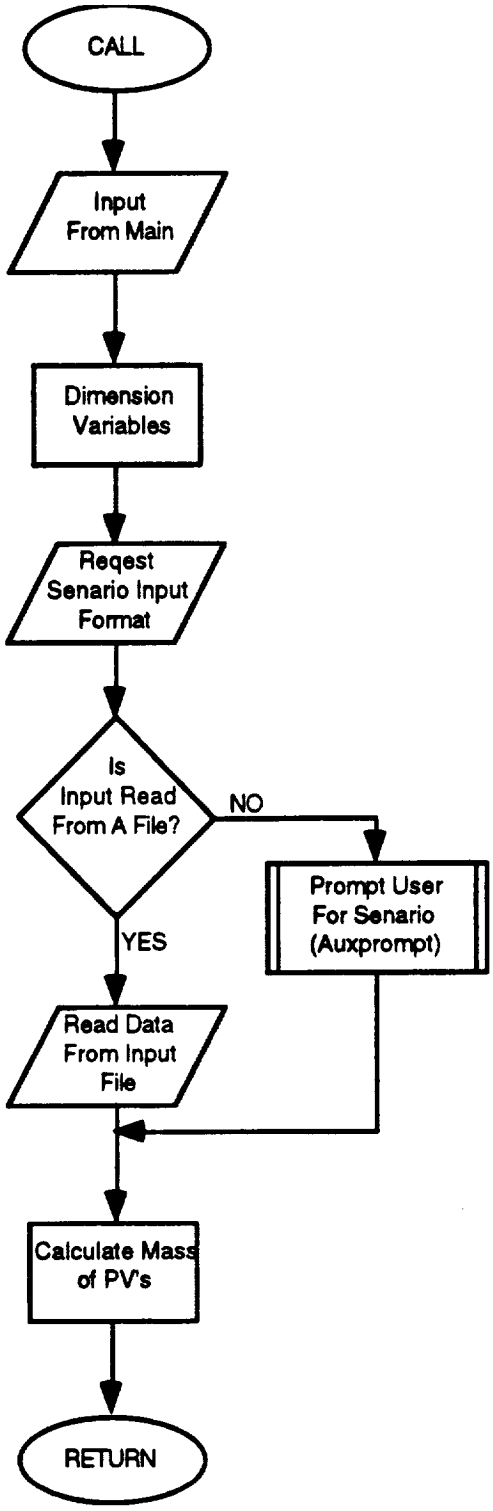

ROVOUT SUBROUTINE

Flow Chart

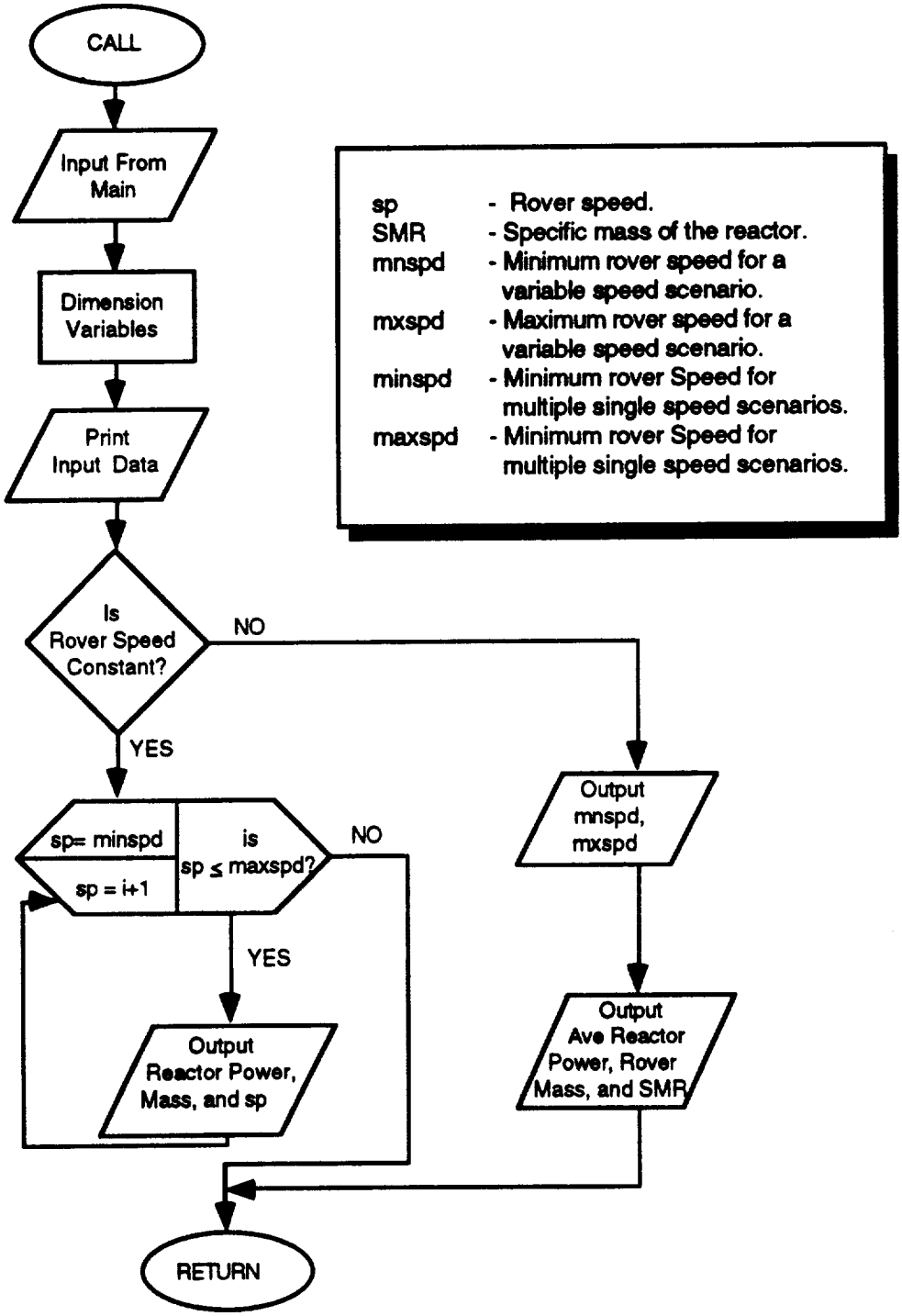

ZEROIN SUBROUTINE

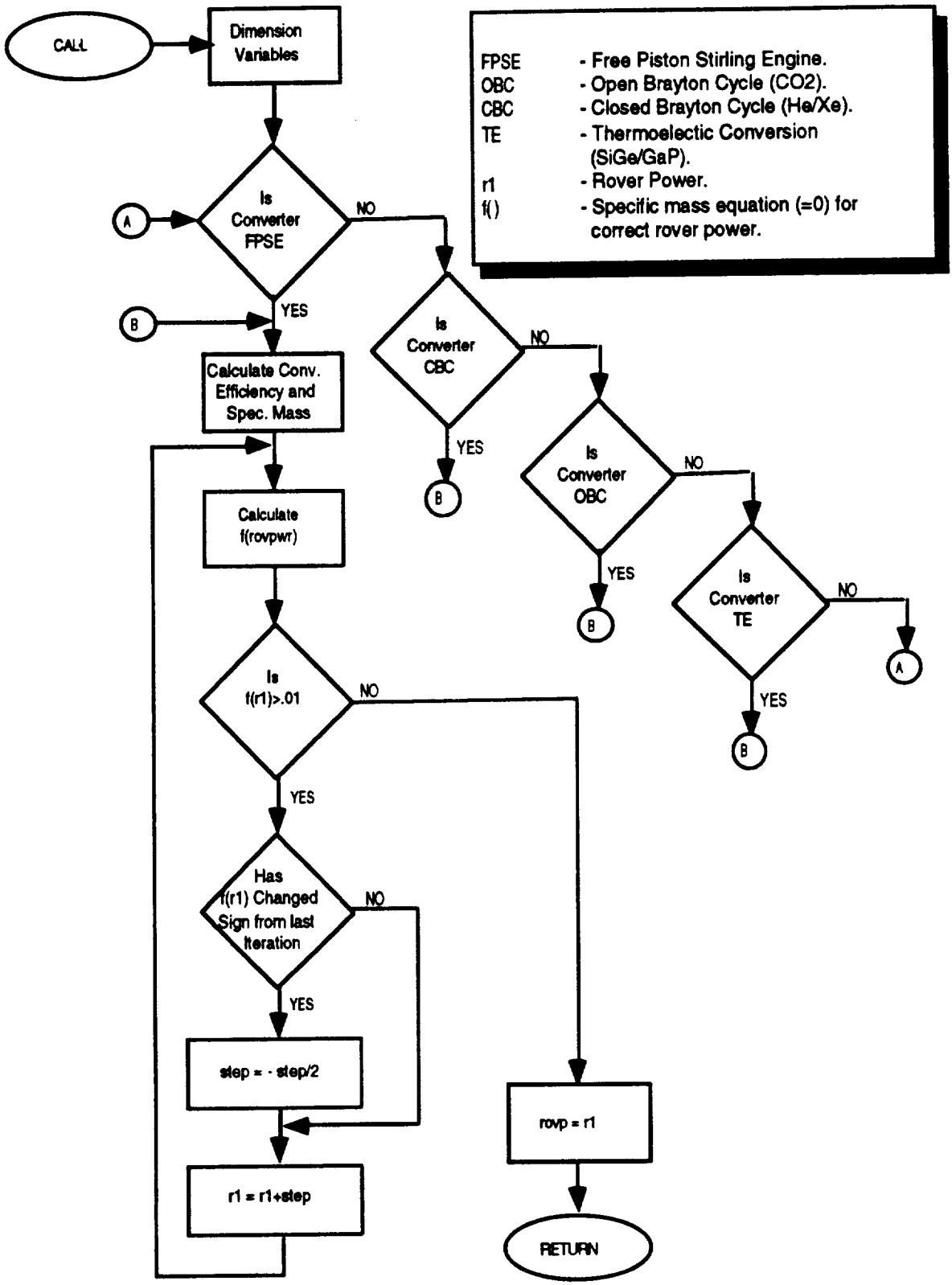

SPDAVE SUBROUTINE

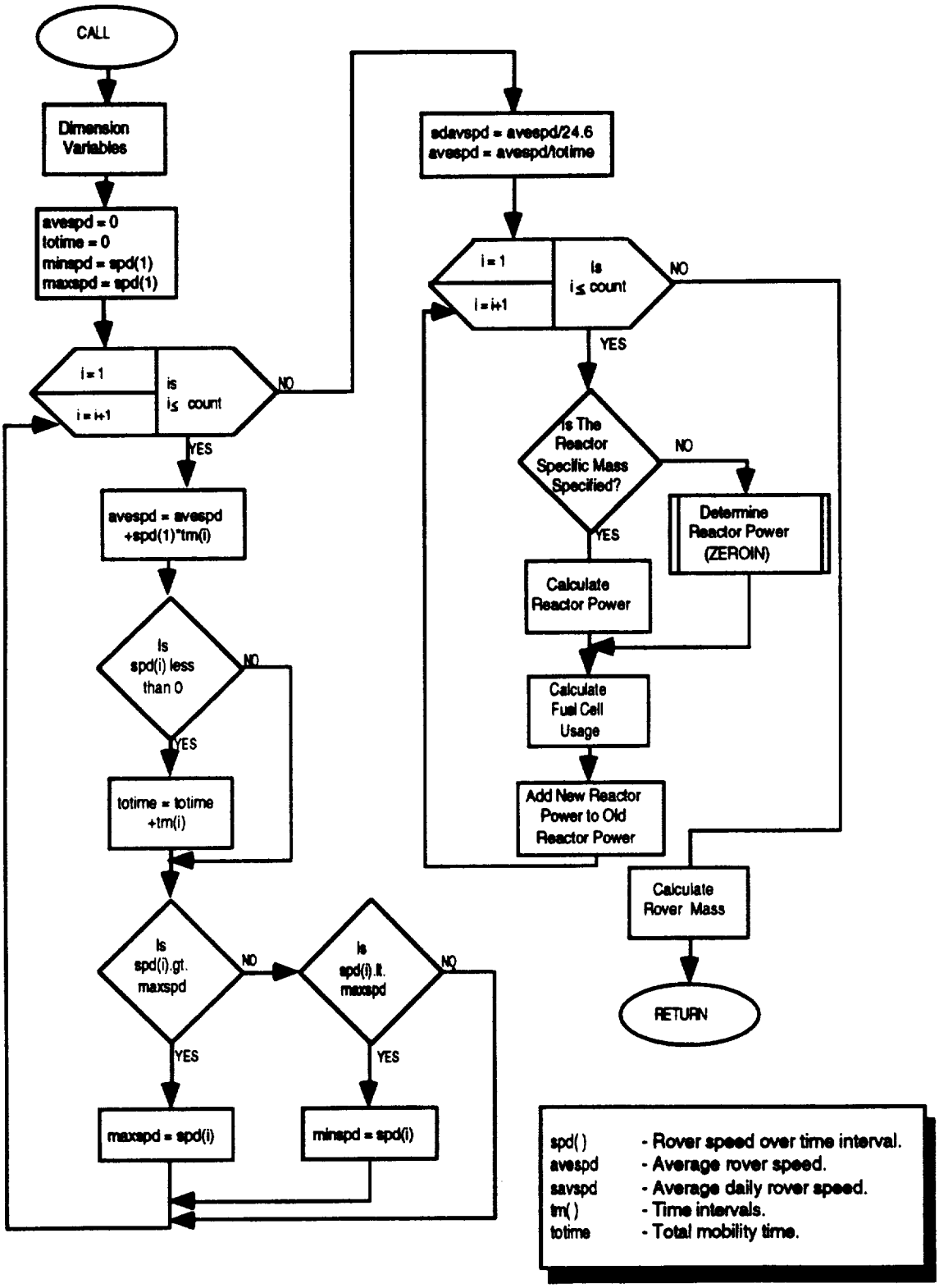

APPENDIX B

LISTING FOR ROVER MASS PROGRAM

```
c              Program Reactor Mass
c
c
c
c
      real     rovmas(0:50,5), pa, x, mpcv1, mpcv2, meu, msc, v,
     &         rovp(0:50,5), mpv, mrov, fc, smr(0:50,5),
     &         spd(0:50), tm(0:50), mxspd, mnspd
      integer i, j, range, systyp, modtyp, auxtyp, smtyp, syst,
     &         count, minspd, maxspd
      character*60  xaxis, yaxis, title, consc(11), intype,
     &              rerun
c
      print*,'Do you what an input prompt (yes or no)?'
      read(5,10)intype
      open(unit=40,file='pvmas',status='new')
 10   format(a)
      if (intype.eq.'no') then
        open (unit=16,file='rdat',status='old')
        rewind 16
        read(16,*)pa, smr(1,1), mnspd, mxspd, x, mpcv1, mpcv2, meu,
     &            msc, na, modtyp, systyp, smtyp, auxtyp, syst
        if (modtyp.eq.1) then
          read(16,*)count
          tmck = 24.6
          do 11 i2 = 1, count
            read(16,*) tm(i2), spd(i2)
            tmck = tmck-tm(i2)
            print*, tm(i2), spd(i2)
 11       continue
          if (tmck.gt.0.01) then
            count      = count+1.0
            tm(count)  = tmck
            spd(count) = 0.0
          endif
        endif
      else
        call rovdat(pa, smr(1,1), mnspd, mxspd, x, mpcv1, mpcv2, meu,
     &              msc, na, modtyp, systyp, smtyp, auxtyp, syst, spd,
     &              tm, count)
      endif
c
      open(unit=35,file='pwrout',status='new')
      j = 1
  15  write(35,16)j
  16  format(/,35x,'RUN #',i2,///)
c
c
      if (auxtyp.eq.1) then
        fc   = 0.0
        fcef = 1.0
        mpv  = 0.0
      else
        call pvfc(na, mpcv1, mpcv2, x, mpv, meu, msc, fc, fcef)
      endif
c
      print*,'fc = ',fcef
      mrov = mpcv1+float(na)*mpcv2+meu+msc+mpv+fc
      if (modtyp.eq.1) then
        call spdave(pa, mrov, x, smr, smtyp, rovp, rovmas, spd, avespd,
     &              savspd, totime, mnspd, mxspd, count, tm, j, pave,
     &              psave, fcef)
      else
        minspd = mnspd
        maxspd = mxspd
```

```
          range = maxspd-minspd
          do 30  i = 0, range
            v = float(i+minspd)
            if(smtyp.eq.1) then
              call zeroin(syst, rovp(i,j), mrov, x, v, pa, smr(i,j),0)
            else
              rovp(i,j) = (pa+x*0.08/1000.0*(mrov*v))/(1.0-x*
     &                    (0.088/1000.0*(smr(1,j)*v)))
            endif
            rovmas(i,j) = rovp(i,j)*1.1*smr(i,j)+mrov
   30     continue
        endif
c
c
c                ** Output Values **
c
        call rovout(pa, j, smr, minspd, maxspd, x, mpcv1, mpcv2, meu,
     &              msc, na, systyp, mpv, rovp, rovmas, modtyp, avespd,
     &              savspd, mnspd, mxspd, count, tm, spd)
c
        print*,'Do you want to change any of the values (yes or no)?'
        read(5,35)rerun
   35   format(a)
        if (rerun.eq.'yes') then
          j = j+1
          smr(1,j) = smr(1,j-1)
          call newval(pa, smr(1,j), mnspd, mxspd, x, mpcv1, mpcv2, meu,
     &                msc, na, modtyp, systyp, smtyp, auxtyp)
          go to 15
        endif
        stop
        end
c
c*******************************************************************************
c*******************************************************************************
c
c
c
        subroutine rovdat(pa, smr, mnspd, mxspd, x, mpcv1, mpcv2,
     &                    meu, msc, na, modtyp, systyp, smtyp, auxtyp,
     &                    syst, spd, tm, count)
c
c
c
c
        real  pa, smr, x, mpcv1, mpcv2, meu, msc, spd(0:50), tm(0:50),
     &        mnspd, mxspd
        integer na, cartyp, systyp, modtype, smtyp, auxtyp, syst, count
c
c
        print*,'Enter number of cars in the rover excluding the ',
     &         'reactor car.'
        read(5,*)numcar
        print*,' '
        print*,' '
        do 1010 i = 1, numcar
 1000     print*,' '
          print*,' '
          print1005,i
 1005     format(' Enter the type of car number ',i1)
          print*,'Primary Control Vehicle (PCV) - 1'
          print*,'Experimental Unit       (EU)  - 2'
          print*,'Storage and Supply Car  (SC)  - 3'
          read(5,*)cartyp
          if (cartyp.eq.1) then
```

```
        print*,' '
        print*,' '
        print*,'Enter the mass of the PCV independent of the'
        print*,'number of Astronauts (in kg).'
        read(5,*)pcv1
        mpcv1 = mpcv1+pcv1
        print*,' '
        print*,' '
        print*,'Enter the mass of the PCV dependent of the'
        print*,'number of Astronauts (in kg/astro.).'
        read(5,*)pcv2
        mpcv2 = mpcv2+pcv2
       else
        if (cartyp.eq.2) then
         print*,' '
         print*,' '
         print*,'Enter the mass of the EU (in kg).'
         read(5,*)eu
         meu = meu+eu
        else
         if (cartyp.eq.3) then
          print*,' '
          print*,' '
          print*,'Enter the mass of the SC (in kg).'
          read(5,*)sc
          msc = msc+sc
         else
          print*,' '
          print*,' '
          print*,'***INVALID ENTRY***'
          go to 1000
         endif
        endif
       endif
1010 continue
     print*,' '
     print*,' '
     print*,'Enter the number of astronauts.'
     read(5,*)na
     print*,' '
     print*,' '
     print*,'Enter the power req.''d in addition to mobility (in kWe).'
     read(5,*)pa
     print*,' '
     print*,' '
     print*,'Enter the traction factor modifier x.'
     read(5,*)x
     print*,' '
     print*,' '
     print*,'Enter the method of reactor specific mass determination.'
     print*,'User specified     - 0'
     print*,'Program calculated - 1'
     read(5,*)smtyp
     print*,' '
     print*,' '
1020 if (smtyp.eq.0)then
       print*,'Enter the reactor specific mass (in kg/kWe).'
       read(5,*)smr
       print*,' '
       print*,' '
     elseif(smtyp.eq.1) then
1021    print*,'Enter the converter type.'
        print*,'     1 - Free Piston Stirling Engine (He working',
    &          ' fluid).'
        print*,'     2 - Closed Brayton Cycle (He/Xe working fluid).'
```

```
        print*,'     3 - Open Brayton Cycle (CO2 working fluid).'
        print*,'     4 - Thermoelectric conversion (SiGe/GaP).'
        read(5,*)syst
        print*,' '
        print*,' '
        if (syst.lt.1.or.syst.gt.4) then
          print*,' '
          print*,' '
          print*,'***INVALID ENTRY***'
          print*,' '
          go to 1021
      elseif (smtyp.lt.0.or.smtyp.gt.1) then
          print*,' '
          print*,' '
          print*,'***INVALID ENTRY***'
          print*,' '
          go to 1020
        else
          smr = 0.0
        endif
      endif
1040  print*,'Enter the traversing scenario.'
      print*,'Constant speed - 0'
      print*,'Variable speed - 1'
      read(5,*)modtyp
      print*,' '
      print*,' '
      if (modtyp.eq.0) then
        print*,'Would you like to calculate the mass for a'
        print*,'Single speed    - 0'
        print*,'Range of speeds - 1.'
        read(5,*)systyp
        print*,' '
        print*,' '
1050    if (systyp.eq.1) then
          print*,'Enter the minimum Rover speed (in km/hr).'
          read(5,*)mnspd
          print*,' '
          print*,' '
          print*,'Enter the maximum Rover speed (in km/hr).'
          read(5,*)mxspd
          print*,' '
          print*,' '
        else
         if (systyp.eq.0) then
           print*,'Enter the Rover speed (in km/hr).'
           read(5,*)mnspd
           mxspd = mnspd
           print*,' '
           print*,' '
         else
           print*,' '
           print*,' '
           print*,'***INVALID ENTRY***'
           go to 1050
         endif
        endif
      else
        if (modtyp.eq.1) then
          call sendat (count, tm, spd)
        else
           print*,' '
           print*,' '
           print*,'***INVALID ENTRY***'
           go to 1040
```

```
        endif
      endif
      print*,'Enter '
      print*,'0 - Photovoltaic auxiliary power system'
      print*,'1 - No PV''s in the auxilairy system'
      read(5,*)auxtyp
      return
      end
c
c
c*****************************************************************************
c
c
c
c
      subroutine pvfc(na, mpcv1, mpcv2, x, mpv, meu, msc, fc, fceff)
c
c
c
c
      real    mpvd, mpcv1, mpcv2, mpcv, mfc1, mcells, meu, msc, fc,
     &        mfc2, mfc3, mpv
      integer i, j, na
c
 2000 print*,'This routine is designed to either accept input from'
      print*,'the emergency scenario from a data file called auxdat.'
      print*,'If this file does file does not exist then you may '
      print*,'specify a full prompting for this information enter:'
      print*,'          0 - Senario prompting'
      print*,'          1 - Read from Auxdat'
      read(5,*)ptyp
      if (ptyp.eq.0) then
        call auxpromt (sma, tc, fceff, tmd, tmn, pls, ve, ta,
     &                 g, pveff, ta2, ta3, apvs)
        print*,tmd,tmn,ta,tc
      else
        if (ptyp.eq.1) then
          open(unit=30,file='auxdat',status='old')
          rewind 30
          read(30,*)sma, tc, fceff, tmd, tmn, pls, ve, ta, g, pveff,
     &              ta2, ta3, apvs
          close(unit=30)
        else
          print*,'***INVALID ENTRY***'
          go to 2000
        endif
      endif
      td     = 24.62
      mcells = 2.0
      mfc1   = ta*pls*na*(0.5+mcells)
      mpcv   = mpcv1+mpcv2*float(na)+mfc1
      smpv   = sma/(g*pveff)*1000.0
      tmm = 12.3
      do 2006 j = 0,3
      tmm = float(j)*4.1
      do 2005 i = 12,0,-1
      tmn = float(i)/1.5
      tc  = 12.3-tmn
      tmn = tmn+tmm
      mpvd   = (na*pls*(tc+(td-tc)/fceff)-12.3*apvs*g*pveff/1000.+x*
     &          (0.08/1000.0)*(mpcv+apvs*sma)*ve*(tmd+tmn/fceff))*smpv/
     &          (tc-x*(0.08/1000.0)*ve*(tmd+tmn/fceff)*smpv)
      mpv    = mpvd+apvs*sma
      write(40,*)tc, mpv
 2005 continue
```

```
 2006 continue
      mfc2   = ta2*pls*na*(0.5+mcells)
      mfc3   = ta3*pls*na*(0.5+mcells)
      fc     = mfc1+mfc2+mfc3
      tatot  = (ta+ta2+ta3)*pls*na
      write (35,2010)
      write (35,2020)smpv, fceff, tc, apvs, tmd, tmn, pls, ve, tatot,
     &               mfc1, mfc2, mfc3
 2010 format(25x,'Auxiliary Power System Input',//)
 2020 format(15x,'PV specific mass                = ',f7.2,' kg/kWe',/,
     &       15x,'Fuel cell efficiency            = ',f7.2,/,
     &       15x,'Deployable PV collection time   = ',f7.2,' hr',/,
     &       15x,'Stationary PV area              = ',f7.2,'m**2',/,
     &       15x,'Mobility time during the day    = ',f7.2,' hr',/,
     &       15x,'Mobility time during the night  = ',f7.2,' hr',/,
     &       15x,'Power needed for emergency LS   = ',f7.2,' kWe/Astro'
     &       ,/,
     &       15x,'Auxiliary cruising speed        = ',f7.2,' km/hr',/,
     &       15x,'Total fuel cell reserve         = ',f7.2,' kWh',/,
     &       15x,'PCV fuel cell mass              = ',f7.2,' kg',/,
     &       15x,'EU fuel cell mass               = ',f7.2,' kg',/,
     &       15x,'SC fuel cell mass               = ',f7.2,' kg',///)
      return
      end
c
c
c*******************************************************************************
c*******************************************************************************
c
c
      subroutine zeroin(syst, rovp, mrov, x, v, pa, smpw, m2)
c
c
c
c
      real    rovp, mrov, x, v, pa, k1, k2, k3, ma, step
      integer syst, m2
      double precision c1, c2, c3, c4, c5, c6, c7, c8, c9, c10, c11,
     &                 c12, eta1, eta2, eta3
c
      ma   = 5.0
      sig  = 5.67e-8
      f    = 0.8
      tamb = 200.
      alph = 0.2
      eps  = 0.85
      step = 100.
c
      k1   = pa+x*(0.08/1000.*mrov*v)
      k2   = x*0.088/1000.*v
      print*,k1,k2
      print*, syst
c
      if (syst.eq.1) then
        trad = 500.
        tr   = 2.7
        smc  = 6.0
        c1  =  0.0543767273338744
        c2  = -0.3981779728928814
        c3  =  0.9497880537528545
        c4  = -0.7477923527039820
        c5  = -0.7487642015184974
        c6  =  5.5454480019398034
        c7  =-13.4344707466661930
        c8  = 10.7927102688699961
```

```
        c9  =  2.6978636228013784
        c10 =-20.2721544168889523
        c11 = 50.0956199839711189
        c12 =-40.5948684886097908
c
        eta1 = (c1*(tr**3)+c2*(tr**2)+c3*tr)*smc**2
        eta2 = (c4*smc**2)+(c5*(tr**3)+c6*(tr**2)+c7*tr)*smc
        eta3 = (c8*smc)+(c9*tr**3)+(c10*tr**2)+(c11*tr)+c12
        eta  = eta1+eta2+eta3
        eta = (1.-1./tr)*eta
c
        smc = smc*eta
      elseif(syst.eq.2) then
        eta  = 0.361
        trad = 395.
        smc  = 15.75
      elseif(syst.eq.3) then
        eta  = 0.43
        trad = 1000.0
        smc  = 50.0
      elseif(syst.eq.4) then
        eta  = 0.053
        smc = 0.609
        trad = 800.
      endif
        print*,eta,smc
      k3  = (1-eta)*ma/(sig*f*(eps*trad**4-alph*tamb**4))*1000.
     &      +smc
      print*,k3
c
      err = 0.01
      r1  = 10.
      lchk = 1
      nchk = 1
      fr   = err+1.
c
      if (m2.eq.1)then
        smpw = 66.54*rovp**(-0.7189)+1494.*rovp**(-0.6203)+k3
        go to 7075
      else
7000  smpw = 66.54*r1**(-0.7189)+1494.*r1**(-0.6203)+k3
      if ((k2*smpw/eta).ge.1.) go to 7050
      fr   = k1/(1.-k2*smpw/eta)-r1
      print*, r1, fr, step, smpw
      nchk = abs(fr)/fr
      print*,nchk,lchk
      if(nchk.ne.lchk) step = -step/2.
7050  if(abs(fr).gt.err) then
        r1 = r1+step
        lchk = nchk
        go to 7000
      endif
c
      rovp = r1
      endif
c
 7075 return
      end
c
c*********************************************************************
c*********************************************************************
c
c
c
      subroutine rovout (pa, j, smr, minspd, maxspd, x, mpcv1, mpcv2,
```

```
     &                    meu, msc, na, systyp, mpv, rovp, rovmas,
     &                    modtyp, avespd, savspd, mnspd, mxspd, count,
     &                    tm, speed)
c
c
c
c
      real pa, smr(0:50,5), mpcv1, mpcv2, meu, msc, mpv,
     &     rovp(0:50,5), rovmas(0:50,5), avespd, savspd,
     &     mnspd, mxspd, tm(0:50), speed(0:50)
      integer j, i, na, systyp, maxspd, minspd, spd, modtyp, count
c
c
      write(35,3000)
 3000 format(22x,'Mass and Power Requirements for Nuclear',/,
     &       28x,'Reactor Powered Mars Rover',//,36x,'Input Values',/)
      if (modtyp.eq.0)then
        write(35,3010)pa, minspd, maxspd, x, mpcv1, mpcv2,
     &              meu, msc, mpv, na
 3010   format(15x,'Supplemental power above mobility  = ',f8.2,' kWe'
     &  ,/,
     &  15x,'Rover minimum speed                    = ',i8,' km/h',/,
     &  15x,'Rover maximum speed                    = ',i8,' km/h',/,
     &  15x,'Rover traction factor                  = ',f8.2,/,
     &  15x,'Astronaut independent PCV mass         = ',f8.2,' kg',/,
     &  15x,'Astronaut dependent mass               = ',f8.2,' kg/astr'
     &  ,/,
     &  15x,'Mass of experimental unit              = ',f8.2,' kg',/,
     &  15x,'Mass of the supply car                 = ',f8.2,' kg',/,
     &  15x,'Mass of the Photovoltaics              = ',f8.2,' kg',/,
     &  15x,'Number of astronaunts                  = ',i8,///)
        write(35,3020)
 3020   format(31x,'Output Values',/,13x,'Rover Speed',5x,'Reactor ',
     &  'Power',3x,'Rover Mass',3x,'Reactor SM',/,16x,'km/h',14x,'kWe',
     &  11x,'kg',10x,'kg/kWt')
        do 3030 i = 0, maxspd-minspd
          sd = i+minspd
          write(35,3040)sd, rovp(i,j), rovmas(i,j), smr(i,j)
 3030   continue
      else
        write(35,3031)pa, mnspd, mxspd, avespd, savspd, x, mpcv1,
     &              mpcv2, meu, msc, mpv, na
 3031   format(15x,'Supplemental power above mobility  = ',f8.2,' kWe'
     &  ,/,
     &  15x,'Rover minimum speed                    = ',f8.2,' km/h',/,
     &  15x,'Rover maximum speed                    = ',f8.2,' km/h',/,
     &  15x,'Rover ave speed per travel time        = ',f8.2,' km/h',/,
     &  15x,'Rover ave speed per day speed          = ',f8.2,' km/h',/,
     &  15x,'Rover traction factor                  = ',f8.2,/,
     &  15x,'Astronaut independent PCV mass         = ',f8.2,' kg',/,
     &  15x,'Astronaut dependent mass               = ',f8.2,' kg/astr'
     &  ,/,
     &  15x,'Mass of experimental unit              = ',f8.2,' kg',/,
     &  15x,'Mass of the supply car                 = ',f8.2,' kg',/,
     &  15x,'Mass of the Photovoltaics              = ',f8.2,' kg',/,
     &  15x,'Number of astronaunts                  = ',i8,///)
        write(35,3032)
 3032   format(30x,'Rover Speed Power Breakdown',//,23x ,'Rover Speed',
     &         2x,'Travel Time',2x,'Rover Power',/,26x,'(km/h)',9x,
     &         '(h)',8x,'(kWe)')
        do 3033 i2 = 1, count
          write(35,3034) speed(i2),tm(i2),rovp(i2,j)
 3033   continue
 3034   format(26x,f5.2,9x,f5.2,6x,f7.3)
        write(35,3035)
```

```
 3035   format(//,31x,'Output Values',//,13x,'Rover Speed',2x,'Ave Re',
     &  'actor Power',2x,'Rover Mass',3x,'Reactor SM',/,16x,'km/h',14x,
     &  'k','We',11x,'kg',10x,'kg/kWt')
        write(35,3045)avespd, rovp(count+1,j), rovmas(1,j), smr(1,j)
       endif
 3040 format(16x,i3,10x,f9.3,7x,f8.2,5x,f8.2)
 3045 format(16x,f5.2,8x,f9.3,8x,f8.2,4x,f8.2)
      write(35,3050)
 3050 format(///,80('*'))
      return
      end
c
c
c*****************************************************************************
c*****************************************************************************
c
c
c
      subroutine auxpromt(smpv, tc, fceff, tmd, tmn, pls, ve, ta, g,
     &                    pveff, ta2, ta3, apvs)
c
c
c
c
      print*,' '
      print*,' '
      print*,'Enter the specific mass of the PV cells (in kg/m**2).'
      read(5,*)smpv
      print*,' '
      print*,' '
      print*,'Enter the time of reserve power in PCV''s fuel cells',
     &       '(in hours).'
      read(5,*)ta
      print*,' '
      print*,' '
      print*,'Enter the time of reserve power in EU''s fuel cells',
     &       '(in hours).'
      read(5,*)ta2
      print*,' '
      print*,' '
      print*,'Enter the time of reserve power in SC''s fuel cells',
     &       '(in hours).'
      read(5,*)ta3
      print*,' '
      print*,' '
      print*,'Enter the efficiency of the Fuel Cell cycle.'
      read(5,*)fceff
      print*,' '
      print*,' '
      print*,'Enter the power needed for life support (in kWe/Astro).'
      read(5,*)pls
      print*,' '
      print*,' '
      print*,'Enter the daily collection time for deployable PV''s',
     &       ' (in hours).'
      read(5,*)tc
      print*,' '
      print*,' '
      print*,'Enter the area of stationary PV''s (in sq. meters)'
      read(5,*)apvs
      print*,' '
      print*,' '
      print*,'Enter the average solar insolation (in kW/m**2).'
      read(5,*)g
      print*,' '
```

```
      print*,' '
      print*,'Enter the efficiency of the PV panels.'
      read(5,*)pveff
      print*,' '
      print*,' '
      print*,'Enter the time of mobility during the day (in hours).'
      read(5,*)tmd
      print*,' '
      print*,' '
      print*,'Enter the time of mobility during the night (in hours).'
      read(5,*)tmn
      print*,' '
      print*,' '
      print*,'Enter the speed for emergency return (km/hr).'
      read(5,*)ve
      print*,' '
      print*,' '
c
      return
      end
c
c*******************************************************************************
c*******************************************************************************
c
      subroutine newval (pa, smr, minspd, maxspd, x, mpcv1, mpcv2,
     &                   meu, msc, na, modtyp, systyp, smtyp, auxtyp)
c
c
c
c
      real mpcv1, mpcv2, meu, msc, minspd, maxspd
c
 4000 write(5,4010)pa, smr, minspd, maxspd, x, mpcv1, mpcv2, meu,
     &             msc, na
 4010 format(1x,'Which value would you like to change?',/,
     &      5x,' 1-Supplemental power above mobility  = ',f8.2,' kWe',/,
     &      5x,' 2-Specific mass of the reactor       = ',f8.2,' kg/kWe'
     &        ,/,
     &      5x,' 3-Rover minimum speed                = ',f8.2,' km/h',/,
     &      5x,' 4-Rover maximum speed                = ',f8.2,' km/h',/,
     &      5x,' 5-Rover traction factor modifier     = ',f8.2,/,
     &      5x,' 6-Astronaut independent PCV mass     = ',f8.2,' kg',/,
     &      5x,' 7-Astronaut dependent mass           = ',f8.2,' kg/astr'
     &        ,/,
     &      5x,' 8-Mass of experimental unit          = ',f8.2,' kg',/,
     &      5x,' 9-Mass of the supply car             = ',f8.2,' kg',/,
     &      5x,'10-Number of astronaunts              = ',i8,/,
     &      5x,'11-None',//)
      read(5,*) nval
c
      if (nval.eq.1) then
       print*,'Enter the new power value (in kWe).'
       read(5,*)pa
       go to 4000
      elseif (nval.eq.2) then
       print*,'Enter the new reactor specific mass (in kg/kWe).'
       read(5,*)smr
       go to 4000
      elseif (nval.eq.3) then
       print*,'Enter the new minimum speed (in km/hr).'
       read(5,*)minspd
       go to 4000
      elseif (nval.eq.4) then
       print*,'Enter the new maximum speed (in km/hr).'
       read(5,*)maxspd
```

```
        go to 4000
       elseif (nval.eq.5) then
        print*,'Enter the new traction factor modifier.'
        read(5,*)x
        go to 4000
       elseif (nval.eq.6) then
        print*,'Enter the new astronaut dependent mass of the'
        print*,'Primary Control Vehicle (in kg/Astro).'
        read(5,*)mpcv1
        go to 4000
       elseif (nval.eq.7) then
        print*,'Enter the new astronaut independent mass of the'
        print*,'Primary Control Vehicle (in kg/Astro).'
        read(5,*)mpcv2
        go to 4000
       elseif (nval.eq.8) then
        print*,'Enter the new mass of the Experimental Unit (in kg).'
        read(5,*)meu
        go to 4000
       elseif (nval.eq.9) then
        print*,'Enter the new mass of the Supply Car (in kg).'
        read(5,*)msc
        go to 4000
       elseif (nval.eq.10) then
        print*,'Enter the new number of Astronauts.'
        read(5,*)na
        go to 4000
       elseif (nval.ne.11) then
        print*,'***INVALID ENTRY***'
        go to 4000
       endif
c
       return
       end
c
c*************************************************************************
c*************************************************************************
c
       subroutine sendat(count, tm, spd)
c
       real    spd(0:50), tm(0:50), tmchk
       integer count
c
       tmchk = 24.6
       count = 1
       print*,'The length of the Martian day is 24.6 hours.  Therefore'
      &       ,', the sum of the'
       print*,'time intervals should equal 24.6 hours.'
c
 6000  print*,' '
       print*,'Enter the time interval over which the speed is consant.'
       read(5,*)tm(count)
       if((tmchk-tm(count)).lt.0)then
         print*,'current time interval increases the sum past 24.6 hours'
         print*,'Tine interval must be less than or equal to ',tmchk
         go to 6000
       endif
 6010  print*,'Enter the rover speed over the time interval (=> 0km/h).'
       read(5,*)spd(count)
       if (spd(count).lt.0) go to 6010
       tmchk = tmchk-tm(count)
       if (tmchk.gt.0.001) then
         print*,'There are still ',tmchk,'hrs left in the day.'
         count = count+1
         go to 6000
```

```
      endif
c
c
      return
      end
c
c*****************************************************************************
c*****************************************************************************
c
      subroutine spdave(pa,mrov,x,smr,smtyp,rovp,rovmas,spd,avespd,
     &                  savspd,totime,minspd,maxspd,count,tm,j,pave,
     &                  spave,fc)
c
c
c
c
      real     avespd,totime,spd(0:50),rovp(0:50,5),pa,x,v,
     &         rovmas(0:50,5),mrov,smr(0:50,5),savspd,rp,tm(0:50),
     &         maxspd,minspd
      integer  i,j,count
c
      avespd = 0.0
      totime = 0.0
      minspd = spd(1)
      maxspd = spd(1)
      rp     = 0.0
c
c
      do 8000, i = 1, count
        avespd = avespd+spd(i)*tm(i)
        if (spd(i).ne.0.) totime = totime+tm(i)
        print*, totime, tm(i)
        if (spd(i).gt.maxspd) then
          maxspd = spd(i)
        elseif (spd(i).lt.minspd) then
          minspd = spd(i)
        endif
 8000 continue
c
      savspd = avespd/24.6
      avespd = avespd/totime
c
      do 8050 i = 1, 2
        if (i.eq.1) then
          v = avespd
        else
          v = savspd
        endif
        if (smtyp.eq.1) then
          call zeroin(syst,rovp(i,j),mrov,x,v,pa,smr(i,j),0)
        else
          rovp(i,j) = (pa+x*(0.08/1000.)*(mrov*v))/(1.0-x*
     &                ((0.088/1000.)*(smr(1,j)*v)))
        endif
        if(i.eq.1) then
          pave  = rovp(i,j)
        else
          psave = rovp(i,j)
        endif
 8050 continue
      print*,pave, psave
c
c
      rp = 0.0
      do 8100, i = 1, count
```

```
        v = spd(i)
        if (smtyp.eq.1) then
          call zeroin(syst,rovp(i,j),mrov,x,v,pa,smr(i,j),0)
        else
          rovp(i,j) = (pa+x*(0.08/1000.)*(mrov*v))/(1.0-x*
     &                ((0.088/1000.)*(smr(1,j)*v)))
        endif
        if(rovp(i,j).gt.psave) rovp(i,j)=(rovp(i,j)-psave)/fc+psave
        rp = (rovp(i,j)-pa)*tm(i)+rp
        print*,rovp(i,j)
 8100 continue
      rovp(count+1,j)   = rp/24.6+pa
      if (smtyp.eq.1) then
        call zeroin(syst,rovp(count+1,j),mrov,x,v,pa,smr(1,j),1)
      endif
      rovmas(1,j) = rovp(count+1,j)*1.1*smr(1,j)+mrov
c
      return
      end
```

APPENDIX C

VALUES OF PHYSICAL CONSTANT

The mass absorption coefficient (μ_a/ρ) for several materials, in cm^2/g*

Material	Gamma-ray energy, MeV																	
	0.1	0.15	0.2	0.3	0.4	0.5	0.6	0.8	1.0	1.25	1.50	2	3	4	5	6	8	10
H	.0411	.0487	.0531	.0575	.0589	.0591	.0590	.0575	.0557	.0533	.0509	.0467	.0401	.0354	.0318	.0291	.0252	.0255
Be	.0183	.0217	.0237	.0256	.0263	.0264	.0263	.0256	.0248	.0237	.0227	.0210	.0183	.0164	.0151	.0141	.0127	.0118
C	.0215	.0246	.0267	.0288	.0296	.0297	.0296	.0289	.0280	.0268	.0256	.0237	.0209	.0190	.0177	.0166	.0153	.0145
N	.0224	.0249	.0267	.0288	.0296	.0297	.0296	.0289	.0280	.0268	.0256	.0236	.0211	.0193	.0180	.0171	.0158	.0151
O	.0233	.0252	.0271	.0289	.0296	.0297	.0296	.0289	.0280	.0268	.0257	.0238	.0212	.0195	.0183	.0175	.0163	.0157
Na	.0289	.0258	.0266	.0279	.0283	.0284	.0284	.0276	.0268	.0257	.0246	.0229	.0207	.0194	.0185	.0179	.0171	.0168
Mg	.0335	.0276	.0278	.0290	.0294	.0293	.0292	.0285	.0276	.0265	.0254	.0237	.0215	.0203	.0194	.0188	.0182	.0180
Al	.0373	.0283	.0275	.0283	.0287	.0286	.0286	.0278	.0270	.0259	.0248	.0232	.0212	.0200	.0192	.0188	.0183	.0182
Si	.0435	.0300	.0286	.0291	.0293	.0290	.0290	.0282	.0274	.0263	.0252	.0236	.0217	.0206	.0198	.0194	.0190	.0189
P	.0501	.0315	.0292	.0289	.0290	.0290	.0287	.0280	.0271	.0260	.0250	.0234	.0216	.0206	.0200	.0197	.0194	.0195
S	.0601	.0351	.0310	.0301	.0301	.0300	.0298	.0288	.0279	.0268	.0258	.0242	.0224	.0215	.0209	.0206	.0206	.0206
Ar	.0729	.0368	.0302	.0278	.0274	.0272	.0270	.0260	.0252	.0242	.0233	.0220	.0206	.0199	.0195	.0195	.0194	.0197
K	.0909	.0433	.0340	.0304	.0298	.0295	.0291	.0282	.0272	.0261	.0251	.0237	.0222	.0217	.0214	.0212	.0215	.0219
Ca	.111	.0489	.0367	.0318	.0309	.0304	.0300	.0290	.0279	.0268	.0258	.0244	.0230	.0225	.0222	.0223	.0225	.0231
Fe	.225	.0810	.0489	.0340	.0307	.0294	.0287	.0274	.0261	.0250	.0242	.0231	.0224	.0224	.0227	.0231	.0239	.0250
Cu	.310	.107	.0594	.0368	.0316	.0296	.0286	.0271	.0260	.0247	.0237	.0229	.0223	.0227	.0231	.0237	.0248	.0261
Mo	.922	.294	.141	.0617	.0422	.0348	.0315	.0281	.0263	.0248	.0239	.0233	.0237	.0250	.0262	.0274	.0296	.0316
Sn	1.469	.471	.222	.0873	.0534	.0403	.0346	.0294	.0268	.0248	.0239	.0233	.0243	.0259	.0276	.0291	.0316	.0339
I	1.726	.557	.260	.100	.0589	.0433	.0366	.0303	.0274	.0252	.0241	.0236	.0247	.0265	.0283	.0299	.0327	.0353
W	4.112	1.356	.631	.230	.121	.0786	.0599	.0426	.0353	.0302	.0281	.0271	.0287	.0311	.0335	.0355	.0390	.0426
Pt	4.645	1.556	.719	.262	.138	.0892	.0666	.0465	.0375	.0315	.0293	.0280	.0296	.0320	.0343	.0365	.0400	.0438
Tl	5.057	1.717	.791	.285	.152	.0972	.0718	.0491	.0393	.0326	.0301	.0288	.0304	.0326	.0349	.0354	.0406	.0446
Pb	5.193	1.753	.821	.294	.156	.0994	.0738	.0505	.0402	.0332	.0306	.0293	.0305	.0330	.0352	.0373	.0412	.0450
U	9.63	2.337	1.096	.392	.208	.132	.0968	.0628	.0482	.0383	.0346	.0324	.0332	.0352	.0374	.0394	.0443	.0474
Air	.0233	.0251	.0268	.0288	.0296	.0297	.0296	.0289	.0280	.0268	.0256	.0238	.0211	.0194	.0181	.0172	.0160	.0153
NaI	1.466	.476	.224	.0889	.0542	.0410	.0354	.0299	.0273	.0253	.0242	.0235	.0241	.0254	.0268	.0281	.0303	.0325
H_2O	.0253	.0278	.0300	.0321	.0328	.0330	.0329	.0321	.0311	.0298	.0285	.0264	.0233	.0213	.0198	.0188	.0173	.0165
Concrete	.0416	.0300	.0289	.0294	.0297	.0296	.0295	.0287	.0278	.0272	.0256	.0239	.0216	.0203	.0194	.0188	.0180	.0177
Tissue	.0271	.0282	.0293	.0312	.0317	.0320	.0319	.0311	.0300	.0288	.0276	.0256	.0220	.0206	.0192	.0182	.0168	.0160

*From L. T. Templin, editor, *Reactor Physics Constants*, ANL-5800, 2nd ed., 1963; based on G. W. Grodstein, National Bureau of Standards circular 583, 1957.

APPENDIX D

Sample TWODANT Input File

```
    2     0     0
 CORE MODEL FOR MANNED MARS ROVER. 12-1-89
 ADAPTED FROM INPUT CREATED BY JOHN MCGHEE.
/
/  ********** block 1 - controls and dimensions ************
/
 IGEOM=   7              / r/z geometry
 NGROUP=  42             / # of neutron groups
 ISN=     8              / Sn order
 NISO=    60             / # of isotopes on xslib
 MT=      11             / # of materials
 NZONE=   27             / # of model zones
 IM=      10             / # of r coarse mesh intervals
 IT=      27             / # of r fine mesh intervals
 JM=      14             / # of z coarse mesh intervals
 JT=      32             / # of z fine mesh intervals
 MAXLCM=  281500         / maximum large core memory
 MAXSCM=  18500          / maximum small core memory
 NOGEOD=  1              / 1 = suppress geometry input
 NOMIX=   1              / 1 = suppress mixing input
 NOASG=   1              / 1 = suppress material zone assignment input
 NOMACR=  1              / 1 = suppress genration of macroscopic xs
 NOSLNP=  1              / 1 = suppress generation of solver input
 NOSOLV=  1              / 1 = suppress solver module
 NOEDIT=  0              / 1 = suppress edit module
 T
/
/  ********* block 2 - geometry details *********************
/
/ r coarse mesh point coordinates (cm):
XMESH=  0 3 8 13 16 17 19 23 27 30 230
/ z coarse mesh point coordinates (cm):
YMESH= 0 50 53 60 65 73 76 110 113 130 132 133 147 150 200;
/ fine intervals per r coarse interval:
XINTS=  1 2 2 2 1 1 2 2 2 12
/ fine intervals per z coarse interval:
YINTS=  5 2 2 2 1 2 4 2 2 1 1 1 2 5
/ zone number for each coarse mesh interval:
 ZONES= 14 14 14 14 14 14 14 14 14 14;
        27 27 27 27 27 27 27 27 27 14;
         1 26 26 26 26 26 26 26 27 14;
         1  2  4  2  3  0  0  0 27 14;
         6  2  5  2  3  0  0  0 27 14;
         6  7  8  7  7  0 15 13 27 14;
         6  9 10 11 12  0 15 13 27 14;
         6 18 22 20 12  0 15 13 27 14;
        17 18 22 20 12  0  0  0 27 14;
        17 21 24 21 21  0  0  0 27 14;
        17 23 24 25 25  0  0  0 27 14;
        17 23 23 25  0  0  0  0 27 14;
        27 27 27 27 27 27 27 27 27 14;
        14 14 14 14 14 14 14 14 14 14;
T
/
/ ****************** block 3 - nuclear data ***************
/
 LIB=      BXSLIB        / cross section source
 MAXORD=   1             / highest legendre order
 IHT=      4             / total xs row #
 LNG=      30            / last neutron group
 ITITL=    1             / title cards included
 SAVBXS=   0             / 1 = save binary xs file
 KWIKRD=   0             / 1 = no error checking
/ names for each isotope:
 NAMES= H1    D2    T3    HE3   HE4   LI6   LI7   BE9   B10
```

```
        B11    C12    N14    O16    F19    NA23   MG     AL27   SI
        CL     K      CA     TI     V      CR     MN55   FE     CO59
        NI     CU     ZR     NB93   MO     RH103  AG107  AG109  CD
        BA138  TA181  W182   W183   W184   W186   RE185  RE187  AU197
        PB     TH232  PA233  U233   U234   U235   U236   U237   U238
        NP237  PU238  PU239  PU240  PU241  PU242
/ NOTE: IN EBOUND ARRAY THE LAST NEUTRON GRP LOWER BOUND IS .139-9 MEV
 EBOUND=
        1.700+1  1.500+1  1.350+1  1.200+1  1.000+1  7.790    6.070
        3.680    2.865    2.232    1.738    1.353    0.823    0.500
        0.303    0.184    0.676-1  2.480-2  9.120-3  3.350-3  1.235-3
        4.540-4  1.670-4  6.140-5  2.260-5  8.320-6  3.060-6  1.130-6
        0.414-6  0.152-6
       10.00     9.00     8.00     7.00     6.00     5.50     4.00
        3.00     2.00     1.00     0.50     0.10     0.01
 VEL=  54.8   51.9  49.6   45.0    40.8    36.1    29.4    24.8
       21.9   19.3  17.1   14.2    11.1     8.67    6.79    4.83
        2.95   1.81  1.07   0.63    0.39    0.237   0.144   0.087
        0.053  0.032 0.020  0.012   0.007   0.003   12R300
/ names for each edit xs:
 EDNAME= FISS
T
/
/ ************** block 4 - mixing details ********************
/
/  atom densities (atoms/b-cm) for each material:
 MATLS=
        FUEL97   U238   .0009564 U235   .0309236 N14   .0318800;
        FUEL73   U238   .0086080 U235   .0232720 N14   .0318800;
        LINER    RE187  .0412847 RE185  .0246653                 ;
        PWC11    NB93   .0525700 ZR     .0005414 C12   .0004112;
        B4C      B10    .0684000 B11    .0076000 C12   .0190000;
        BEO      BE9    .0676600 O16   .0676600                 ;
        BE       BE9    .1196000                                ;
        BAFFLE   TA181  .0540800                                ;
        CLNT     LI6    .0027500 LI7    .0343100                ;
        LIH      H1     .059     LI6    .0045500 LI7   .0561200;
        TUNG     W182 .0171600  W183 .0093300  W184 .0200200  W186 .0186700;
/  material volume fractions in each zone:
 ASSIGN=  1 PWC11 .190;
          2 CLNT  1.0;
          3 PWC11 .350 CLNT .650;
          4 PWC11 .038 CLNT .800;
          5 PWC11 .038 CLNT .800 BEO .134;
          6 PWC11 .190 BEO  .670;
          7 PWC11 .800 CLNT .200;
          8 PWC11 .678 CLNT .160 BEO .134;
          9 PWC11 .129 CLNT .176 FUEL97 .594 LINER .066;
         10 PWC11 .141 CLNT .141 FUEL97 .475 LINER .053 BEO .134;
         11 PWC11 .129 CLNT .176 FUEL97 .594 LINER .066;
         12 PWC11 .250 CLNT .650 BAFFLE .100;
         13 BEO   .7   B4C  .3;
         14 LIH   1.0;
         15 BEO   .550 B4C .450;
         16 BEO   .878;
         17 PWC11 .190 B4C  .670;
         18 PWC11 .129 CLNT .176 LINER .107;
         19 PWC11 .141 CLNT .141 LINER .086 BEO .134;
         20 PWC11 .129 CLNT .176 LINER .107;
         21 PWC11 .200 CLNT .800;
         22 PWC11 .678 CLNT .160 B4C   .134;
         23 CLNT  1.0;
         24 PWC11 .038 CLNT .800 B4C   .134;
         25 PWC11 .250 CLNT .750;
         26 BE    1.0;
```

```
        27 TUNG  1.0;
T
/
/  ***************  block 5 - solver details  ********************
/
 IEVT=    1                        / eigenvalue search
 ISCT=    0                        / scattering legendre order
 IBL=     1                        / left boundary reflective
 IBR=     0                        / right boundary vacuum
 IBT=     0                        / top boundrary vacuum
 IBB=     0                        / bottom boundary vacuum
 T
/
/  ************* block 6 - edit input details **********************
/
/ spectrum data
/
 PTED=   1                         / edit by mesh point
 ZNED=   0                         / no zone edits
 POINTS= 30I27,864
/ POINTS= 25I1,27
/ POINTS= 25I838,864
/ POINTS= 3, 432, 840
/
/ edit location: lower plenum, lecore, hecore, rod plenum, upper plenum
/ fine intr (r,z):    (11,14), (6,40), (16,40),   (11,70),      (9,94)
/ edit points = r+44(z-1):
/
 RESDNT= 1                         / use edit xs resident macro xs
 IGRPED= 2                         / print broad groups and totals
 ICOLL= 30, 12                     / energy group collapsing
 POWER= 0.5                        / normalize output to this value (mw)
 MEVPER= 200.0                     / mev per fission
 RSFE= F1.0                        / responce function multiplier
 RZFLUX=0
 T
```

APPENDIX E

Tungsten Nuclear Cross Section Data

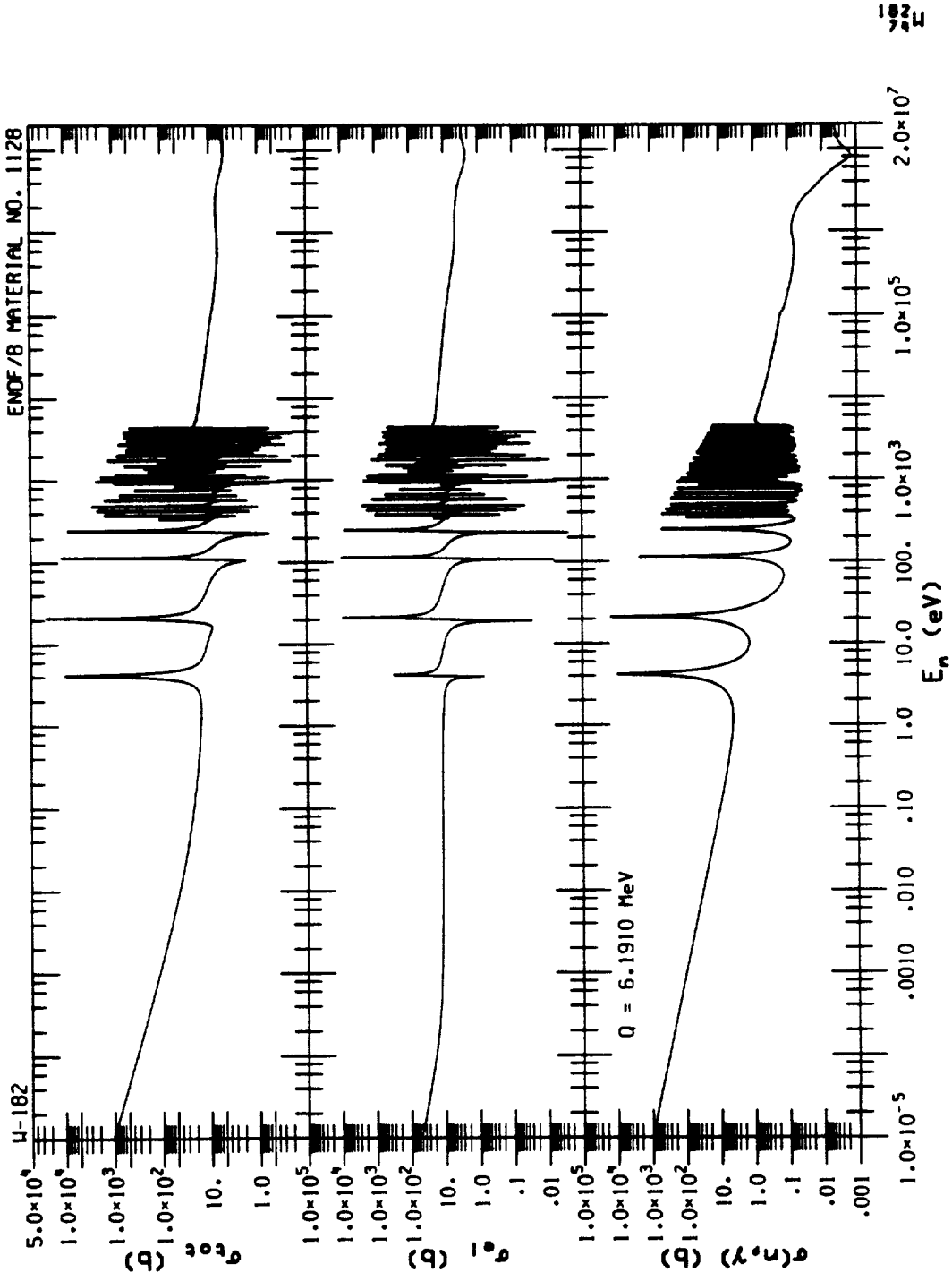
$^{182}_{74}W$
ENDF/B MATERIAL NO. 1128
W-182
Q = 6.1910 MeV
$\sigma(n,\gamma)$ (b)
σ_{el} (b)
σ_{tot} (b)
E_n (eV)

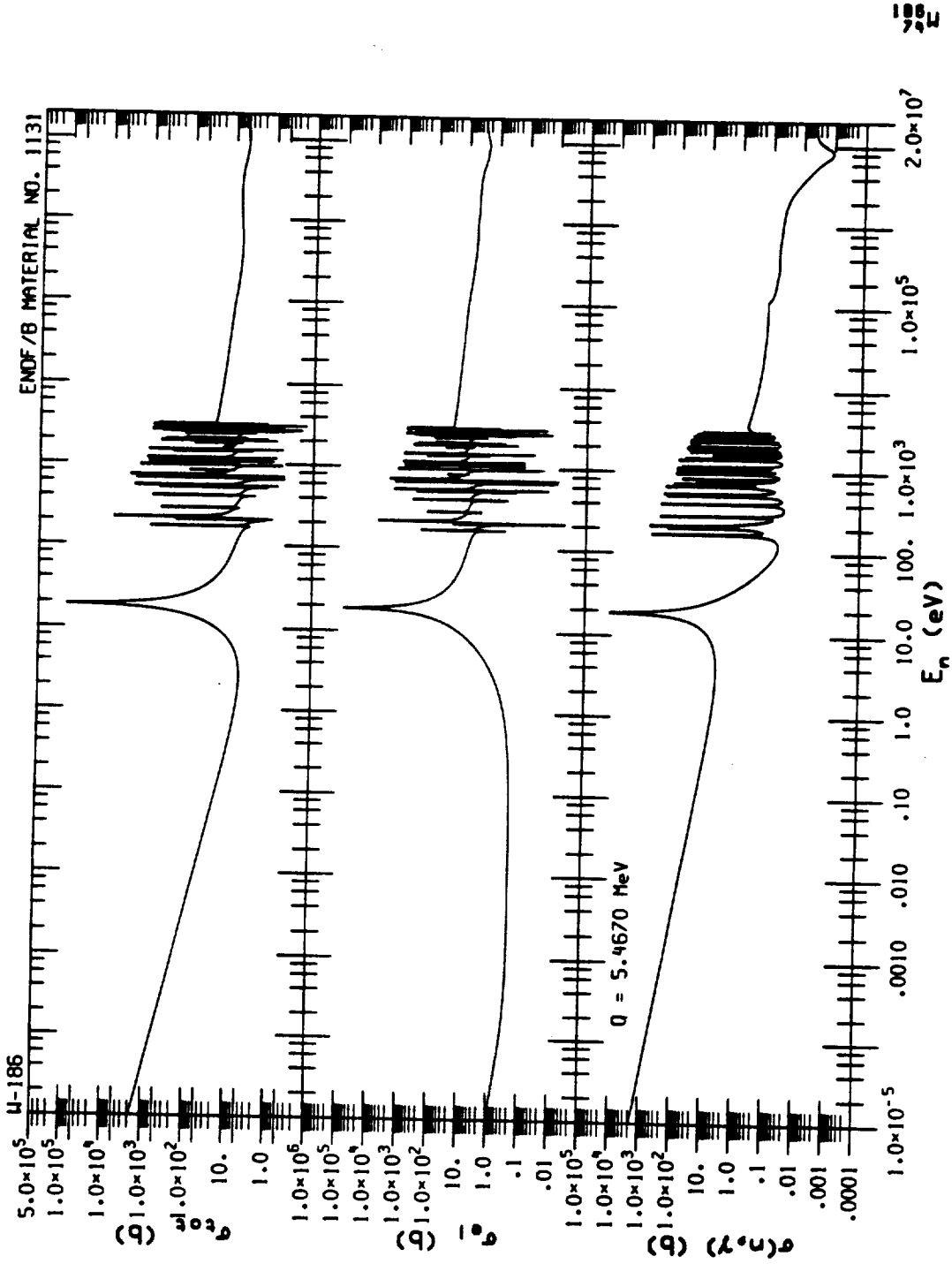
ENDF/B MATERIAL NO. 1131
W-186
Q = 5.4670 MeV
E_n (eV)
$\sigma(n,\gamma)$ (b)
σ_{el} (b)
σ_{tot} (b)

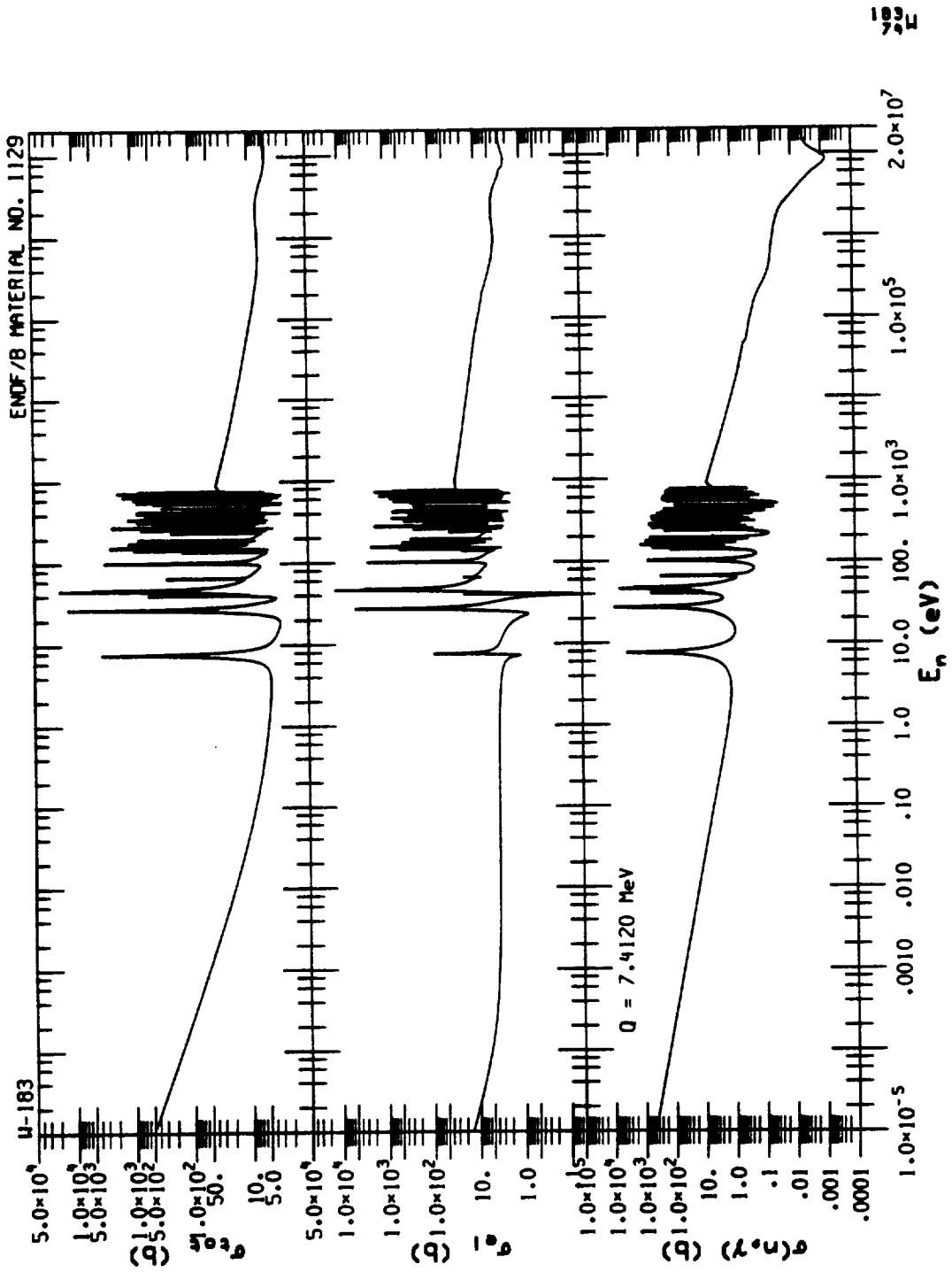
183 74W
ENDF/B MATERIAL NO. 1129
W-183
Q = 7.4120 MeV
E_n (eV)
σ_{tot} (b)
σ_{el} (b)
$\sigma(n,\gamma)$ (b)